Genome wide identification of transcriptional targets of Foxa2 in midbrain dopaminergic cells by ChIP-Seq

Emmanouil Metzakopian

Presented for the degree of Doctor of Philosophy
April 2010

Division of Developmental Neurobiology
National Institute for Medical Research
The Ridgeway, Mill Hill
London NW7 1AA
Department of Anatomy and Developmental Biology
University College London
University of London

Declaration of Authenticity

I, **Emmanouil Metzakopian**, confirm that the work presented in this thesis is my own. Where information has been derived from other sources, I confirm that this has been indicated in the thesis.

Emmanouil Metzakopian
28/04/2010

Abstract

Midbrain dopaminergic (mDA) neurons are involved in the regulation of movement and behavior, and their loss causes severe neurological disorders, such as Parkinson's disease. Foxa1 and Foxa2 (Foxa1/2), members of the Foxa family of forkhead/winged helix transcription factors, are expressed in mDA neurons throughout their development and display overlapping functions. Previously, it has been shown that Foxa1/2 regulate specification and differentiation of mDA neuron development. During specification, Foxa1/2 are required for the expression of Lmx1a, an intrinsic determinant of mDA identity. Recent data strongly suggests that Foxa2 cooperate with Lmx1a and Nurr1 (Nr4a2) in subsequent feed forward loops to regulate differentiation of mDA neurons. However, Foxa2 regulated direct targets and the mechanisms underlying its roles in mDA development are largely unknown.

In this study, we performed chromatin immunoprecipitation (ChIP) and massively parallel Illumina 2G sequencing (ChIP-seq) using *in vitro* and *in vivo* DA systems. We produced a genome wide profile of Foxa2 binding sites at two stages of mDA neuron development: specification (*in vitro*), and differentiation (E12.5 and E14.5 *in vivo* tissue). Foxa2 binding was observed on known regulated elements, the Shh brain enhancer and the Foxa2 floor plate enhancer in both *in vivo* and *in vitro* data sets. Validation of candidate targets was carried out by independent *in vivo* ChIP-qPCR analysis and reverse transcriptase-qPCR expression assays using ventral midbrain tissue from both wild type and transgenic *Foxa1;Foxa2* null mice. Furthermore, genomic regions in the Lmx1a and Lmx1b loci identified in our ChIP-seq analysis were validated for enhancer activity by transgenic LacZ reporter mice. These results strongly suggest that Foxa2 directly regulates the Lmx1a and Lmx1b enhancers emphasizing its key role in mDA

specification. In addition, luciferase reporter assays in P19 cells demonstrate the combinatorial role of Foxa2 with Lmx1a and/or Nurr1 in regulating candidate enhancer regions of genes expressed in mDA neurons. These results confirm the quality of our data sets in predicting Foxa2 regulated target genes.

Acknowledgements

Firstly, I would like to thank my supervisor for providing me with an interesting and challenging project and for her support throughout this process. I would like to thank all past and present members of the Ang laboratory; I would especially like to thank Simon, Martin and Neal for their encouraging discussions and support. I would not have been able to achieve any of my goals if it were not for their help and friendship. I would also like to thank further Julie, Martin and Simon for sharing their data with me. Finally. I would also like to thank members of the Briscoe and Wilkinson labs for their suggestions and for their reagents.

I would like to acknowledge Diogo Castro and Nicky Harker for their advice regarding the ChIP experiments performed in this project. I have to thank my mid-term report examiners Drs Francois Guillemot and Robin Lovell-Badge for inspiring discussions and insightful comments regarding my project. Finally I would like to thank my family and Eleanna who always supported me throughout my studies and encouraged me when work in the laboratory was hard and always reminded me of the light at the end of the tunnel.

Table of Contents

LIST OF FIGURES

Index

AADC	L-aromatic amino acid decarboxylase
ANR	Anterior neural ridge
AP	Anteroposterior
AR	Androgen receptor
AVE	Anterior visceral endoderm
b-HLH	Basic helix loop helix
BMP	Bone morphogenic protein
BSA	Bovine serum albumin
CA	Catecholamines
cDNA	Complementary DNA
ChIP	Chromatin immunoprecipitation
CNS	Central nervous system
CR (1 or 2)	Conserved region (1 or 2)
DA	Dopamine
DAT	Dopamine transporter
DBH	Dopamine β-hydroxylase
DNA	Deoxyribonucleic acid
DV	Dorsoventral
En1	Engrailed 1
En2	Engrailed 2
ES cells	Embryonic Stem cells
FDR	False discovery rate
Fgf8	Fibroblast growth factor 8
Foxa (1 or 2)	Forkhead box (a1 or a2)
Foxa2 CKO	Foxa2 conditional knockout mice
IsO	isthmic organizer
L-DOPA	L-dihydroxyphenylalanine
Lmx1 (a or b)	LIM-homeodomain transcription factors
mDA	Midbrain dopaminergic
MHB	Midbrain-hindbrain boundary
NGS	Next Generation Sequensing

PBS	Phosphate-buffered saline
PD	Parkinson's disease
PFA	Paraformaldehyde
RNA	Ribonucleic acid
SEM	Standard error mean
Seq	Sequencing
Shh	Sonic hedgehog
SNc	Substantia nigra
SNr	Substantia nigra
TGF-β	Transforming growth factor-beta
TSS	Transcription Start Site
VTA	Ventral tegmental area
Wt	Wild type
ZLI	Zona limitans intrathalamica

1. Introduction

The mesencephalon is one of the most interesting regions of the central nervous system (CNS), and it provides a good model to study the mechanisms of how neural tissues are patterned and subdivided to generate distinct structures. Different neuronal populations within the mesencephalon have differing essential functions. The midbrain dopaminergic (mDA) neurons are members of this population that play important roles in movement control and behavior. These neurons are generated in specific spatial locations along both the anterior-posterior and dorsal-ventral axes in response to signals emanating from signaling centers positioned along the neural tube. In order to appreciate the mechanisms involved in the generation of mDA neurons, it is important to understand the events which are critical for the correct specification and patterning of the mesencephalon from the primitive neural tube.

1.1 Early neural tube patterning lead to create functionally diverse compartments

Cells in the neural plate respond to multiple signals originating from primary signalling centres (organisers) and finally give rise to the central nervous system (CNS). The anterior visceral endoderm (AVE) plays an important role in anterior patterning and establishing the anterior limit of the developing embryo. Hensen's node is another organizer that produces tissue which neurolizes the ectoderm and is important for maintaining and extending the anterior pattern in the mouse (Beddington and Robertson, 1999; Stern, 2001; Wurst and Bally-Cuif, 2001). As a result of the signals from these organizers the neural plate roles up to form the neural tube and a series of vesicles develop in the anterior end of the neural tube indicating the position of the future prosencephalon or forebrain, mesencephalon or midbrain, and rhombencephalon or hindbrain (Wurst and Bally-Cuif, 2001).

The prosencephalon undergoes a further subdivision to yield the telencephalon, which will give rise to the cerebral hemispheres, and the diencephalons, which will contain the thalamus and hypothalamus. The rhombencephalon also undergoes a further subdivision, yielding the metencephalon, which gives rise to the cerebellum and the pons, and the myelencephalon, which gives rise to the medulla (Figure 1-1). However, the mesencephalon does not undergo any further subdivision (Gilbert, 2003).

After the closing of the neural tube and initial vesicular development of its anterior end, the three main domains in the brain premordium are subjected to further structural refinement by secondary signaling centres or secondary organizers. Secondary signaling

centers can be defined as focal transverse domains with morphogenetic activity across the anterior-posterior axis (Echevarría et al., 2003).

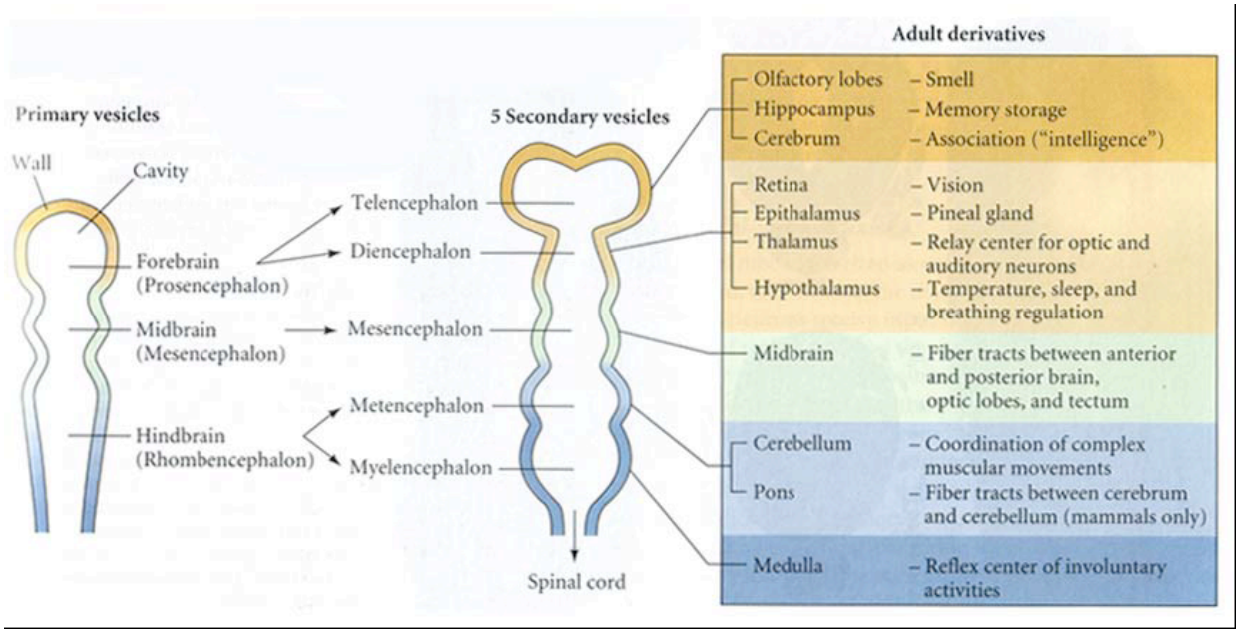

Figure 1-1: Compartmentalisation of the neural tube. The anterior region of the neural tube forms specialised vesicles along the anterior-posterior axis and regions of the adult brain are derived from these vesicles (Adapted from Gilbert, 2003).

Three regions have been identified as secondary signaling centers in the anterior neural tube; the anterior neural ridge (ANR), the zona limitans intrathalamica (ZLI) and the isthmic organizer (IsO) (Echevarría et al., 2003; Kiecker and Lumsden, 2005).

The ANR is a morphologically defined structure located at the junction between the most rostral part of the neural plate and non-neural ectoderm. It plays a crucial role in patterning the telencephalon (Echevarría et al., 2003). The ZLI is described as a compartment and source of local morphogenetic properties, which coincides with a surface constriction in the prospective thalamus, separating the dorsal from the ventral thalamus (Echevarría et al., 2003; Kiecker and Lumsden, 2004). The IsO, the best characterized organizer, is located at the boundary between the midbrain and anterior hindbrain (Bally-Cuif and Wassef, 1995). The IsO plays a critical role in inducing and polarizing midbrain and anterior hindbrain structures by emitting signals that have morphogenetic properties (Echevarría et al., 2003; Simeone, 2000; Wurst and Bally-Cuif, 2001). The function of the IsO will be discussed in detail below.

The main subdivisions of the CNS: the forebrain, midbrain, hindbrain and spinal cord, are established along the rostrocaudal axis of the neural tube. These events require an orchestration of signals emitted from multiple organizing centers within this signaling system. Another signaling system of similar complexity is the dorsoventral axis of the neural tube and it plays a critical role in establishing cell type diversity within these rostrocaudal subdivisions. Antagonistic interactions between ventralizing and dorsalizing signals ultimately lead to distinct regions of the neural tube known as the floor plate, the roof plate, the basal plate and the alar plate (Echelard Y, 1993; Jessell, 2000; Lee and

Jessell, 1999; Martí et al., 1995; Roelink et al., 1995). The floor plate will be discussed in detail later in this chapter.

1.2 The IsO and its role in midbrain development

The IsO has been identified in all studied vertebrates and is described as a local organizer of the embryonic brain. The IsO plays an important role in organizing the growth and the ordered rostrocaudal specification of the midbrain and hindbrain territories (Wurst and Bally-Cuif, 2001). The position of the IsO has been shown to depend on the expression of two homeodomain transcription factors *Otx2* and *Gbx2*.

Otx2 and *Gbx2* are expressed by the headfold stage in the anterior and posterior neuroectoderm, respectively (Ang and Rossant, 1994). Genetic analysis of mutant mice lacking Otx2 demonstrates the absence of the anterior most regions of the neural tube, corresponding to the midbrain and forebrain regions (Acampora et al., 1995; Ang et al., 1996). This is accompanied with the anterior expansion of Gbx2 expression and enlargement of the cerebellum. In contrast, mutant mice lacking Gbx2 protein results in the loss of the cerebellum at the expense of midbrain expansion. This is due to ectopic posterior expression of Otx2 (Liu and Joyner, 2001a; Martinez-Barbera et al., 2001). It has also been reported that *Otx* genes might cooperate and that a critical threshold of OTX proteins is required for regionalization and subsequent patterning of the developing brain. Also evidence has been provided that *Otx* gene dosage is required in controlling the boundary of the IsO (Acampora et al., 1997). Ectopic expression studies using either *Otx2* or *Gbx2* have produced similar results (Broccoli et al., 1999; Millet et al., 1999).

All these results clearly demonstrate that the IsO is positioned in the MHB between the expression domains of *Otx2* and *Gbx2*, and that the correct position of the IsO is critical for determining the size of the mesencephalon and metencephalon. Recently it has been demonstrated that the establishment and specification of the IsO at the MHB is not dependent on the actions of either *Otx2* or *Gbx2*, as genes such as Fgf8 and Wnt1 normally expressed in a restricted manner at the MHB are still observed in *Otx2/Gbx2* double mutants. However, they are essential for negatively regulating *Fgf8* and *Wnt1*, respectively, and thus subdividing the presumptive midhindbrain region into two different domains (Figure1-3) (Liu and Joyner, 2001a; Martinez-Barbera et al., 2001).

In recent years, studies have demonstrated the inducing capabilities of the IsO. Ectopically placing tissue from the MHB region into the host Forebrain can induce a new MHB region around the transplanted tissue (Liu and Joyner, 2001a; Nakamura H, 2005). Two classes of signaling molecules, Wnts and FGFs are expressed at the MHB. *Wnt1* was originally identified as an oncogene due to frequent insertions of the mouse mammary tumour virus which lead to the over-expression of its transcript (Nusse and Varmus, 1982), and is first expressed at the first somite stage and by the 6-8 somite stage is expressed throughout the presumptive midbrain (Echelard et al., 1994; Wilkinson DG). The expression of *Wnt1* in the midbrain gradually becomes restricted to the ventral and dorsal midlines and to a small semi-circular domain at the posterior limit of the *Otx2* domain (Zervas et al., 2004). *Fgf8* is first expressed during gastrulation and is eventually restricted to several signaling centers along the anterior-posterior axis (Crossley and Martin, 1995). The expression of *Fgf8* within the MHB region is restricted posteriorally

to the expression of *Wnt1*, and forms a semi-circular domain of expression around the MHB (Crossley and Martin, 1995; Meyers et al., 1998).

The MHB region is lost in *Wnt1* knockout (*Wnt1* -/-) embryos demonstrating the importance of this signaling molecule (McMahon AP, 1990; McMahon AP, 1992), but further studies have shown that *Wnt1* is only required for the proliferation and survival of these cells (Danielian and McMahon, 1996; McMahon AP, 1992). Furthermore, *Wnt1* does not illustrate the inducing properties of the IsO as demonstrated in gain of function studies (Danielian and McMahon, 1996).

Fgf8 was demonstrated to posses the inducing capabilities of the IsO. Fgf8-soaked beads can transform the anterior forebrain into a MHB region (Crossley et al., 1996; Liu et al., 1999; Martinez et al., 1999). The requirement for *Fgf8* during the development of the MHB was also demonstrated by using *Fgf8* conditional knockout mice, as classical knockout mice have gastrulation defects (Sun et al., 1999). The loss of *Fgf8* from the MHB results in the loss of the midbrain and anterior hindbrain (Chi et al., 2003). Furthermore, another role for FGF signaling from the IsO has been described in zebrafish. Fgf8 signals acting together with the *Engrailed* genes are important in the maintenance of the boundary between the midbrain and hindbrain (Scholpp S, 2003).

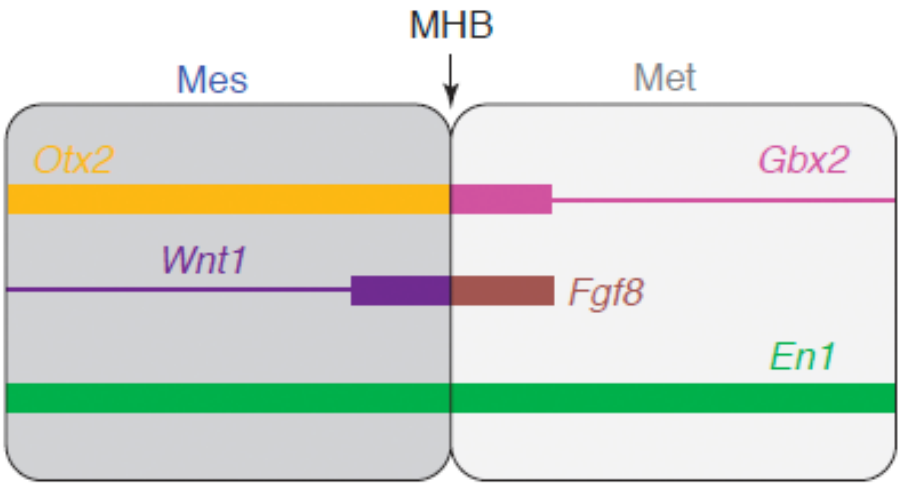

Figure 1-2:The molecular code defining the midbrain hindbrain boundary (MHB).

At E10.5the Otx2, Wnt1, Gbx2, Fgf8 and En1 domains of expression define a molecular code centered on the MHB. (Modified from Simeone,, 2000)

Signaling molecules from the IsO interact with signals from the floor plate to further refine, pattern and specify distinct neuronal populations along its neuraxis. For the purpose of this thesis, mechanisms for the specification of midbrain dopaminergic neurons will be discussed in following chapters.

.

1.3 The Floor plate

The specification of functionally diverse neuronal populations in the CNS depends on signaling molecules along the anterior-posterior and dorso-ventral axes. As discussed earlier in this chapter, signals coming from signaling centers are responsible for cell type specification along the dorso-ventral axis as it is for the anterior-posterior axis. The two signaling centers playing a central role in cell type specification along the dorso-ventral axis are the roof plate (dorsally) and the floor plate (ventrally). And the interaction of these dorsal and ventral signals are responsible for the specification of neurons along this axis (Jessell, 2000).

The floor plate is described as a small group of cells located at the ventral midline of the neural tube that influences strongly the development of the vertebrate nervous system (Placzek and Briscoe, 2005). The floor plate was originally identified by its morphology by W. His, and was described as a group of cells in the ventral midline with an ependimal structure and lack of any differentiated neurons (Kingsbury, 1930). The floor plate cells participate in governing the specification of glial and neuronal cell types through secreting a key signalling molecule Shh (Briscoe and Ericson, 1999; Kessaris et al., 2001; Martí et al., 1995; Patten and Placzek, 2000; Placzek and Briscoe, 2005).

Shh is first expressed in the midline mesoderm of the head at the late streak stages of gastrulation, and then extends to the notochord (Echelard et al., 1993). Shh expression initiates in the CNS at the ventral midline of the midbrain at 8-somite stage, and extends rostrally into the forebrain and caudally into the hindbrain and spinal cord. In the hindbrain and spinal cord, Shh expression is restricted to the FP, whereas it extends ventrolaterally in the midbrain (Echelard et al., 1993). Gain and loss of function data

have demonstrated the requirement of Shh to induce floor plate cells. It has been shown in studies where cells transfected with Shh expression vector and placed in close proximity with explants from naïve neural plate tissue are able to induce the differentiation of floor plate cells and motor neurons (Roelink et al., 1994). This has been supported by loss of function data where Shh -/- mice display a complete loss of floor plate structures (Chiang C. et al., 1996). It has also been demonstrated that Shh is the inductive signal derived from the FP that is responsible for the induction of midbrain dopaminergic (DA) and motor neurons (Hynes M. et al., 1995a).

The Forkhead transcription factor *Foxa2* has been shown to be one of the target genes of Shh signaling which plays a role as a major regulator of floor plate development (Sasaki and Hogan, 1994a; Sasaki et al., 1997; Sasaki et al.). Ectopic expression of *Foxa2* is sufficient to induce ectopic expression of Shh leading to the generation of ectopic floor plate structures (Sasaki and Hogan, 1994a). Moreover, Foxa2 loss of function results in loss of floor plate due to loss of Shh expression in the notochord (Ang and Rossant, 1994; Weinstein et al., 1994).

The floor plate has long been thought of as an organizer and involved in patterning nearby cells to their destined fates. The floor plate was not known to contribute to a specific neuronal population. Recently it was shown that in the midbrain this was not the case. Lineage tracing of mDA neurons using Shh-Cre driving the LacZ gene has shown that all the mDA neurons are generated from floor plate cells (Joksimovic et al., 2009). Moreover, cell sorting experiments coupled with immunostainig for DA specific markers using the membrane floor plate marker Corin has

further confirmed this finding (Ono et al., 2007). Thus in the ventral midbrain, the floor contributes to the mDA population in parallel to performing its patterning functions.

1.4 The midbrain DA neurons

1.4.1 Dopamine

Dopamine (DA) belongs to the family of catecholamines (CA), which include noradrenalin and adrenaline. It is regarded as one of the classical neurotransmitters of the central nervous system. Dopamine, noradrenalin and adrenalin are synthesized from the amino acid tyrosine, and the first and rate-limiting step of this biosynthesis is catalyzed by the enzyme tyrosine hydroxylase (TH). TH converts tyrosine into L-dihydroxyphenylalanine (L-DOPA) (Eells, 2003; Levitt et al., 1965; Nagatsu et al.). The enzyme L-aromatic amino acid decarboxykase (AADC or Ddc) catalyzes the decarboxylation of L-DOPA to form dopamine (Zhou and Palmiter, 1995). The enzymes dopamine β-hydroxylase (DBH) can further convert dopamine into noradrenalin by, and then to adrenalin by phenylethanolamine N-methyltransferase (Figure 1-3) (Goridis and Rohrer, 2002). DA neurons do not produce DBH; therefore, the CA synthesis terminates at DA.

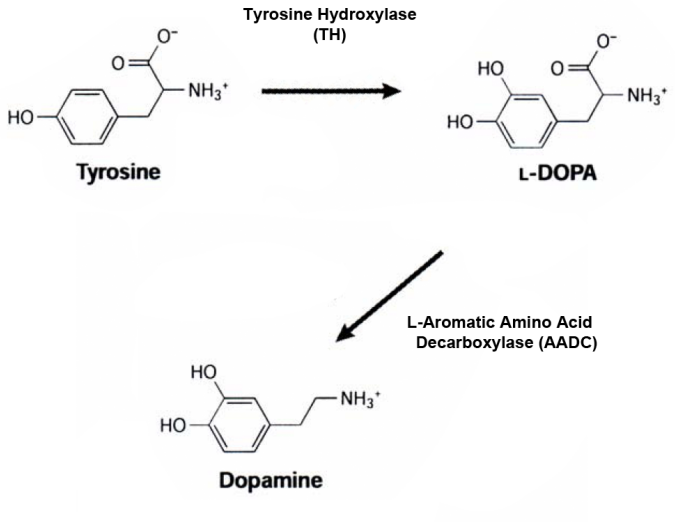

Figure 1-3: Biosynthesis of dopamine neurotransmitter.

Tyrosine Hydroxylase (TH) is the rate-limiting step of dopamine synthesis and is required to hydrolyse tyrosine and produce $_{L}$-DOPA. L-Aromatic Amino Acid Decaboxylase (AADC) then converts $_{L}$-DOPA into dopamine. (Diagram modified from Goridis and Rohrer, 2002)

1.4.2 The midbrain DA populations

The DA neurons are one of the first systems to be described in detail. This was due to the ease of their detection by a histofluorescence method known as formaldehyde-induced fluorescence (Falck et al., 1962; Goridis and Rohrer, 2002; Hokfelt et al., 1984; Zhou and Palmiter, 1995). Distinct subgroups of midbrain DA neurons can be identified according to cell body topology and axon connectivity with postsynaptic targets. Midbrain DA neurons are located in the substantia nigra (SN), ventral tegmentum (VTA) and retrorubral field (RRF), also known as subgroups A8-A10. It is interesting to note that the SN is divided into two sub groups: the pars compacta (SNc) and pars reticulata

(SNr). The SNc is composed of medium sized cells that are more darkly stained and closely spaced compared to the SNr. The SNc cells are mostly DA neurons whereas the SNr cells are mostly non-DA cells (Beckstead et al., 1979; Burbach et al., 2003; Goridis and Rohrer, 2002). In humans, approximately 75% of the midbrain DA neurons are located in the SN and project to the dorsal striatum forming the nigrostriatal pathways, which is involved in the control of voluntary motor movement (Figure 1-4) (Wallén and Perlmann, 2003; Zhou and Palmiter, 1995). DA neurons located in the VTA project to the nucleus acumbens, other limbic brain areas, and the cortex forming the mesolimbic/cortical pathways involved in the control of emotion and reward behaviors (Tzschentke, 2000; Tzschentke and Schmidt, 2000).

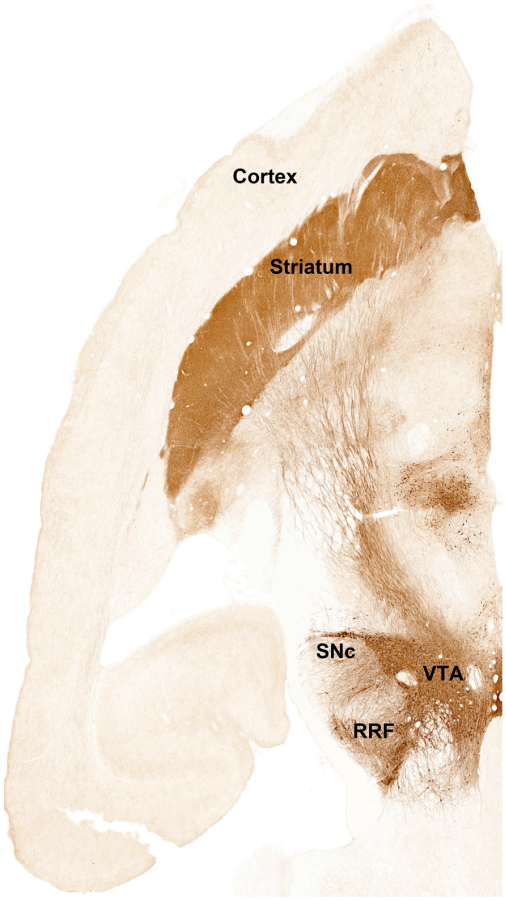

Figure 1-4:The Nigrostriatal Pathway.

A horizontal section of the adult rat brain stained with an antibody against tyrosine hydroxylase (TH). A dense bundle of fibres project rostro-laterally, beginning from the Substantia nigra compacta (SNc) towards the Striatum. VTA: Ventral tegmental area. RRF: Retrorubral field. (Kind contribution by Dr. Simon Stott).

1.4.3 Midbrain DA neurons and Parkinson's disease

In 1817, James Parkinson first described the clinical manifestations of Parkinson's disease (PD), of which the main symptoms are tremor, bradykinesia, and balance disturbances. Depression may also occur, but is less well defined. PD is a progressive

neurodegenerative disorder that affects 1-2% of the population over 65 years of age. At the onset of the disease, a large proportion (70–80%) of DA neurons in the SNc has already been lost, resulting in reduced DA synthesis and release from the striatal nerve terminals (Hirsch et al., 1988; Jiang et al., 2005; Simon et al., 2003). DA neuron cell death is also associated with the presence of cytoplasmic protein aggregates called Lewi bodies (Goldman et al., 1983). It remains unclear what causes cell death of the SNc DA neurons. However, environmental toxins, ageing, and genetic susceptibility are key elements to consider for this disease (Eells, 2003; Hirsch, 1998; Jenner; 1998; Schapira, 1997).

The importance of genetic factors involved in Parkinson's disease has been the centre of debate for decades, and an understanding of these genetic factors could hold the key to possible therapeutic treatments. Investigations with siblings from patients of Parkinson's disease demonstrate that there is a higher possibility of developing Parkinsonian symptoms compared to the siblings of non-affected parents (Pankratz and Foroud, 2004), and several genes have now been identified which are considered to have the potential to increase the incidence of Parkinson's disease, such as *α-synuclein*, *parkin* and *DJ-1*.

1.4.4 The development of midbrain DA neurons (induction and molecular specification)

As discussed earlier, the vertebrate nervous system is composed of multiple cell types that are organized at specific stereotypic locations along the anterior-posterior and dorso-ventral axis. It has been shown that signaling centers along these axes such as the roof plate, floor plate and the IsO play crucial roles in instructing cell fates that will characterize the midbrain and hindbrain regions (Ye et al., 1998). A number of secreted

factors released from these signaling centers have been shown to modify cell fates along their axis of distribution, and this is in agreement with the notion that extracellular molecules establish information grids to instruct cell fate changes (Crossley et al., 1996; Kiecker and Lumsden; Ye et al., 1998). Such signals are Shh from the floor plate, BMP from the roof plate, Fgf8 and Wnt1 from the IsO region. These secreted molecules will be discussed in detail below.

1.4.4.1 Induction of midbrain DA neurons by signaling molecules

1.4.4.1.1 Shh

Shh expression initiates in the CNS at the ventral midline of the midbrain at 8-somite stage, and extends rostrally into the forebrain and caudally into the hindbrain and spinal cord. In the hindbrain and spinal cord, Shh expression is restricted to the FP, whereas it extends ventrolaterally in the midbrain (Echelard et al., 1993). In the developing midbrain, DA neurons were first suggested to develop in close proximity to the FP, which is also sufficient for the induction of DA neurons in midbrain explant cultures and in the dorsal midbrain with an ectopic FP (Hynes M. et al., 1995b). Shh is subsequently demonstrated to be the inductive signal derived from the FP that is responsible for the induction of DA neurons (Hynes M. et al., 1995a).

1.4.4.1.2 Fgf8

Fgf8 expression is detected in the prospective MHB between E8.0 and E8.5, and become restricted to the isthmic constriction at around E9.0 to E9.5 (Crossley and Martin,

1995). *Fgf8* has been shown to mimic the inducing capabilities of the IsO by transforming the anterior forebrain when an Fgf8 source is placed close to it into a MHB region (Crossley et al., 1996; Liu et al., 1999; Martinez et al., 1999). Fgf8 signaling has been shown to directly regulate Wnt1 and En1/2 expression, which are also implicated in the development of midbrain DA neurons. This made it difficult to determine if Fgf8 directly controls DA development (Crossley et al., 1996; Shamim et al., 1999). A recent study of mutant mice carrying different combinations of Fgfr1, Fgfr2, and Fgfr3 mutations demonstrate redundant contributions of these receptors in receiving signals from the IsO and regulating the development of midbrain DA neurons without affecting the expression of Wnt1, Shh signaling and neurogenic gene expression in the ventral midbrain (Saarimäki-Vire et al., 2007). This suggests a more direct role of Fgf signaling in midbrain DA neuron development.

1.4.4.1.3 Wnt1

Wnt1 has been shown to regulate midbrain development by maintaining En1 expression (Danielian and McMahon, 1996; McMahon AP, 1992; Wurst et al., 1994). In addition to the expression anterior to the isthmus, Wnt1 is also detected in two stripes adjacent to the floor plate of the midbrain and overlaps with the region where mDA progenitors first appear (Prakash et al., 2006). The function of Wnt1 in mDA neuron development has been shown by both *in vitro* and *in vivo* studies. Treatment of rat ventral midbrain cultures with Wnt1 conditioned media show that Wnt1 is a key regulator for the proliferation of mDA progenitors by exhibiting a dose depended increase in TH+ neurons. This effect is not specific to mDA progenitors but rather an effect on all ventral

midbrain progenitors (Castelo-Branco et al., 2003). The mechanism for this effect has been shown to be through the upregulation of cyclins D1 and D3, which promote cell cycle progression, and down-regulation of the expression of cell cycle inhibitors p27 and p57 (Prakash et al., 2006). Other than the role of Wnt1 in mDA precursor proliferation *in vitro*, it is also required for the proper differentiation of mDA neurons. In *Wnt1-/-* mutant embryos, only very few DA neurons were generated that expressed the mature mDA markers Nurr1 and TH, but these cells fail to express Pitx3 (Prakash et al., 2006)

1.4.4.2 Molecular specification

Midbrain DA neurons are known to have anatomical and functional differences. Despite these differences they share the dopamine biosynthesis and transmission machinery. The coordinated expressions of a cascade of transcription factors play key roles in these events (Burbach et al., 2003). A few of these transcription factors will be discussed here.

1.4.4.2.1 The LIM-homeodomain transcription factors Lmx1a and Lmx1b

Lmx1a and Lmx1b are LIM-homeodomain transcription factors. Lmx1a and Lmx1b are both expressed in the ventral midbrain and caudal forebrain where midbrain DA neurons are generated (Andersson et al., 2006b). *Lmx1a* transcript and protein are first detected in the ventral midbrain at E8.5 and E9 respectively (Andersson et al., 2006b; Millen et al., 2004). Lmx1a is specifically expressed in midbrain DA progenitors and maintained in midbrain DA postmitotic neurons (Andersson et al., 2006b). Lmx1b is expressed broadly around the presumptive MHB at E8.5, and becomes restricted to the ventral midbrain and caudal forebrain at E9.5 (Guo et al., 2007).

Lmx1b plays an early essential role in the development of the midbrain by

regulating the expression of Fgf8, Wnt1, En1 and Pax2 that are required for the midbrain and hindbrain development (Guo et al., 2007; Matsunaga et al., 2002). In the mDA system, Lmx1b is proposed to be required for the differentiation and maintenance of mDA neurons. The Lmx1b -/- mutant mice developed Th+ neurons that do not express the mature midbrain DA neuron marker Pitx3. These Th+ neurons are eventually lost during embryonic maturation. These results suggested the presence of two molecular cascades during the specification of midbrain DA neurons, one essential for the neurotransmitter phenotype and another essential for other midbrain DA neuron differentiation aspects (Smidt et al., 2000).

Lmx1a is both required and sufficient to induce DA neurons in the ventral midbrain (Andersson et al., 2006a). Mis-expression of Lmx1a in chick midbrain at HH stage 10 extensively induces ectopic DA neurons in the ventral midbrain region, whereas siRNA knockdown of Lmx1a reduces postmitotic DA neurons. Lmx1a is both sufficient and required for the expression of Msx1 in midbrain DA progenitors. Lmx1a was shown to be a much more potent inducer of Th+ neurons than Lmx1b when transfected into mouse embryonic stem (mES) cells treated by Shh and Fgf8. Furthermore a study using Lmx1a mouse mutant dreher has shown a significant reduction in midbrain DA neurons. These results illustrate the requirement of Lmx1a in midbrain DA neuron differentiation (Ono et al., 2007).

1.4.4.2.2 The homeodomain transcription factors En1 & En2

Engrailed 1 (En1) and Engrailed 2 (En2) are homeobox transcription factors with a high sequence homology (Joyner et al., 1985; Joyner and Martin, 1987). En1 and *En2* start to be expressed during the early hours of somite formation in the presumptive MHB

region (Davis and Joyner, 1988). En genes play an early role in maintaining the expression of Fgf8 in the MHB (Liu and Joyner, 2001b).

In the mDA system, En1/2 are expressed in the mDA neurons during embryonic stages and the SN, and VTA at postnatal day 0 (P0). En1 is highly expressed by mostly all midbrain DA neurons in the SN and VTA, whereas En2 is expressed by a subset of them (Simon et al., 2001). In the development of mDA neurons, En1/2 substantially compensate for the loss of one another such that single mutants of either *En1* or *En2* display a relatively normal appearance of SN and VTA. The double mutant analysis shows complete loss of SN and VTA DA neurons suggesting their strong requirement for midbrain DA neuron development. Moreover, the expression of α-synuclein, which has been genetically linked to PD in humans, is diminished at early stages of development in En 1 mutants and lost in En1/2 double mutants before the loss of the Th+ neurons (Simon et al., 2001).

1.4.4.2.3 Msx1

Msx1 (Muscle segment homeobox gene) is first expressed in mDA progenitors at E9.5, and remains restricted to a medial midbrain DA progenitors domain until E12.5 (Andersson et al., 2006b). Although electroporation of Lmx1a into the chick ventral midbrain can induce Msx1 expression and DA fate, overexpression of Msx1 is insufficient to induce ectopic DA neurons in the midbrain (Andersson et al., 2006b). Similarly, transfection of Msx1 driven by the Nestin enhancer is insufficient to induce DA fate in mouse embryonic stem cells. Instead of mediating the induction of midbrain DA fate by Lmx1a, Msx1 functions to suppress alternative cell fate by repressing Nkx6.1, and to promote pan-neuronal differentiation. Therefore, it is suggested that Msx1 controls

the timing of DA cell neurogenesis. However, in *Msx1* knockout embryos, there is only 40% reduction in Ngn2+ progenitor cells and Nurr1+ DA neurons, suggesting that other factors, possibly *Msx2*, may compensate for the loss of *Msx1* in DA neuron generation (Andersson et al., 2006b).

1.4.4.2.4 Neurogenin 2 (Neurog2)

The proneural gene Neurog2 is a BHLH transcription factor and is important for neuronal differentiation and neuronal subtype specification in various regions of the nervous system (Bertrand et al., 2002; Brunet and Ghysen, 1999; Guillemot, 1999). Neurog2 is expressed in midbrain DA progenitors but also in a few post mitotic Nurr1+ cells in the intermediate zone separating the progenitors from the Th+ mature neurons (Kele et al., 2006).

Mutational studies in mouse show that Neurog2 is the major proneural gene involved in the development of midbrain DA neurons. The Neurog2 null mice have a substantial reduction of TH+ neurons at early stages of development, and only a few TH+ cells can be detected in the lateral edges of the DA domain. This phenotype gradually recovers later in development and is probably due to the compensation of other proneural genes such as Mash1 (Andersson et al., 2006b; Kele et al., 2006). Substituting *Mash1* allele into the *Ngn2* locus can only partially accelerate the development of midbrain DA neurons without providing a full recovery. This illustrates the unique requirement of Neurog2 for neurogenesis of the ventral midbrain DA neurons (Kele et al., 2006).

1.4.4.2.5 Nurr1

Nurr1 (Nr4a2) is a member of the nuclear hormone receptor family of ligand inducible transcription factors. It is known as an “orphan nuclear receptor” since its

ligand has not yet been identified. It is widely expressed in the CNS as well as in midbrain DA neurons at the time when they become postmitotic (Wallén et al., 1999). Mutant studies of the Nurr1 -/- mice show that these cells lose the expression of TH. They do maintain the expression of En1, AHD2, and Pitx3 during early development, but are lost at later stages. This illustrates that Nurr1 is not required for the initial specification step of midbrain DA neurons but is crucial for the maturation, migration and guidance of axons to their targets in the striatum. This is achieved by regulating the expression of mature mDA markers involved in these processes (Hermanson et al., 2003; Jacobs et al., 2009; Wallén et al., 1999). The identification of Nurr1 mutations in patients with familial PD has emphasized its clinical significance (Le et al., 2003).

1.4.4.2.6 Pitx3

The paired-like homeodomain transcription factor Pitx3 is expressed in the ventral midbrain from E11.5 onwards and its expression correlates with the appearance of midbrain DA neurons (Holland and Takahashi, 2005; Smidt et al., 1997). A knock-in GFP reporter of Pitx3 shows overlapping expression of GFP and TH in the vast majority of the mDA neurons in the SN and VTA (Zhao et al., 2004). On the contrary, a double immunohistochemistry study demonstrates the heterogeneity of Pitx3 expression in the midbrain DA populations (van den Munckhof et al., 2003). A study of naturally occurring Pitx3 mutant mice known as the aphakia mice suggests that Pitx3 functions in protecting DA neurons from cell death. Since the subpopulation expressing Pitx3 was more susceptible to cell death in these mutants (van den Munckhof et al., 2003). These results demonstrate the requirement of Pitx3 for the development and survival of at least a subpopulation of midbrain DA neurons.

1.4.4.2.7 The Forkhead box transcription factors Foxa1 and Foxa2

In the CNS, Foxa1 and Foxa2 (previously know as HNF-3α and HNF-3β respectively) are expressed in the ventral midline of the neural tube, and it is spread more dorsally in the midbrain than in the posterior neural tube (Lai et al., 1990; Lai et al., 1991; Sasaki and Hogan, 1993). The requirement of Foxa factors for the development of the ventral midbrain and more specifically DA neuron development will be discussed in following chapters.

1.4.5 How to make a midbrain DA neuron *in vitro*

Embryonic stem (ES) cells are clonal cell lines derived from the inner cell mass of the developing blastocyst that can proliferate extensively *in vitro* and are capable of adopting all the cell fates in a developing embryo (Evans et al., 1981). So far there have been two protocols developed specifically to differentiate ES cells towards a DA fate, one involves cell aggregation and the application of Shh and Fgf8 (Lee et al., 2000) and the other is via co-culture of ES cells with PA6 stromal cells (Kawasaki et al., 2000). The nature of stromal cell-derived inducing activity (SDIA) is unclear as PA6 neural inducing activity remains when the cells are fixed (and unable to secrete soluble factors), or when the PA6 cells are separated from the ES cells. It is suggested that SDIA may be a secreted factor that is restrained to the cell surface, as treatment with heparin removes the neural inducing activity (Kawasaki et al., 2000).

A serum-free adherent monolayer culture method has been developed in which ES cells can develop into neural precursors, and subsequently DA neurons can be produced upon addition of Fgf8 and Shh (Ying et al., 2003). Recently this method was used to differentiate ES cells that were first transfected with an expression vector containing the Lmx1a cDNA driven by the Nestin enhancer. The Nestin enhancer is only active when the ES cells acquire a neuronal progenitor fate. Since Lmx1a is a key player in the specification of the midbrain DA neuronal fate a large percentage of the transfected ES cells differentiated to midbrain DA neurons when compared to cells transfected with a control GFP construct driven by the Nestin enhancer (Figure 1-5) (Andersson et al., 2006b). Midbrain DA neurons can now be efficiently produced *in vitro* to be used for further studies, especially for experiments that are difficult to execute using *in vivo* tissue.

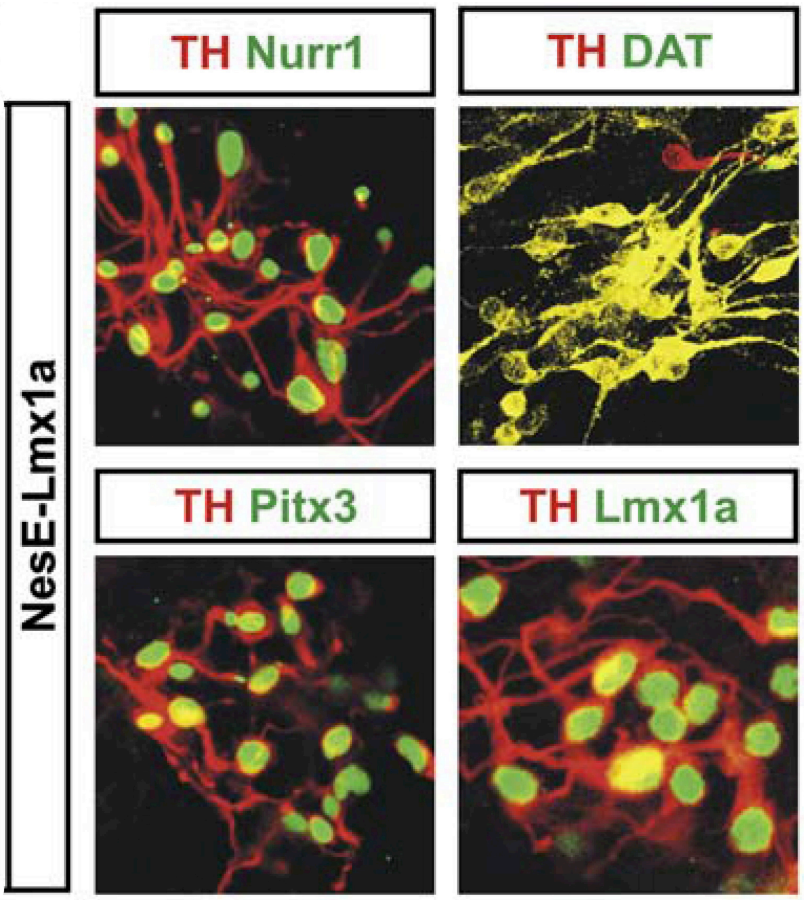

Figure 1-5: TH expressing neurons derived from ES cells.

NesE-Lmx1a genetically modified ES cells differentiated in serum free media upon the addition of Shh and Fgf8. The TH+ neurons from this assay also express Nurr1, DAT, Pitx3, and Lmx1a. (Modified From Anderson, 2006)

1.5 The Forkhead transcription factors

1.5.1 History of the Forkhead genes

In the 1990s, chromosomal walking was used to clone the Forkhead gene in Drosophila. The product of this gene did not posses a known, at the time, protein motif. Nor was its sequence similar at the time to any other known protein. Mutational analysis in Drosophila illustrated the importance of Forkhead for the development of terminal structures of the embryo that give rise to the anterior and posterior gut. The homeotic transformation of the gut structures into head structures created a two pronged mutant embryo, hence the name Forkhead (Weigel et al., 1989).

Mammals also express Forkhead proteins and they were originally identified as proteins enriched in the rat liver and were given the name Hepatocyte nuclear factor 3 (HNF-3). The first gene identified was HNF-3α (Lai et al., 1990). Following HNF-3α two other members of this transcription factor family were identified, HNF-3β, and HNF-3γ (Liu et al., 1991). The DNA binding domain of the HNF-3 proteins is composed of ~110 amino acids and presents a high degree of conservation between the three members of this family (Figure 1-6) (Weigel and Jäckle, 1990).

The solution of HNF-3γ three dimensional structure revealed a core of 3 α-helices and β-Sheets flanked by two large loops or "wings" and factors possessing this DNA binding domain were referred to as winged-helix transcription factors (Clark et al., 1993).

Now over 100 new members of this family have been identified and all the members of this family are referred to as Forkhead box transcription factors (Fox). 15

subclasses have been created depending on the similarities between each protein. The HNF-3 proteins have been allocated to subclass A with HNF-3α now called Foxa1, HNF-3β is Foxa2, and HNF-3γ is Foxa3.

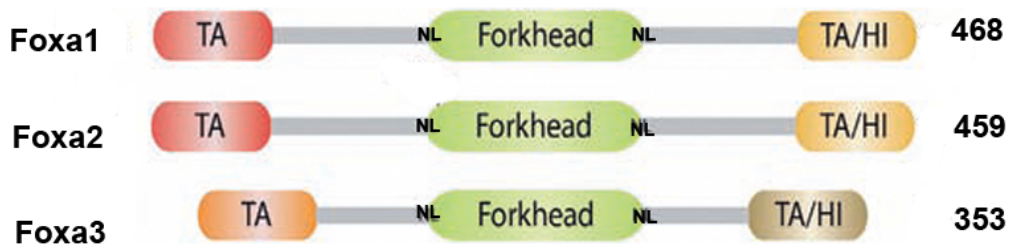

Figure 1-6: Schematic representation of functional domains present in Foxa1–3.

Amino acid numbering is for the mouse proteins. All three family members share 95% identity within the forkhead domain, while outside this domain Foxa1 and Foxa2 are 39% identical and 51% similar. Outside of the forkhead domain, Foxa3 is only weakly similar to Foxa1 and Foxa2, with the greatest homology in the N-terminal and C-terminal transactivation domains. The C-terminal region has also been shown to interact with the core histones H3 and H4 (Cirillo et al., 2002). TA, transactivation domain; HI, histone interaction domain; NL, nuclear localization. (Modified from Friedmana and Kaestner, 2006)

1.5.2 Control of Foxa2 expression within the floor plate

Foxa2 is expressed in the notochord and in the ventral midline of the neural tube at embryonic days 8.5.(Ang and Rossant, 1994; Sasaki and Hogan, 1994a). The initial expression of Foxa2 within the ventral midline of the neural tube occurs within the presumptive mesencephalon. Foxa2 expression spreads more laterally in the midbrain when compared to the posterior neural tube (Ang and Rossant, 1994; Sasaki and Hogan, 1994b). Foxa2 has been shown to be able to induce Floor plate, one of the main signaling centres involved in midbrain DA neuron development. The analysis was done by expresing Foxa2 under the control of the En1 prormoter. Floor plate markers such as Foxa1, and BMP1 were detected in the dorsal domain where Foxa2 is expressed suggesting that a Floor plate structure was generated ectopicaly (Sasaki and Hogan, 1994b). Shh, an important morphogen for the correct specification of midbrain DA neurons, has been suggested to be induced by Foxa2 within the notochord and Floor plate(Echelard et al., 1993; Hynes et al., 1995). It was later determined that due to Shh signaling Foxa2 is induced by Gli1, a downstream target of Shh. This way Foxa2 and Shh expression is induced and maintained within the floor plate (Figure 1-7)(Hynes et al., 1997; Sasaki et al., 1997).

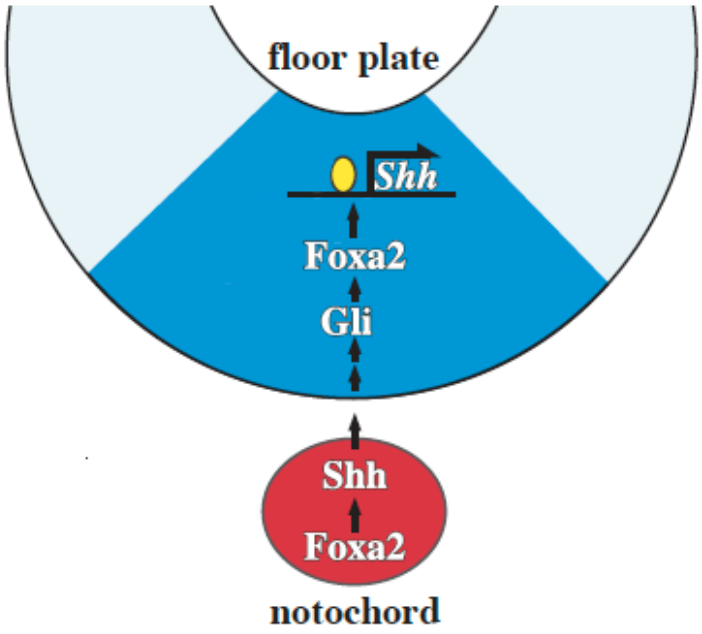

Figure 1-7: Schematic of the notochord and floor plate showing the transcriptional cascade resulting in Shh expression.

In the notochord, Foxa2 activates Shh, which then signals to the overlying neural plate. In response to Shh signaling, Gli2 activates Foxa2 expression in the neural plate. Foxa2, in turn binds the Shh regulatory elements to stimulate Shh transcription in the floor plate. (Adapted from Jeong, et al 2003)

1.5.3 Role for Foxa2 in midbrain DA neuron development

Recently it was shown that Foxa1 and Foxa2 are expressed in mDA progenitors and mature neurons and their expression is maintained up to adulthood (Figure 1-8). This suggests that Foxa1 and Foxa2 may be required for the development and maintenace of mDA neurons (Ferri et al., 2007; Kittappa et al., 2007). Cre recombinase driven by the Nestin promoter of Foxa2 in the mutant background of Foxa1 null mice deletes all Foxa proteins from the ventral midbrain region from E10.5 onwards. It is observed that mDA progenitors develop normaly and the region is properly specified since progenitor markers Lmx1a and Lmx1b can be detected in the progenitor domain at E10.5. In these mutants mDA neurons fail to mature properly since mature markers such as Th, Nurr1, and AADC are not detected. It is suggested that this is due to a block in neurogenesis since Neurog2 is misregulated in these mutants (Ferri et al., 2007). In a recent study where Cre recombinase was driven by the En1 promoter it was shown that Foxa factors are required for the expression of Lmx1a, the key specifier of midbrain DA neurons. This study also illustrated the requirement of Foxa factors for the correct specification of the mDA region by inhibiting the expression of the homeodomain transcription factor Nkx2.2(Lin et al., 2009). Chromatin Immunoprecipitation analysis suggests that Foxa2 regulation of TH and Nkx2.2 gene expression is direct (Lin et al., 2009). More recently Foxa2 has been shown to synergise with other factors through a feed forward loop for the induction of the mDA phenotype (Ang, 2006 2010, Lee, 2010). It has been suggested that Lmx1a can only perform its downstream functions within a Foxa2 positive domain suggesting their cooporations for the proper differentiation of mDA neurons (Nakatani et al., 2010). Furthermore, Chromatin immunoprecipitation analysis of the TH promoter

demonstrates the requirement of Nurr1 for the efficient recruitment of Foxa2 to its binding site (Lee et al., 2010).

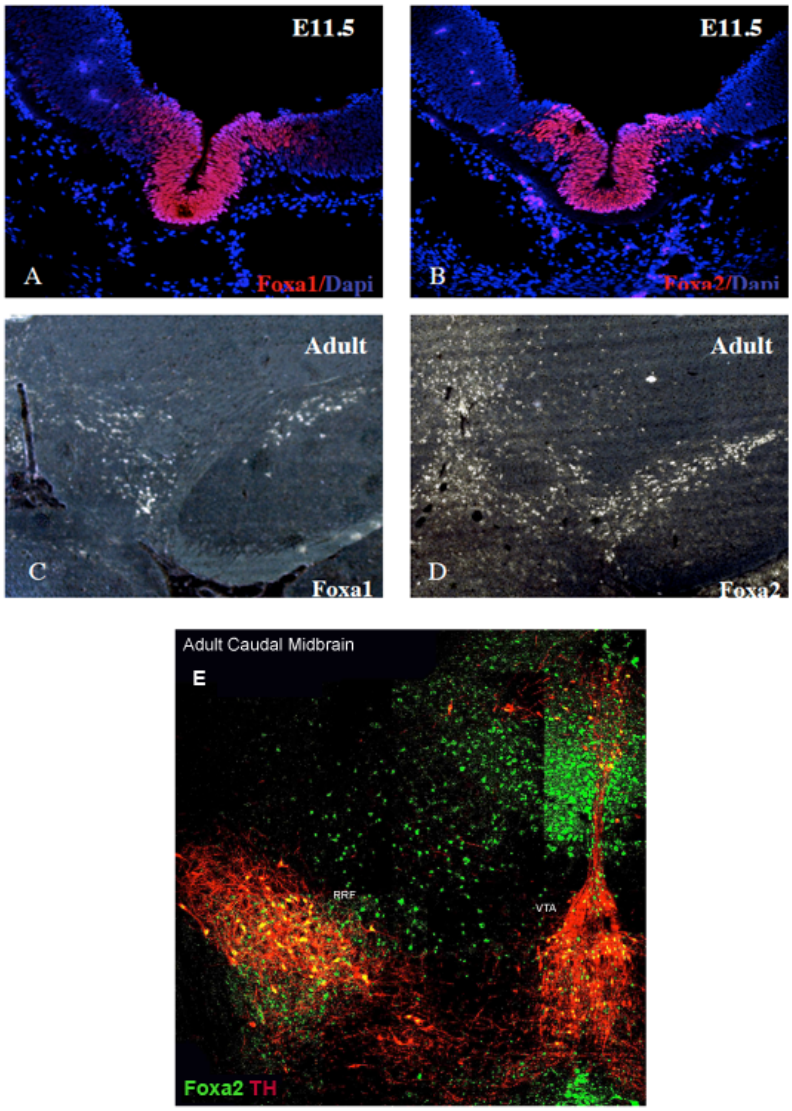

Figure 1-8:Foxa2 expression during mouse ventral midbrain development.

Coronal sections through E11.5 and adult mouse midbrain show (A-B) Expression of Foxa1 and Foxa2 (Red) is restricted to the ventral midbrain region were DA neurons are born at E11.5. (C-D) Foxa1 and Foxa2 expression persists through adulthood as shown by ISH (E) Immunostaining of Foxa2 (Green) and TH (Red) indicates a high degree of overlap. (Figure 'E' is a Kind contribution by Dr. Simon Stott).

Moreover, reduced levels of Foxa2 protein in the adult mouse mDA neurons leads to progressive loss of these neurons that is accompanied with motor behavioural defficit (Kittappa et al., 2007). These mutant mice provide a new model of Parkinson's disease that exhibits both the late onset and patholgical characteristics. These studies show the importance of Foxa1 and Foxa2 for the generation and maitenance of mDA neurons. Further studies are required to clarify the mechanisms by which Foxa1 and Foxa2 function to control the proper differentiation of mDA neurons.

1.5.4 Foxa role in regulation of gene expression

1.5.4.1 Nucleosome positioning and Chromatin opening

The nucleosome (the basic unit of chromatin) consists of DNA wrapped nearly twice around an octamer of four core histone proteins. This structure is dynamic and open to transcriptional regulation (Felsenfeld, 1992). It is generally accepted that transcription is regulated by transcription factors, which modulate the recruitment of the basal transcriptional machinery to a nearby promoter (Ptashne and Gann, 1997). Nucleosomes positioned on promoters ensure that transcription will not occur spontaneously at the wrong time. This in turn requires transcriptional regulators to overcome this chromatin barrier and access their sites in order to affect transcription (Lomvardas and Thanos, 2002). In the mouse liver, the N1, N2, and N3 nucleosomes are positioned over the serum albumin enhancer when active. The transcriptional machinery is bound on the nucleosomal DNA and not the linker DNA. Foxa binding sites have been identified in the N1 nucleosomal particle and have been shown to be required for the activity of this enhancer (Liu et al., 1991; Zaret, 1995). In 1993 Foxa transcription factors have been

described to have a structure similar to linker histones, which have the capability to bind and compact chromatin. It was suggested that Foxa factors may possess similar nucleosomal binding capabilities (Clark et al., 1993). It was later revealed that Foxa proteins have the capability to position nucleosomes and this way organize the chromatin to a moor loose structure and allow further access to other transcription factors (Cirillo et al., 2002; Shim et al., 1998).

1.5.4.2 Foxa function revealed by genome wide analysis of its recruitment to chromatin

1.5.4.2.1 Chromatin immuno-precipitation

Transcriptional regulation is a complex process that can be understood with the help of genome-wide mapping of protein-DNA interactions. A detailed map of binding sites for transcription factors and the core transcriptional machinery, which regulate various biological processes, can now be obtained and used to understand the regulatory networks involved in these processes (Park, 2009). Chromatin immuno-precipitation (ChIP) is the main tool used to investigate these mechanisms (Figure 1-9) (Solomon et al., 1988). In ChIP antibodies are used to select and enrich for a specific proteins that are bound to genomic DNA fragments. These DNA fragments can then be purified and used for down stream analysis. Quantitative PCR is the method used to obtain an accurate estimation of enrichment for predicted bound genomic regions, whereas the introduction of microarrays allowed the fragments from ChIP to be hybridized to a microarray chip (ChIP-chip). Therefore allowing the genome wide identification of DNA-protein interactions (Blat and Kleckner, 1999; Ren et al., 2000).

Recent advances in next generation sequencing (NGS) are now enabling the sequencing of hundreds of millions of short DNA fragments in a single run (Shendure and Ji, 2008). Chromatin immuno-precipitation followed by sequencing was one of the first applications of NGS (Barski et al., 2007; Robertson et al., 2007). Here the DNA fragments are sequenced directly instead of hybridizing them on an array. The higher resolution and greater coverage are just a few examples where ChIP-seq excels over ChIP-chip, thus providing substantially improved data. Te main disadvantage of ChIP-seq is the cost and availability but these situations are being improved as well and we can expect ChIP-seq to become the method of choice in the near future for all ChIP experiments (Park, 2009).

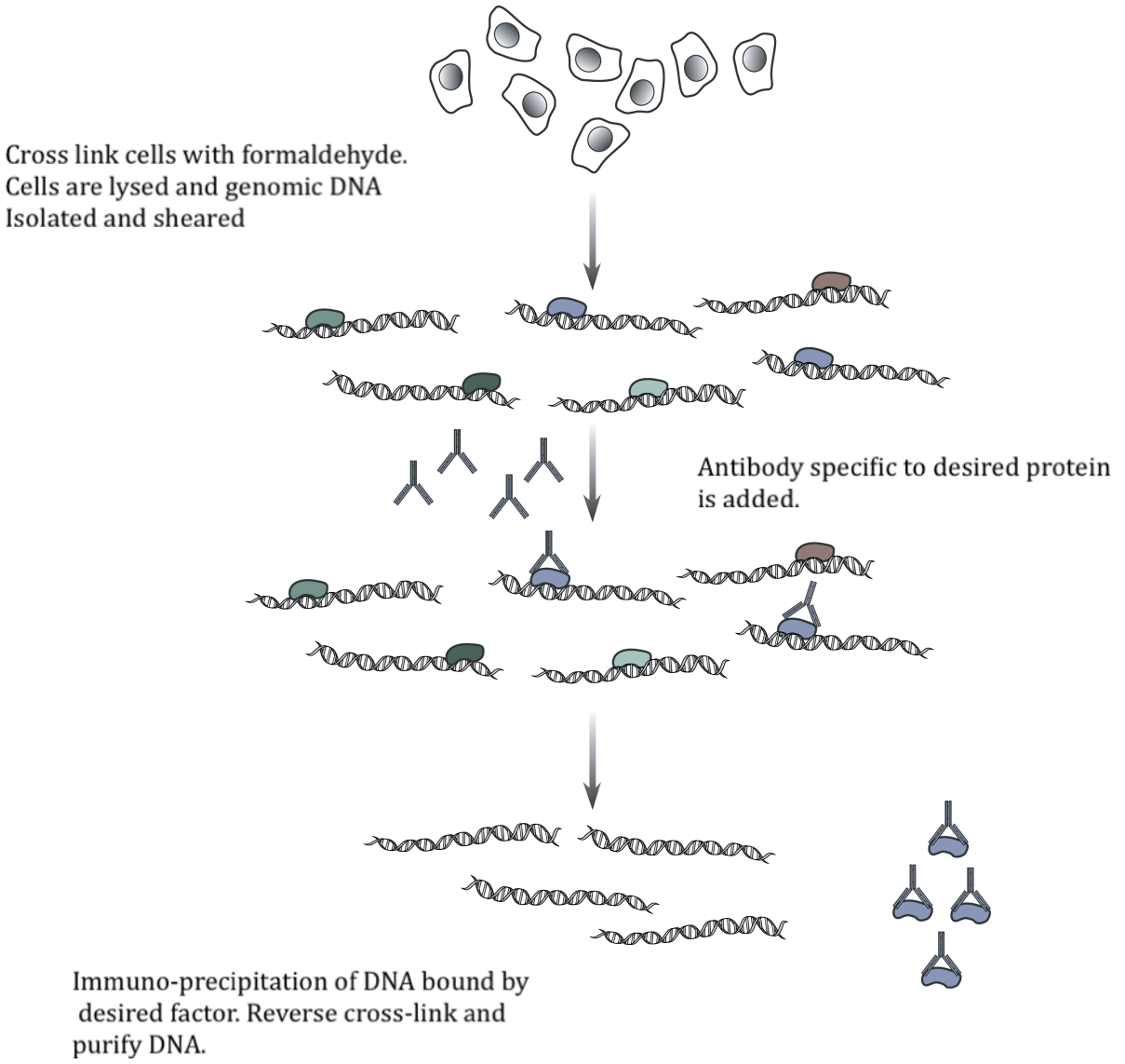

Figure 1-9: An overview of the chromatin immuno-precipitation (ChIP) procedure.

Cells are initially cross-linked by 1% Formaldehyde agent that links DNA-interacting proteins to the DNA. The genomic DNA is then isolated and sheared by sonication, into a suitable fragment size distribution (100–300 bp used for ChIP- Seq). An antibody that specifically recognizes the protein of interest is then added and immuno-precipitation used to isolate appropriate protein–DNA complexes. The cross-links are then reversed and the DNA fragments purified (Modified from Hoffman and Jones, 2009)

1.5.4.2.2 Chromosome wide analysis of Foxa1 targets in breast and prostate cancer models

Foxa1 is commonly found highly expressed in tumors arising from prostate and estrogen receptor positive breast tumors (Lacroix and Leclercq, 2004). In a recent study curried out to identify Estrogen-regulated gene targets on a chromosome wide level identified Foxa proteins as cofactors required for the Estrogen mediated activity. Two families of nuclear receptors mediate the Estrogen regulation of gene expression, ERα, and ERβ. Chromatin immuno-precipitation of ER coupled with tiled arrays of Chromosomes 21-22 of breast cancer cells identified ER gene targets. Chromatin immuno-precipitation coupled with qPCR analysis of Foxa1 binding to the ER recruited regions identified ~50% co-recruitment. Foxa1 was also shown to be required for the recruitment of ER to its targets (Carroll et al., 2005).

Androgens are male hormones that play important roles in prostate development and development of other male sex organs and their function is mediated through nuclear receptors known as androgen receptors (AR). Foxa1 was shown to interact with AR in prostate cancer cells (Gao et al., 2003). In a later study where gene targets were identified for ER in breast cancer cells and for AR in prostate cancer cells, the authors show that Foxa1 differential activity in these breast and prostate cells relies on its differential recruitment to its target sites and its alternative collaboration with the lineage specific factors ER and AR at tissue specific enhancers. Foxa1 recruitment was also shown to correlate with histone modifications identified in transcriptionally active regions in these cancer cells and is required for their activity in transcription initiation. Conversely, Foxa1 is not required for their maintenance as shown by siRNA silencing experiments (Lupien

et al., 2008). This data suggests an important role for Foxa proteins in chromatin remodeling and transcription initiation.

1.5.4.2.3 Foxa2 function revealed by ChIP-Seq analysis

Foxa2 has been shown to be an initiating factor in the earliest stages of liver development in the mouse embryo. Foxa2 was also shown to be involved in the later functions of the adult liver, such as bile acid and glucose homeostasis (Ang and Rossant; Rausa et al., 2000; Wolfrum et al., 2003). Foxa2 directly regulates genes involved in glucose and lipid metabolism such as glucose-6-phosphatase and tyrosine amino transferase (Friedman and Kaestner, 2006; Wolfrum et al., 2003). In 2008, the first study for the global identification of Foxa2 binding targets was performed (Wederell et al., 2008). The authors used adult mouse liver cells for the ChIP-seq experiment. This study presented many new properties of Foxa2 genomic recruitment such the distribution of the binding events throughout the genome and the correlation of genes associated with the peaks and their expression in the adult liver. Interestingly, 48% of the genes expressed in the liver are also associated with a Foxa2 bound region. Moreover, they show that Foxa2 binding events mostly occur within 10 Kb upstream of the transcription start site (TSS) or within the first intronic region, suggesting close relation of Foxa2 binding close to promoters. Also, a few insights have been described through *de novo* motif search performed on the data set for possible co-factors (Wederell et al., 2008).

A more recent ChIP-seq study took a further step in analyzing the transcription factor characteristics of Foxa2 by assessing its interrelationship with the other members of this transcription factor family (Foxa1, and Foxa3). Instead of using *in vivo* obtained tissue as in the previous study they performed ChIP-seq on the Hepatocyte carcinoma cell

line HepG2. They found that Foxa1 and Foxa3 have dissimilar distribution of their binding events. Furthermore, Over 50% Foxa1 peaks overlapped with the Foxa2 peaks. This suggests redundancy in the functions of these two factors, and also their possible physical interaction. Co-immunoprecipitation (IP and ChIP-reChIP) experiments show that Foxa1 and Foxa2 interact and bind to similar genomic locations (Motallebipour et al., 2009).

These studies are good examples of the power ChIP-seq offers for this type of genome wide analysis of transcription regulation and identification of novel mechanistic interactions.

1.6 Aim of project

Foxa2 has been shown to play crucial roles in the specification, development, and maintenance of midbrain DA neurons (Kele et al., 2006; Kittappa et al., 2007; Lin et al., 2009). Many genes involved in this processes have been shown to be regulated by Foxa2 (Lin et al., 2009 2006). Recent global studies of Foxa2 recruitment to the genome in adult mouse liver cells and liver carcinoma cell lines have given many new mechanistic insights to the way Foxa2 functions as a transcriptional regulator (Motallebipour et al., 2009; Wederell et al., 2008).

The primary aim of this project is to identify the global binding events of Foxa2 in the mDA neurons through ChIP-seq experiments performed at two important stages of their development (specification, and differentiation). The results will be used to identify new targets and biological processes that they are involved in.

A secondary aim of the project is to perform enhancer analysis using newly identified regions from the ChIP-seq data and identify possible mechanisms driving their function in regulating gene expression.

2. Materials and Methods

2.1 In Situ Hybridization

Adult brains were dissected and fixed in 4% paraformaldehyde in 1M PBS overnight, washed in PBS and cryo-protected in 30% sucrose in PBS and sectioned on a Leica Jung cryostat at a thickness of 14 um. The in-situ hybridization procedure has been described previously (Conlon and Herrmann, 1993). Foxa1/2 probes used from Ang et al (1993).

2.2 Immunohistochemistry

Cells were fixed with, freshly made, 4% PFA for 10 min. at room temperature. Cells were then washed with 1X PBS. Cells were incubated for 10 min with blocking solution (5%FBS, 0.1% Triton, PBS). Primary Antibody was added and cells were incubated at $4^{o}C$ over night. Cells were then washed 3X with 0.1%Triton PBS. Secondary Antibody was added and cells were incubated at room temperature for 1 hour. Antibodies used: Rabbit anti Nurr1 (Santacruz), mouse anti TH (Chemicon), rabbit anti Lmx1a (J. Ericsson), mouse anti Tuj1 (Chemicon), mouse anti Nestin (Chemicon), rabbit anti Foxa2 (J.A. Whitsett).

2.3 Differentiation of ES Cells

E14.1 (NesE-Lmx1a, NesE-GFP) ES cells were propagated on gelatinized culture dishes in DMEM (Invitrogen) supplemented with 2000 U/ml LIF (Chemicon), 10% KSR, 2% FCS, 0.1 mM nonessential amino acids, 1 mM pyruvate (Invitrogen), and 0.1 mM b2-mercaptoethanol (Sigma). For *in vitro* differentiation 15,000 cells/well were plated on gelatinized 24-well plates, and incubated in ES medium for 12–15 hr. Thereafter, the cells were washed once with PBS and grown in N2B27 differentiation medium (Ying et al, 2003) supplemented with 20 ng/ml bFGF (Invitrogen), 100 ng/ml FGF8, and 100 nM SHH for 0–8 days.

2.4 Chromatin immunoprecipitation of *in vitro* and *in vivo* samples

The samples used were prepared from cells acquired from *in vitro* or *in vivo* DA systems. The *in vitro* sample was generated from Nestin-Enhancer-Lmx1a-stably transfected ES cells that have been differentiated into mDA progenitors as described in Andersson et al 2006. The *in vivo* samples were prepared from dissected ventral midbrains of E10.5, E12.5 and E14.5 mouse embryos. Cells or tissue were cross-linked in 1% formaldehyde for 10 min while rotating at 4^{0} C. Cross-linking was quenched by adding glycine to a final concentration of 0.125 M for 5 min while rotating. The tissue was rinsed in cold PBS and homogenized with a plunger in cold Whole cell lysis buffer (10 mM Tris–Cl, pH 8.0, 10 mM NaCl, 3 mM MgCl2, 1% NP-40, 1% SDS) and protease inhibitors. Cells were incubated at 4°C for 10 min. Lysate was sonicated using the Diagenode Bioruptor for 15 min on high, using 30 s intervals. Debris were removed by centrifugation at 13 000 g for 10 min, and the supernatant was collected and snap frozen

in liquid nitrogen. A 10 uL aliquot was reverse crosslinked by the addition of NaCl to a final concentration of 192 mM, overnight incubation at 65°C, and purification using a PCR purification kit (Qiagen, CA, USA). The chromatin concentration was determined using a NanoDrop 3.1.0 nucleic acid assay (Agilent Technologies, Santa Clara, CA, USA). Ten micrograms of chromatin per sample was precleared by adding 90 uL of protein A-agarose in 1 ml of ChIP dilution buffer (0.01% SDS, 1.1% Triton X-100, 167 mM NaCl, 16.7 mM Tris–Cl, pH 8.1) and rotating the sample for 1 h at 4°C. Protein A-agarose was sedimented by centrifugation at 3000 g for 30 s. Two micrograms of rabbit anti-Foxa2 (kind gift of J.A. Whitsett), anti-Otx2 serum or normal rabbit anti-IgG antibody (Millipore #12-370), was added to the supernatant and incubated overnight at 4°C. Protein A-agarose was blocked overnight at 4°C with 1 mg/ml bovine serum albumin in ChIP dilution buffer, added to the chromatin, and rotated for 1 h at 4°C. Following three consecutive washes of 5 min each with TSE I (0.1% SDS, 1% Triton X-100, 2 mM EDTA, 20 mM Tris–Cl, pH 8.1, 150 mM NaCl), TSE II (0.1% SDS, 1% Triton X-100, 2 mM EDTA, 20 mM Tris–Cl, pH 8.1, 500 mM NaCl) and ChIP buffer III (0.25 M LiCl, 1% NP-40, 1% deoxycholate, 1 mM EDTA, 10 mM Tris–Cl, pH 8.1), chromatin was eluted by adding 100 uL of freshly made ChIP elution buffer (1% SDS, 0.1 M NHCO3) to the pellet and rotating the sample for 10 min. Elution was repeated with an additional 100 uL of ChIP elution buffer, and the eluates were combined. Cross-linking was reversed by the addition of NaCl to a final concentration of 192 mM and overnight incubation at 65°C. The samples were resuspended in Tris-EDTA

2.5 Real-time qPCR

ChIP-qPCRs were assembled using Platinum SYBR Green Super mix (Invitrogen). Reactions were performed in triplicates using the ABI 7900 PCR System (ABI). The enrichment was calculated by comparing input (sheared genomic DNA) to ChIP material ($2^{\mathbf{Ct\ input-Ct\ ChIP}}$). The enrichment of Foxa2 target regions was compared to regions close to the Gli2 and Shh loci (-ve 1, and –ve 2 respectively), which served as a reference for nonspecific DNA. One-way Annova and Dannet test was used to calculate the significance of enrichment of the target region over the negative control region (-ve 1).

Primers were designed using the Primer3 sofware (*www.biotools.umassmed.edu*). All primers were tested using multiple dilutions of input genomic DNA and dissociation curve was set to make sure a single product was generated. Primers are provided in the Appendix chapters.

2.6 ChIP followed by high throughput sequencing

For ChIP-Seq experiments, for the purpose of collecting enough of the immunoprecipitated DNA, 20 independent ChIP assays were performed as described previously and were finally collected in a single PCR purification column (Qiagen). For the *in vitro* system 10^7 cells were required. As for, the *in vivo* samples required 80 E12.5 and 40 E14.5 ventral midbrains respectively. As control sample we used input DNA. 10ng of the ChIP (experiment) or input (control) DNA samples were modified for

sequencing following the manufacturer's protocol (Illumina). Cluster generation and sequence alignment to the mouse genome (mm9) with subsequent pipeline processing were performed following Illumina's protocol. Note, two lanes were sequenced for each sample and merged the tags for deeper sequencing purposes.

2.7 Peak calling using a model based analysis of ChIP-seq (MACS)

MACS analyses the ChIP-seq tags of the experiment against the control sample (Input). MACS linearly scales the total control tag count to be the same as the total ChIP tag count. Since there may be tags that are sequenced repeatedly, more times than expected from a random genome-wide tag distribution. Such tags might arise from biases during amplification of the ChIP sample and preparation of the sequencing library, and are likely to add noise to the final peak calls. Therefore, MACS removes duplicate tags higher in number than what is expected.

The program then Slides 2 dimensional windows across the genome to find candidate peaks with a significant tag enrichment (p value 10e-5). It will then merge overlap peaks, and extend each tag a fixed number of bases from its center. For each candidate peak, the window is centered at the peak location in the control sample and a p-value is calculated and the false peaks are removed. Peaks with p-value below 10e-5 are called (positive peaks).

The false discovery rate (FDR) is calculated by reversing the control and treatment data, calling peaks using the same strategy, and then calculating p-values for these 'negative peaks'. After ranking 'positive' peaks and 'negative' peaks by p-values, one can

calculate an FDR for a certain p-value and is the #control peaks/#ChIP peaks for that p-value.

2.8 Motif analysis

To determine the *de novo* sequence recognized by Foxa2 in our ChIP-Seq data set we performed the ultra conserved motif search using MEME (*www.meme.sdsc.edu*). First we sorted our list according to the FDR, low FDR peaks being at the top of the list and the higher FDR peaks being at the bottom of the list. The peaks were then grouped in groups of 500 peaks, generating 19 groups. The subpeak regions of 60 bp spanning the peak summits from each group were uploaded on MEME and the default parameters were used to do the search.

To search the ChIP-Seq data set for possible enrichment of the Otx2 motif, the position weight matrix provided by Uniprobe (*www.thebrain.bwh.harvard.edu/uniprobe*) was used to search the data set using the Perl module TFBS by Boris Lenhard (Lenhard and Wasserman, 2002). The score threshold was set at 80% similarity. Based on these parameters 629 peak sequences were found to contain the Otx2 PWM. To establish statistical confidence for the motif search results 1000 random datasets, were generated, each with the same number of sequences as the ChIP-Seq dataset, and with the same dinucleotide composition. The same parameters were used to search for the Otx2 PWM in these random data sets.

2.9 Gene Ontology (GO) analysis

The identfication (ID) numbers of the genes used for this analysis were extracted from MGI (*www.informatics.jax.org*). These IDs were used as reference on

GOTOOLBOX (*www.genome.crg.es/GOToolBox*) to identify the overrepresented GO terms. GO categories were taken from the ‘‘biological process’’ level. Only terms with p-value <0.001 were considered for the analysis and the Fold enrichment of the genes found in our list over the reference (whole genome) were calculated for each GO term. Genes in the top terms identified for each category studied can be found in the Appendix chapter.

2.10 Breeding and genotyping of mutant animals.

All mouse strains were maintained in a mixed MF1-129/SV background. *En1*$^{KICre/+}$, *Foxa2*$^{flox/\ flox}$ and *Foxa1* $^{loxp/loxp}$ mouse strains were generated as described (Sapir et al., 2004; Hallonet et al., 2002; Gao et al., 20008 respectively). In this thesis, the *Foxa1*^{loxp} allele will be referred as *Foxa1*^{flox}. *Foxa2* $^{flox/\ flox}$*;Foxa1* $^{flox/\ flox}$ mice were generated by crossing *Foxa2*$^{flox/flox}$ with *Foxa1*$^{flox/flox}$ animals. To obtain conditional *Foxa1/2* double mutants, *En1*$^{KICre/+}$ mice were crossed with *Foxa2*$^{flox/flox}$*;Foxa1* $^{flox/\ flox}$ animals. Subsequently, *En1*$^{KICre/+}$*;Foxa1*$^{fl1ox/+}$*;Foxa2*$^{flox/+}$ F1 male animals were then mated to *Foxa2* $^{flox/\ flox}$*;Foxa1* $^{flox/\ flox}$ females to generate *En1*$^{KIcre/\ +}$ *;Foxa2* $^{flox/\ flox}$*;Foxa1* $^{flox/\ flox}$ double mutants. The *Foxa2*^{flox} and *Foxa1*^{flox} alleles were detected by PCR (Hallonet et al., 2002; Gao et al., 2008), whereas the *Cre* transgene was detected by using a pair of primers and PCR conditions as described by Indra et al. (1999).

The *En1*$^{Cre/+}$*; Otx2*$^{flox/flox}$ and Nestin $^{Cre/+}$*, Foxa2*$^{flox/\ flox}$*;Foxa1* $^{flox/\ flox}$ mice have been described previously (Kele et al., 2006; Puelles et al., 2004).

2.11 RNA extraction

Single E10.5 dissected ventral midbrain tissue or 500 X 10^3 Cells harvested at day 2, day 3.5 and day 5 of *in vitro* diffrentiation were collected in the RNA extraction buffer provided by the Pico pure RNA extraction kit (ARCTURUS). RNA was extracted according to manufacturers specifications.

2.12 Reverse transcriptase qPCR analysis

The cDNA was prepared from *in vitro* differentiated NesE-Lmx1a Es cells or E10.5 single dissected mouse ventral midbrain of the mutant strains described previously. The Pico Pure kit (Arcturus) was used to extract the RNA. Total RNA were transcribed into cDNA with the SuperScript™ III RT (Invitrogen, Carlsbad, CA) and oligo (dT) primers. For quantitative analysis of the expression level of mRNAs, real-time PCR analyses using Platinum SYBR Green Super mix (Invitrogen) were performed in triplicates using the ABI 7900 PCR System (ABI). Oligonucleotides amplifying small amplicons were designed using Primer3 (biotools) software. Amplifications were performed in 20 µl containing 0.5 µM of each primer. 0.5 X SYBR Green (Invitrogen), and 2 µl of 50 fold diluted cDNA. Forty-five PCR cycles were performed with a temperature profile consisting of 95$_o$C for 30 sec, 60^{o}C for 30 sec, 72^{o}C for 30 sec, and 79^{o}C for 5 sec. The

dissociation curve of each PCR product was determined to ensure that the observed fluorescent signals were only from specific PCR products. After each PCR cycle, the fluorescent signals were detected at 79^{o}C. The fluorescent signals from specific PCR products of cDNA prepared from mutant or control (wild type littermate) ventral midbrain tissue were normalized against that of the GAPDH gene ($2^{\text{Ct GAPDH-Ct Gene tested}}$), and then relative values were calculated by setting the normalized value of control as 1. All reactions were repeated using at least three independent samples (biological replicates), and One-way Annova and Dannet test was used to calculate the significance of the fold change of the expression of genes tested in mutant compared to the wild type control.

2.13 Illumina Array Hybridization

Biotinylated cRNA were prepared from 500 ng of total RNA using an Illumina TotalPrep RNA Amplification Kit (Ambion, TX) and cRNA yields were quantified using an ND-1000 spectrophotometer (Nanodrop Technologies). cRNA (1500 ng) were hybridized to Illumina's MouseRef-8 v2.0 expression BeadChips (Illumina) containing 25,000 mouse genes using the hybridization solution supplied by the manufacturer. All reagents and procedures for washing, detection, and scanning were performed according to the Beads Station system protocols.

2.14 Luciferase Assay (Promega)

P19 cells were transfected with constructs containing candidate regulatory elements upstream of a luciferase gene to measure their enhancer activity. Foxa2 candidate cofactors (Otx2, Lmx1a, and Nurr1) including Foxa2 were cloned down stream the CMV

promoter. All transfection plasmid constructs were purified by the Qiagen Maxi-prep method. For each experiment, individual sample plasmids were tested in triplicate. 200 nanograms of sample plasmid DNA were introduced into P19 cells by the Lipofectamine method (Invitrogen). All plasmids tested were cotransfected with 10 ng of Renilla to control for transfection efficiency.. The empty luciferase vector was used as a negative control. Cells were grown in the appropriate media for 2 days after subculturing onto 20 well tissue culture plates to a density of 5 X 10^{4} cells/well. Cells were assayed for luciferase activity using the Promega luciferase assay kit and the analytical luminescence monolight luminometer. Relative light units were determined after a 10-s detection period. The ratio of luciferase activity Luciferase construct/ Renilla was determined, and the average of triplicate readings was expressed as fold expression over background (activity of the empty luciferase vector)

2.15 Generation of Reporter Constructs

Genomic sequences bound by Foxa2 within the *Lmx1a* and *Lmx1b* loci were PCR amplified uding high fidelity Taq (Roche) Fragments were subcloned into the TOPO vector (Invitrogen) and directly sequenced using the T7 promoter. The reporter construct used for the transgenic studies was BGZA, which contains the β-globin minimal promoter, *lacZ* gene, and *SV40* polyadenylation cassette (Helms *et al.,* 2000; Yee and Rigby, 1993). The fragments were then cloned into the Sal1, Nhe1 site upstream of the β-globin minimal promoter. The primers used are:

Lmx1a CR1

F: TTGTAAGCTTCTCTGCCCAGTTCCCCAGGA

R: AGAAGCTTGCTCTGTTTCCACCCTCTCCAC

Lmx1a CR2

F: AGGCTGAAGCTTCACACCCGGACGGCAGTTTT

R: CAAAGCTTGCCGGCCCGAAGGCGCGGCCCCG

Lmx1b CR1

F: AAGAAGCTTCAGGCAGCCAGGGGTTAA

R: AAAAGCTTGTGTGTGTGTGTGTGTGTG

2.16 Production and genotyping of transgenic mice

Transgenes were prepared for microinjection as described (Epstein et al., 1996). The genotyping of transgenic embryos was carried out by PCR using proteinase K digested tail biopsies as DNA templates. Primers directed against *lacZ* (F: GCACATCCCCCTTTCGCCAGCTGGCGTAAT)(R:CGCGTCTGGCCTTCCTGTAGCCAGC TTTCA), generating DNA fragments of (220 bp), were used under the following PCR conditions: 94°C for 1 minute, 60°C for 1 minute, 72°C for 1 minute, for 30 rounds followed by a final extension at 72°C for 10 minutes. For staging embryos, the day of vaginal plug detection corresponded to 0.5 days post coitus (dpc).

2.17 Whole-mount β-galactosidase

β-galactosidase activity was detected in whole-mount embryos by using X-gal (Sigma) as substrate according to Echelard et al. (1994). The embryos were stained from 60 minutes to overnight depending on the strength of transgene expression.

3. Results

In this study, we identified and analyzed genomic regions bound by Foxa2 in DA cells during specification and differentiation. ChIP-qPCR experiments were performed for the purpose of validating the sites identified through genome wide ChIP-Seq analysis. RT-qPCR expression analysis of the candidate target genes was investigated in loss of function models to establish the functionality of the protein/DNA interaction. To identify the possible biological processes Foxa2 may be involved in regulating we performed GO term analysis of Foxa2 candidate target genes. The names of genes mentioned in this thesis, as well as the associated chromosomal regions tested in the independent ChIP-qPCR assays are summarized in the appendix chapters.

3.1 Genome wide analysis of Foxa2 binding in an *in vitro* model for midbrain DA progenitors

Foxa1 and Foxa2 start being expressed in the mouse ventral midbrain progenitors at E8.5 (Hahn et al., 1993). By E10.5 the midbrain progenitor cells express all the markers defining a mDA precursor, such as Lmx1a, Lmx1b, Foxa2, and Shh, but none of the immature and mature neuronal markers such as Nurr1, AADC, Th, DAT, and Pitx3 are expressed at this point (Kele et al., 2006). From a developmental point of view, E10.5 is the proper time point to harvest primary ventral midbrain cells to perform ChIP-Seq. An obstacle for this is that ChIP-seq requires 20 million cells for the analysis and it is extremely difficult and time consuming to dissect enough E10.5 ventral midbrain tissue for a ChIP-Seq experiment. For this reason we decided to use an *in vitro* cell line system

of mDA progenitors character to identify Foxa2 target genes during the specification of these neurons.

3.1.1 Defining the *in vitro* midbrain DA progenitor model

During this thesis there were a number of *in vitro* models for mDA neurons to consider, such as *in vitro* differentiation of ES cells. The protocol by Kawasaki et. al. demanded differentiation of ES cells over a stromal cell line, whereas the protocol by Lee et al required cell aggregation and application of Fgf8 and Shh in the media to induce the proper cell fate (Kawasaki et al., 2000; Lee et al., 2000). Ying et al offered an alternative method by differentiating ES cells as an adherent monolayer culture to produce DA neurons upon the addition of Fgf8 and Shh to the serum free media (Ying et al., 2003). None of these methods using ES cells produce DA neurons efficiently with the proper markers that define ventral midbrain DA neurons (Andersson et al., 2006b; Kawasaki et al., 2000; Lee et al., 2000). These approaches result in a largely heterogeneous population that cannot be used for this experiment. Another cell line to consider is known as MN9D (Rick et al., 2006). MN9D is an immortalized cell line resulting from the fusion of mouse neuroblastoma and ventral midbrain DA neurons. These cells express TH, and also produce and transport DA (Rick et al., 2006). Due to the fact that MN9D cells express mature mDA markers rendering them unsuitable for use in this experiment since we aim at strictly using cells with a DA progenitor character.

The identification of Lmx1a as an intrinsic determinant of mDA neuron differentiation made it possible to produce high yields of mDA progenitors *in vitro* (Andersson et al., 2006b). The method utilizes ES cells transgenic for Lmx1a driven by the promoter of the neural stem cell marker Nestin. The experiment requires 8 days of

differentiation. By day 5 the cells express most if not all the known midbrain DA progenitor markers including Foxa2 and Lmx1a as shown by immunofluorescence, and microarray expression analysis (Figures 3-1, 3-4).

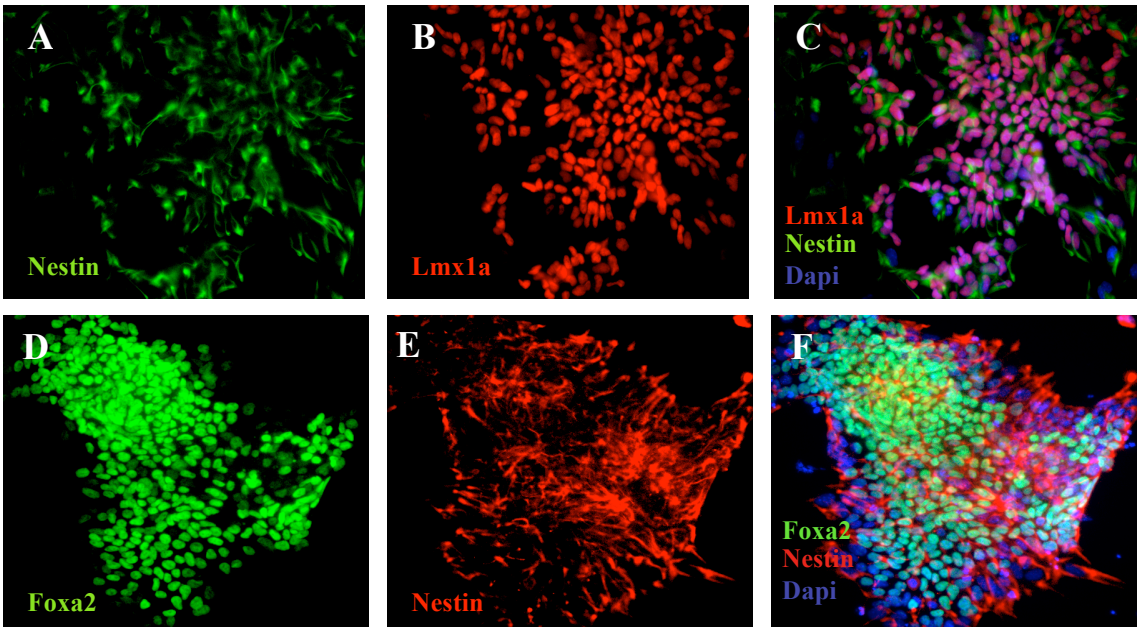

Figure 3-1: Foxa2 and Lmx1a expression after 5 days of in vitro monolayer differentiation of NesE-Lmx1a transgenic ES cells.

(A-C) Lmx1a and Nestin staining followed by counter staining with Dapi. (D-F) Foxa2 and Nestin staining followed by counter staining with Dapi.

By day 8 a large percentage of the colonies (over 80%) express mature mDA neuronal markers and acquire neuronal morphology (Figure 3-2). As a control experiment we differentiated ES cells transgenic for GFP under the Nestin enhancer using the same culture conditions as the previous case. We observed that the efficiency of generating TH+ neurons is very low (below 10% of colonies express TH); suggesting that the transgenic NesE-Lmx1a ES cell line is the proper cell line to use for our experiments (Figure 3-3).

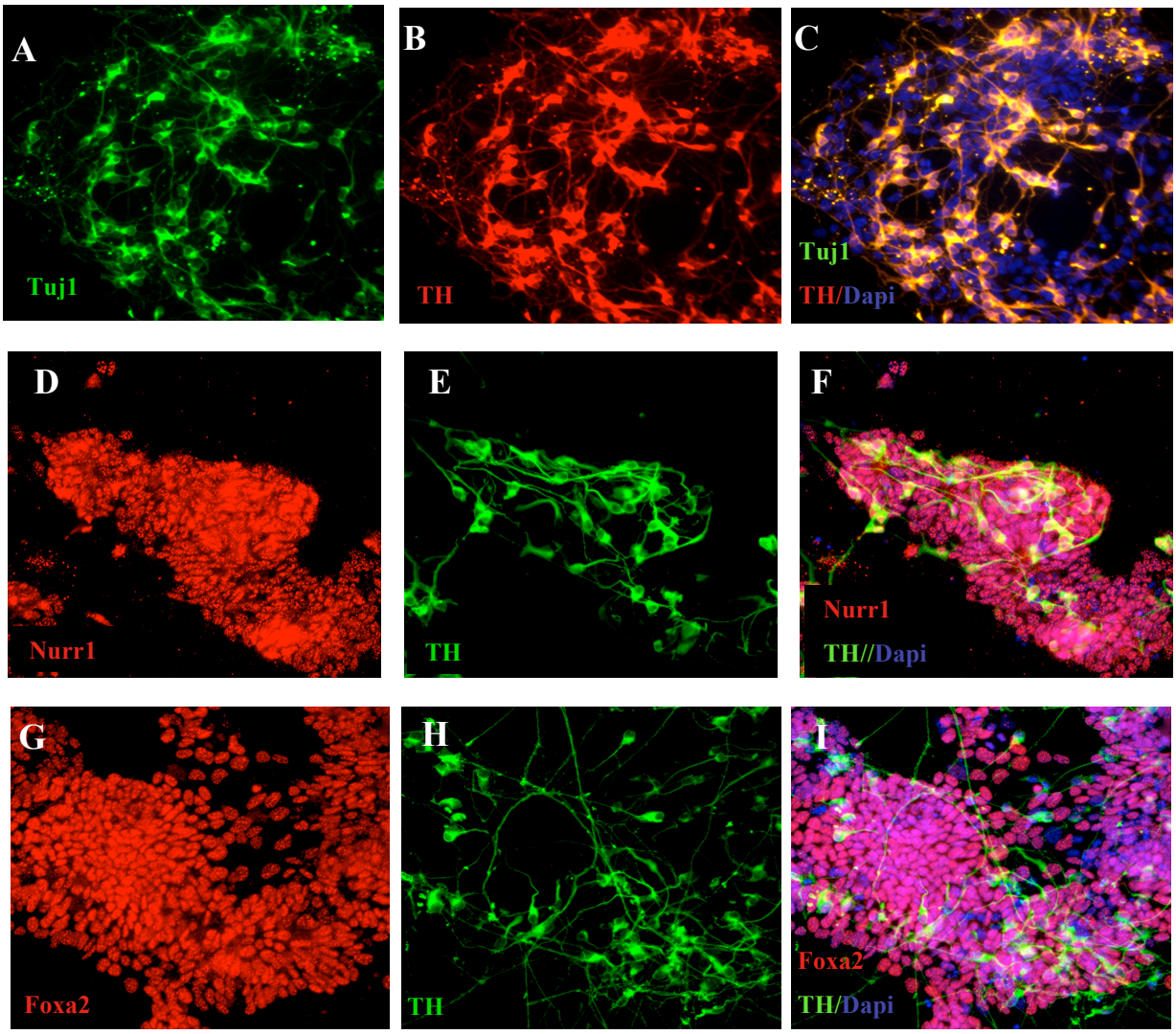

Figure 3-2: Expression profile of neurons generated at day 8 (D8) of in vitro differentiation of NesE-Lmx1a transgenic Es cells.

(A-C) TH overlap with Tuj1. (D-F) TH overlap with Nurr1. (G-I) TH overlap with Foxa2. TH+ neurons are generated with high efficiency by D8, and immuno-histochemical staining suggest co-expression of Nurr1 and Foxa2. Dapi was used as counter staining in all cases.

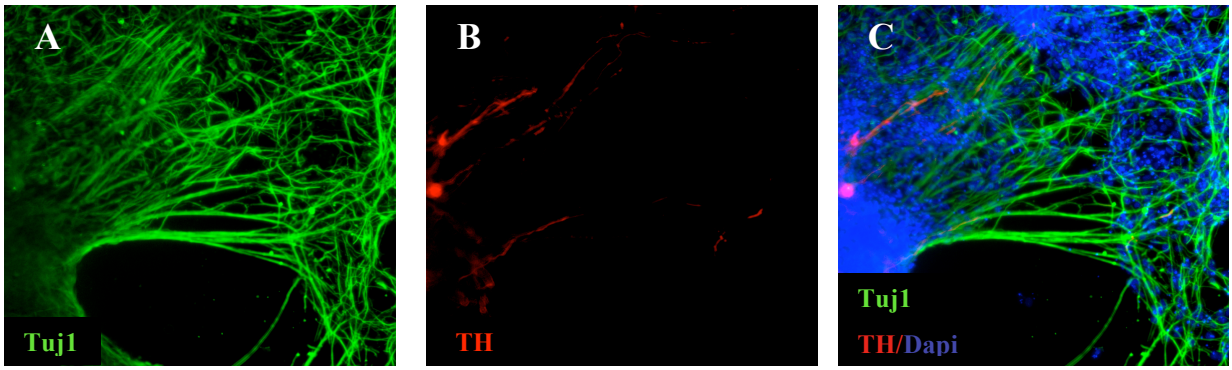

Figure 3-3: Expression profile of neurons generated from the in vitro differentiation of NesE-GFP transgenic Es cells.

(A-C) Overlap of TH with Tuj1 and counter staining with Dapi . TH+ neurons are produced at very low efficiency from an Lmx1a negative context.

3.1.1.1 Day 5 of *in vitro* differentiation of NesE-Lmx1a transgenic Es cells is the best time point to harvest mDA progenitors for ChIP-Seq

Illumina expression arrays were used to profile the cells during their initial stages of differentiation at the defined time points, Day 2 (D2), Day 3.5 (D3.5), and Day 5 (D5). The expression dynamics of known genes normally expressed in the ventral midbrain were assessed at these time points (Figure 2-4). Interestingly, most of the progenitor marker genes detected such as TCF12 (E-box protein expressed in the ventricular zone), Corin (floor plate marker) and Bmp7 reach a peak of expression at D5 and more importantly none of the known mature markers (TH, and AADC) were expressed at this time point (Uittenbogaard and Chiaramello, 2002; Mavromatakis, 2006). Importantly, Shh, a target of Foxa2, was expressed by day 5, and ChIP-qPCR experiments with Foxa2 antiserum on day 5 show that Foxa2 is bound to its target regions on the Shh and Foxa2 regulatory elements (Figure 3-5). This result suggests that Foxa2 is exerting its regulatory

influence on its target genes at D5. All together, this data shows us that D5 is a suitable time point to harvest the differentiated cells for the ChIP-Seq experiment.

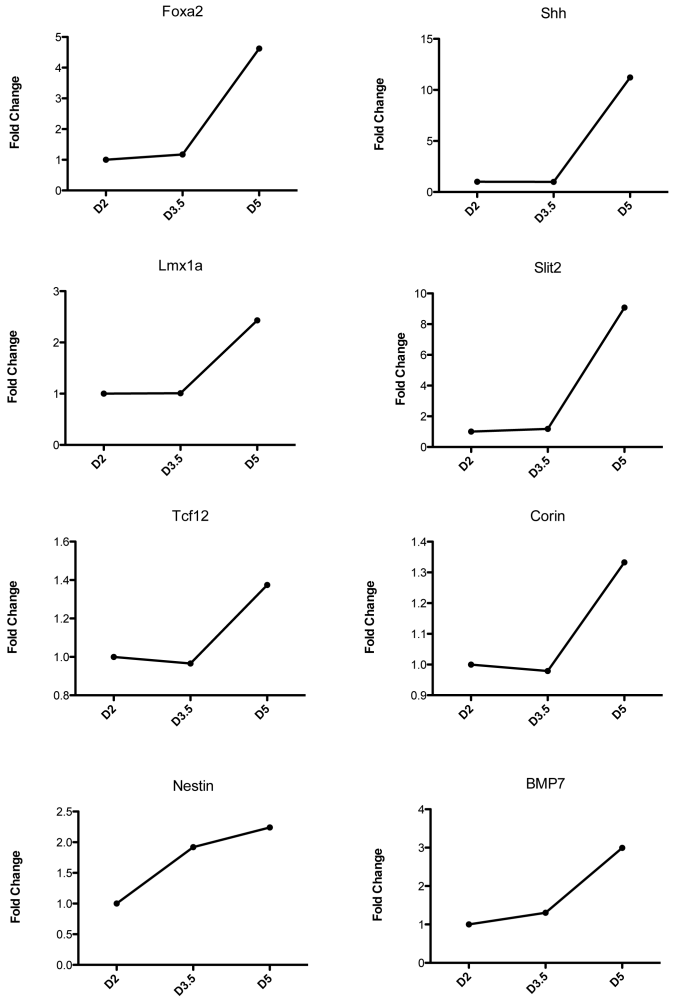

Figure 3-4: Microarray analysis of the expression profile of NesE-Lmx1a ES cells during differentiation towards midbrain DA progenitors.

Genes presented: Foxa2, Shh, Lmx1a, Slit2, Tcf12, Corin, Bmp7, and Nestin. We observe the expression of all these genes arriving at a peak on day 5 (D5) of in vitro differentiation.

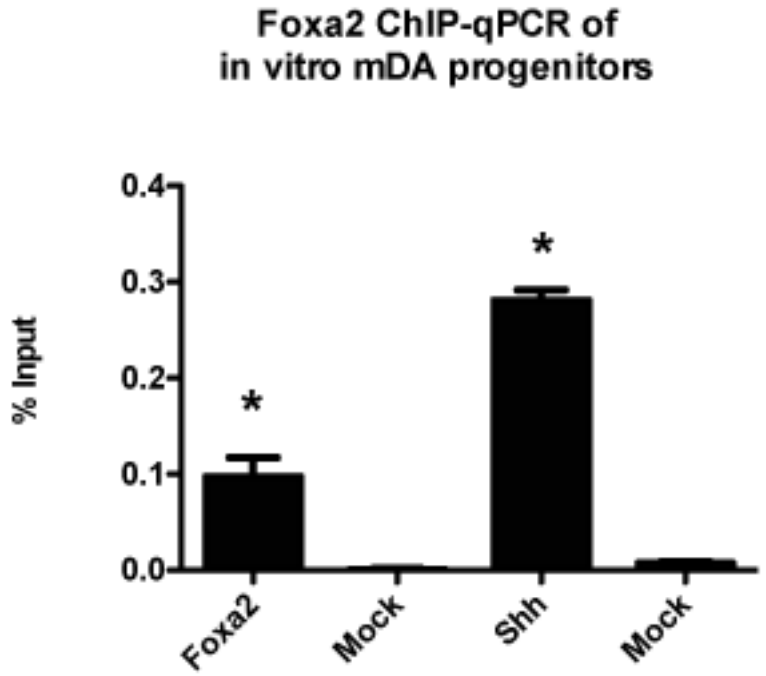

Figure 3-5:ChIP experiments of chromatin from D5 in vitro differentiated mDA progenitors validating the positive control regions, Shh brain enhancer and the Foxa2 floor plate enhancer using Foxa2 antiserum.

Non-specific antibody against IgG was used for the mock ChIP assays. Error bars represent SEM. Each ChIP was performed on chromatin samples from three biological replicates, and enrichment of both control regions over the mock experiments was statistically significant ($P < 0.05$)

3.1.2 Identification and characterization of Foxa2 DNA binding *in vitro*

3.1.2.1 Identification of Foxa2 DNA binding events

Chromatin immunoprecipitation and massively parallel Illumina 2G sequencing (ChIP–Seq) were carried out to identify binding sites of Foxa2 in mDA progenitors derived from our *in vitro* D5 differentiated NesE-Lmx1a ES cells (Andersson et al., 2006b). Sequencing of the ChIP product generated ~10^7 high quality sequences that mapped to the mouse genome and are viewed by the UCSC mm9 genome browser (www.genome.ucsc.edu). Peaks were called by a model-based analysis of ChIP-Seq (MACS), and overlapping mapped sequences represent Foxa2 bound regions (Zhang et al., 2008). By normalizing the ChIP experiment to an input control, a false discovery rate (FDR) was assigned to each peak and false peaks were removed from the list. We identified 9160 peaks with an FDR substantially lower than 5%, providing a good level of confidence. To further establish the quality of the list we examined the known regulatory regions bound by Foxa2, the Shh brain enhancer and the Foxa2 floor plate enhancer using the UCSC genome browser (Jeong and Epstein, 2003; Nishizaki et al., 2001). Statisctorily, clear peaks could be identified in these regions providing initial confidence in the data set (Figure3-6). Furthermore, Foxa2 regulated genes identified in the lab from mouse genetic data such as Lmx1a, lmx1b, and Foxa1 are only a few examples of genes that have been associated with a peak from our list (Figure 3-7) (Lin et al., 2009; Mavromatakis, 2006). Two Regions bound by Foxa2 on each of the Lmx1a and Lmx1b loci have been studied in this thesis and will be known from now on as Lmx1a or Lmx1b Conserved Regions 1 and Conserved Regions 2 (CR1 and CR2 respectively) due to the high conservation of their sequence between many species (Figure 3-7).

A

Shh Brain Enhancer

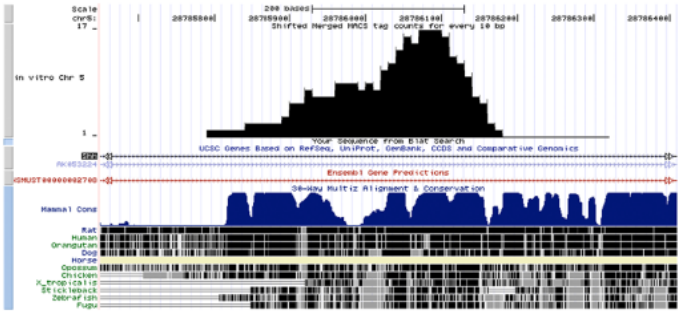

Foxa2 Enhancer

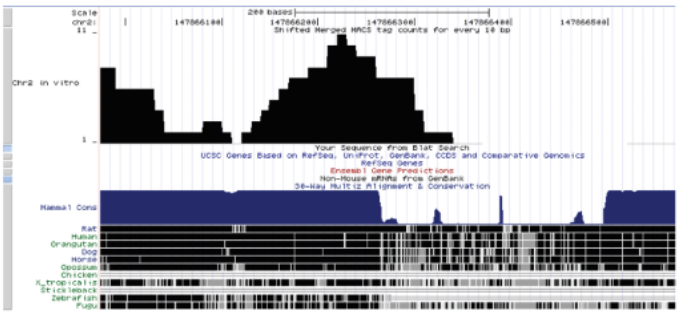

B

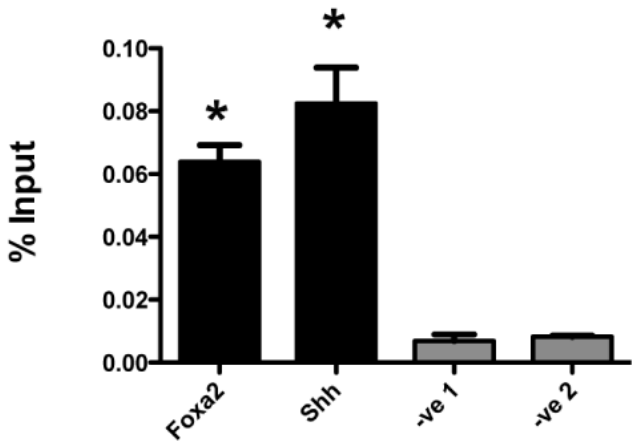

Figure 3-6: Occupancy of Shh and Foxa2 conserved regulatory elements by Foxa2.

(A) Schematic diagrams of the Shh brain and Foxa2 floor plate enhancers indicating peak regions generated from data obtained by Foxa2 in vitro ChIP-Seq experiments. (B) ChIP experiments of chromatin from E12.5 ventral midbrain tissue validating the positive control regions, Shh brain enhancer and the Foxa2 floor plate enhancer using Foxa2 anti serum. Genomic regions (-ve1, -ve2) unbound by Foxa2 were used as negative control. Error bars represent SEM. Each ChIP was performed on chromatin samples from three biological replicates, and enrichment of both control regions over the negative regions in the ChIP samples was statistically significant ($P < 0.05$).

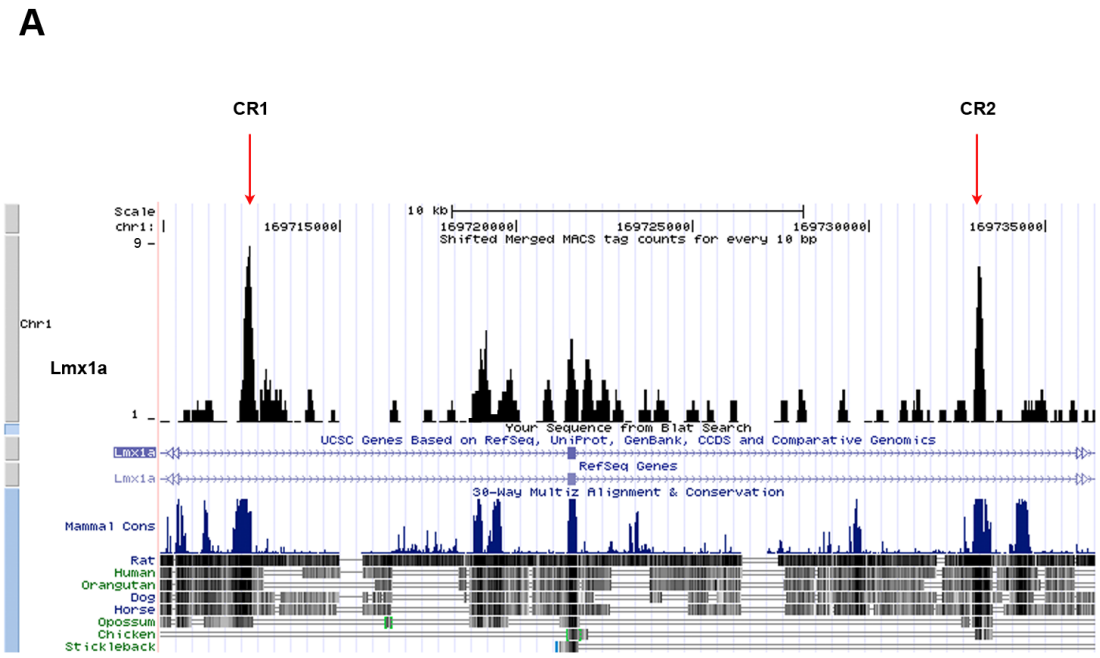

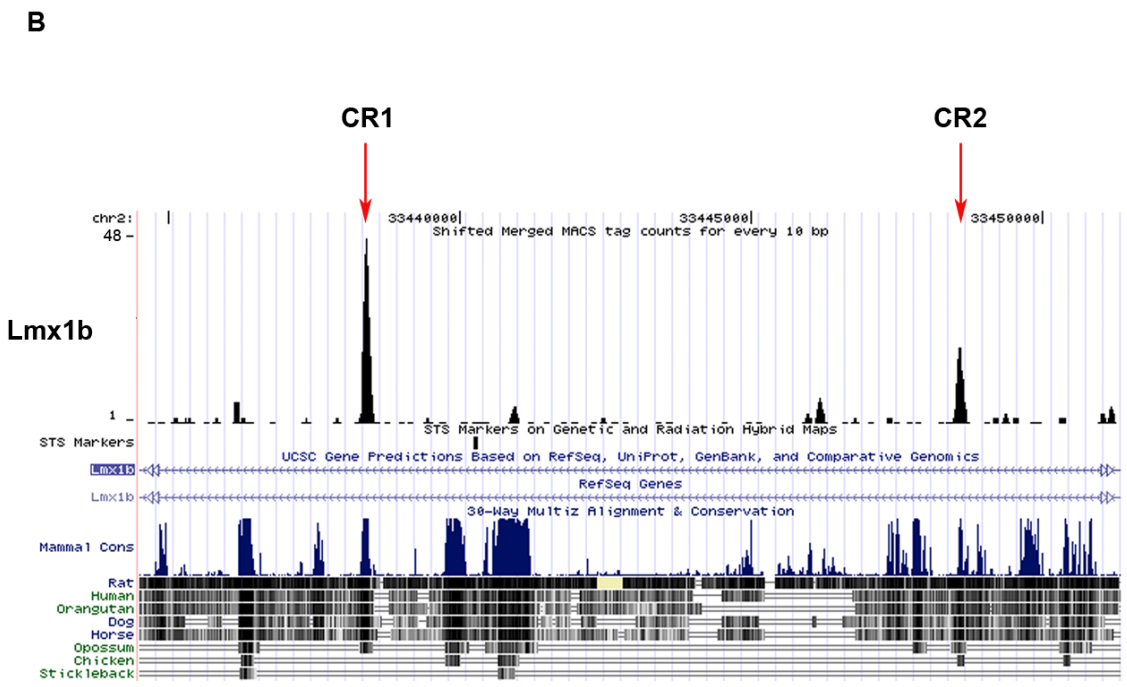

Figure 3-7: Occupancy of Lmx1a and Lmx1b conserved genomic elements by Foxa2.

(A-B) Schematic diagrams of genomic regions occupied by Foxa2 within the Lmx1a and Lmx1b loci from data obtained by Foxa2 in vitro ChIP-Seq experiments. Red arrows indicate peaks called by peak calling algorithm MACS. CR1: First conserved region. CR2: Second conserved region.

3.1.2.2 DNA binding motifs enriched in our data set

To determine the *de novo* sequence recognized by Foxa2 in our ChIP-Seq data set we performed a motif search using MEME (www.meme.sdsc.edu) to look for the best two motifs. First we sorted our list according to the FDR, low FDR peaks being at the top of the list and the higher FDR peaks being at the bottom of the list. The peaks were then grouped in groups of 500 peaks, generating 19 groups. The subpeak regions of 60 bp spanning the peak summits from each group were uploaded on MEME and the default parameters were used to do the search. The first motif was a Foxa2 motif defined by the JASPAR database (Bryne et al., 2008), and was enriched throughout the data set confirming further the validity of the results (Figure 3-8A). Furthermore, a second motif was identified using this method that greatly resembled an E-box motif as defined by the TRANSFAC database (Matys et al., 2006) similar to the Mash1 binding motif (Figure 3-8B). Mash1 is a basic helix loop helix transcription factor and is involved in neuronal differentiation and development. Mash1 acts as a transcription activator by binding on E-box sequences within promoters and enhancers of its target genes (Castro et al., 2006). These data suggests Foxa2 may be co-occupying genomic regions together with an E-box binding protein.

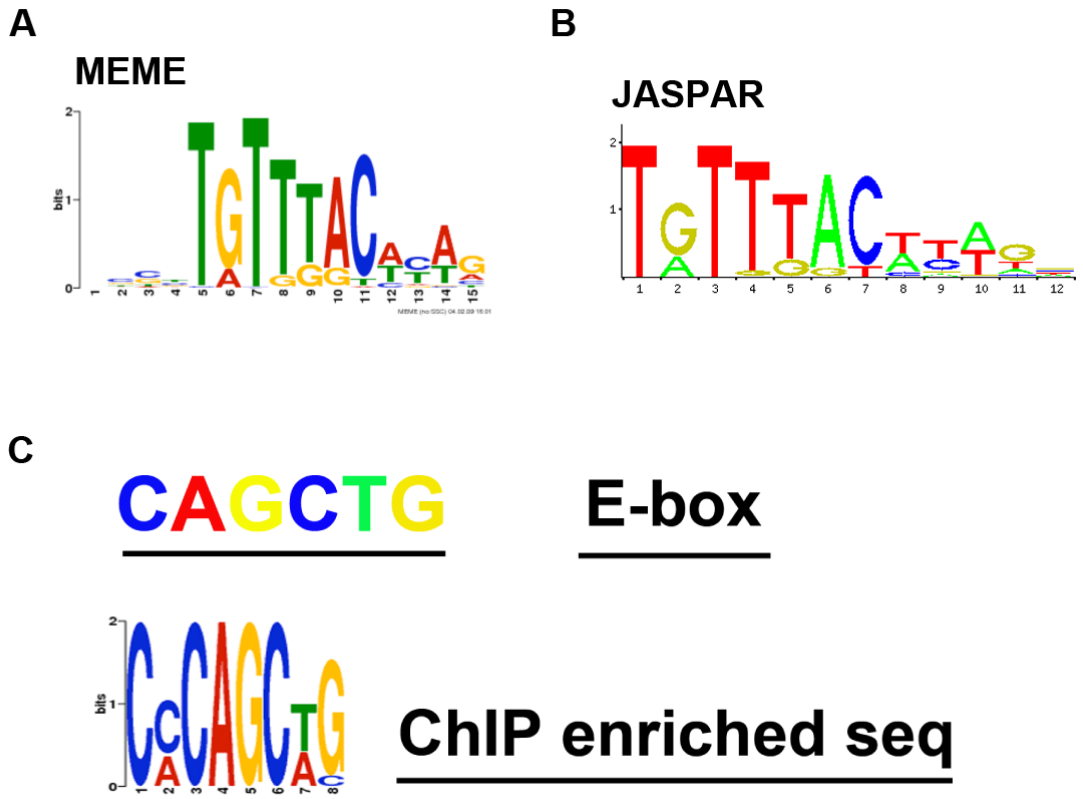

Figure 3-8: De novo motifs identified from the ChIP-seq analysis.

(A) Sequence of first de novo motif enriched in the ChIP-Seq data as identified by MEME. (B) Represents the known Foxa2 DNA binding motif present in the JASPAR database. (C) Sequence of the E-box motif (Castro et al., 2006) commonly bound by Mash1 (top). Sequence of the second enriched de novo motif identified by MEME in the data set (bottom).

3.1.2.3 Characterizing the locations of the high confidence peaks

The locations of the high-confidence peaks were mapped to the nearest TSS of Ensembl annotated genes, and microRNA transcripts. We found that 47% of peaks were located within a gene region (Figure 3-9). Interestingly, only 8% of the peaks were located within 2 kb upstream or downstream of the TSS of annotated genes, while 27.8% of the peaks were located within 10 kb of the TSS (Figure 3-10A). 30% of peaks overlapping genes were localized to a first intron (Figure 3-10B). We also observed that 40% of all peaks were more than 100 kb from the TSS of any annotated gene (Figure 3-10C). Of these peaks, 45% overlapped with conserved genomic regions, suggesting that either Foxa2 may act at remote distances from genes or that a number of Foxa2-regulated genes have yet to be annotated. Thus, Foxa2-binding sites observed are not preferentially located close to an annotated TSS but are situated at a range of locations across the mouse genome.

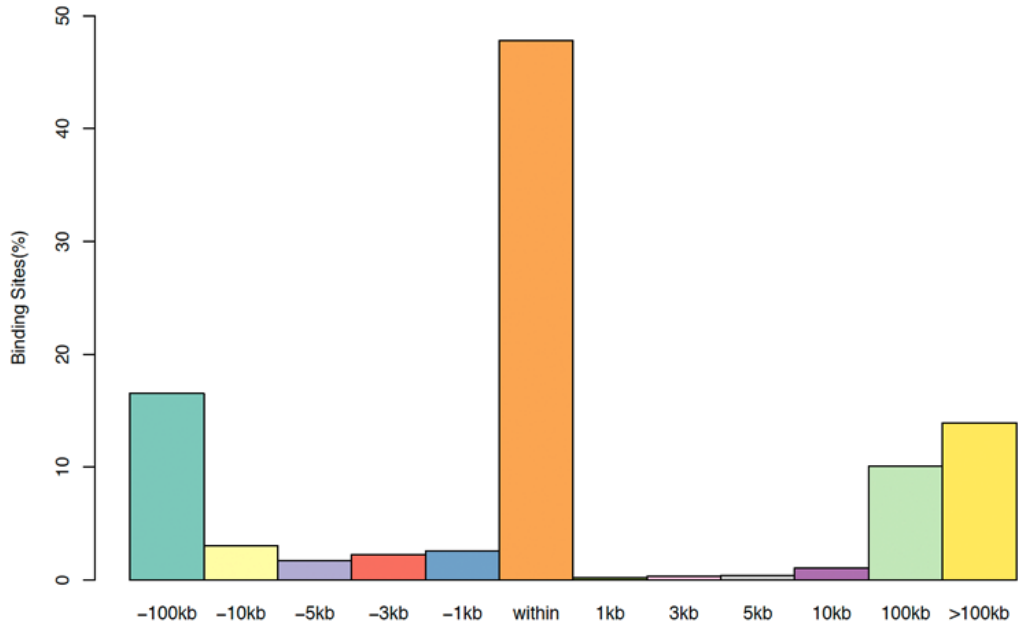

Figure 3-9: Percentage of binding sites at various distances from and within genes. Recruitment at distal regions from or within genes is a general characteristic of Foxa2 binding. 47% of peaks identified are within genes.

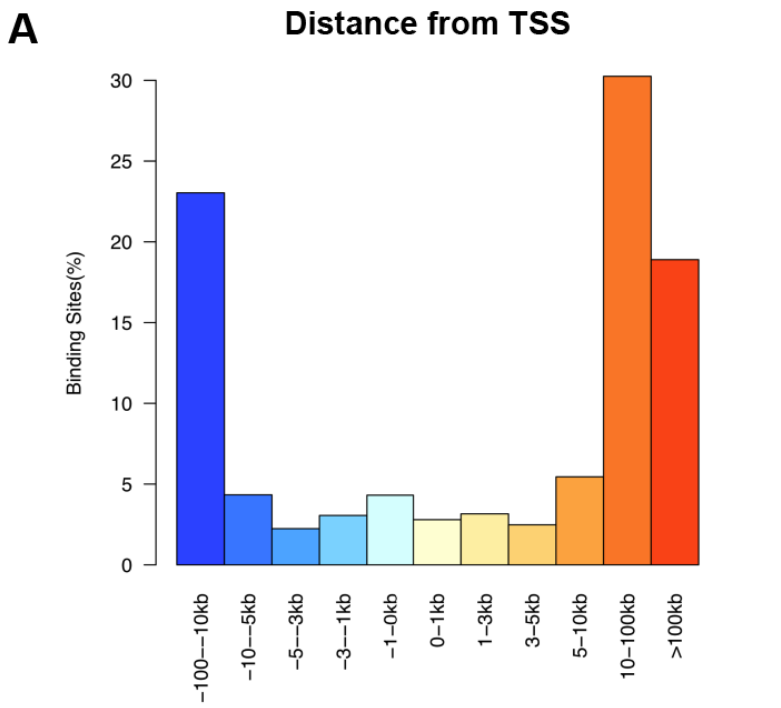
A
Distance from TSS
Binding Sites(%)
30
25
20
15
10
5
0
−100−−10kb
−10−−5kb
−5−−3kb
−3−−1kb
−1−0kb
0−1kb
1−3kb
3−5kb
5−10kb
10−100kb
>100kb

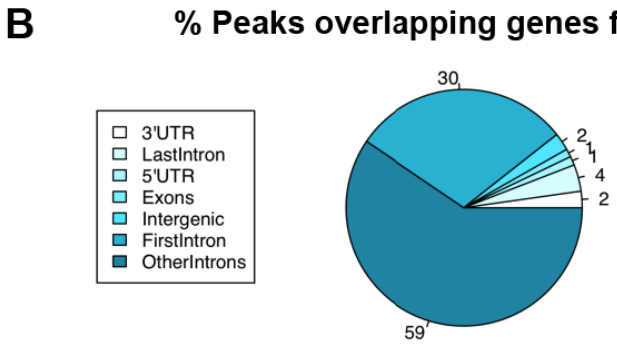
B
% Peaks overlapping genes features
3'UTR
LastIntron
5'UTR
Exons
Intergenic
FirstIntron
OtherIntrons
30
2
1
4
2
59

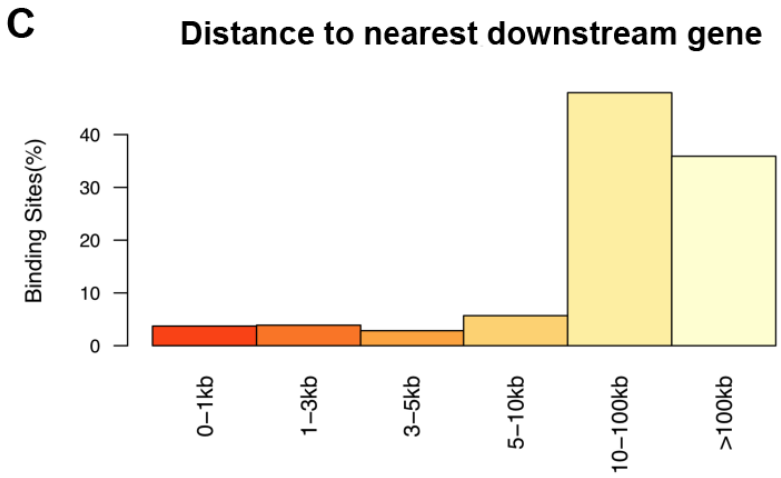
C
Distance to nearest downstream gene
Binding Sites(%)
40
30
20
10
0
0−1kb
1−3kb
3−5kb
5−10kb
10−100kb
>100kb

Figure 3-10: Characteristics of Foxa2 genome wide DNA binding events (in vitro).

(A) Percentage of binding sites at various distances from TSS. Recruitment at distal regions from the TSS is a general characteristic of Foxa2 genomic recruitment. (B) Distribution of peaks within genes. Majority of peaks are distributed within intronic regions with 30% identified within the first intron. (C) Distribution of the peaks from the nearest downstream gene. Most of the peaks are found between 10 and 100 kb away from the nearest downstream gene.

3.1.2.4 Validation of Foxa2 *in vitro* binding events using E12.5 mouse ventral midbrain tissue by ChIP-qPCR

Binding events that occur *in vitro* may not be a direct indication of binding events occurring *in vivo*. To test our *in vitro* model we chose a group of 11 peaks assigned to genes expressed at E12.5 in the mouse ventral midbrain. We then performed ChIP-qPCR experiments using E12.5 mouse midbrain tissue to test these 11 regions. It was very encouraging to see that all sites were enriched in the independent Foxa2 ChIP (Figure 3-11). This suggests that many regions bound by Foxa2 in the *in vitro* data set can be verified by independent detection methods (ChIP-qPCR) in the relevant *in vivo* system.

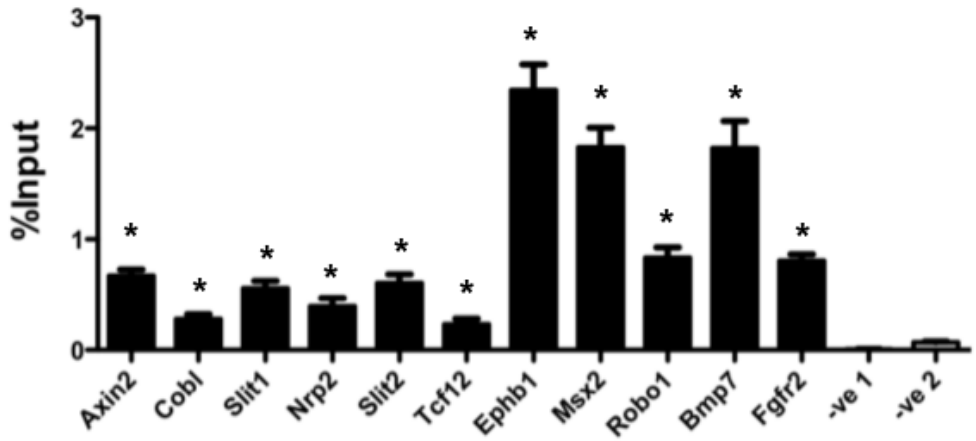

Figure 3-11: Genomic regions validated for Foxa2 binding by an independent ChIP-qPCR assay. ChIP was performed on chromatin extracted from ventral midbrain of E12.5 mouse embryos. All 15 regions tested are enriched compared to negative control regions. Error bars represent SEM. Each ChIP was performed on chromatin samples from three biological replicates, and enrichment Foxa2 bound regions over the negative regions in the ChIP samples was statistically significant (P value < 0.05).*

3.1.2.5 Overlap of ChIP-Seq data with microarray expression data

The candidate target genes from the ChIP-Seq experiment were correlated with differentially expressed (DE) genes identified from the microarray time course assay of in vitro differentiated mDA progenitors described previously. Only DE genes with a p value <0.01 were considered. We observed that 25% of the DE genes correlated with a peak. Out of these peaks 16% are within 2kb of the TSS, 34% are within 10kb, and 72% are within 50kb (Table 1). This observation enhances the previous suggestion that Foxa2 may exert it regulatory influence on gene expression from genomic regions at remote distances in DA progenitor cells.

# Peaks	9160
# DE genes in microarray time course	3326
# DE genes with a peak	824
# Peaks within 2kb of DE gene TSS	160 (16%)
# Peaks within 10kb of DE gene TSS	341 (34%)
# Peaks within 50kb of DE gene TSS	720 (72%)

Table 1. Distribution of Foxa2 peaks from the TSS of candidate targets. Most of the binding events are observed far away from the TSS.

3.1.2.6 GO term analysis of Foxa2 DE target genes identified *in vitro*

To globally categorize the types of genes that are differentially regulated by Foxa2, we determined the enriched Gene Ontology (GO) functional categories that are among genes either up regulated or down regulated between D3.5 and D5, since this is the time point Foxa2 is reaching its peak of expression (Figure 3-4). We found that the up regulated candidate target genes are enriched for neuronal differentiation processes, whereas the down regulated set of targets are enriched for genes involved in alternative cell fate processes such as cardiac muscle and immune system development (Figure 3-12, 3-13).

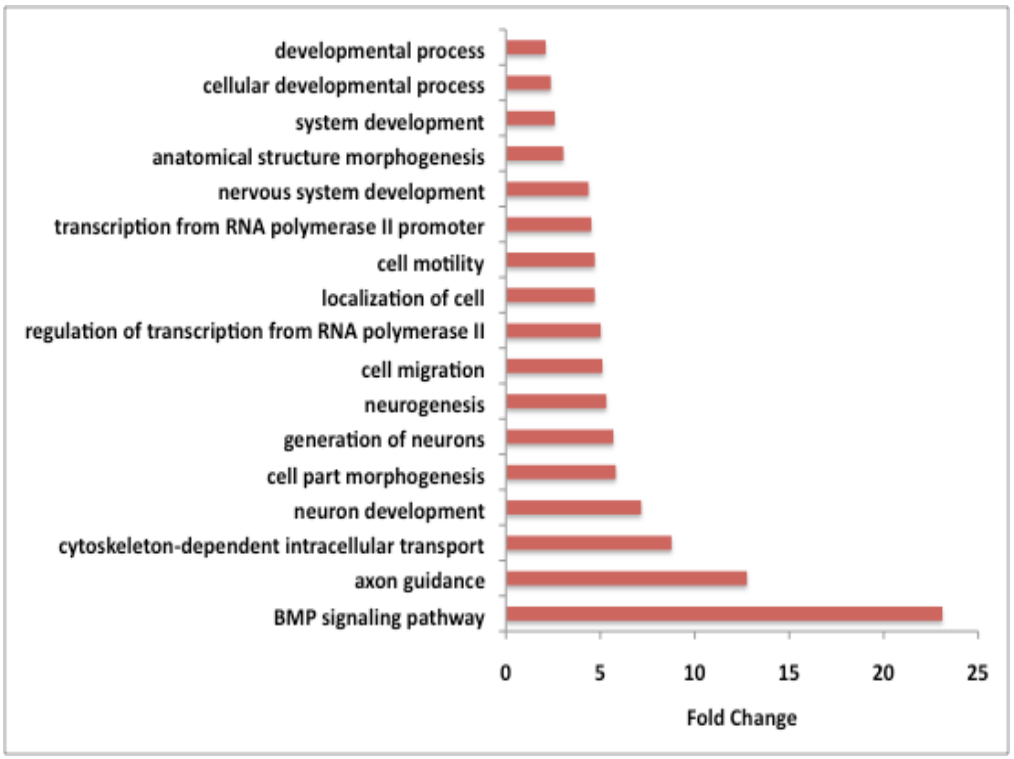

:Figure 3-12: Gene ontology (GO) categories showing the most enriched biological processes of up regulated candidate targets in the system between D3.5 and D5 of in vitro differentiation.

All categories displayed are of p-value<0.001 and are sorted according to fold change of the number of genes in each biological process in the experiment list over the reference list (whole genome).

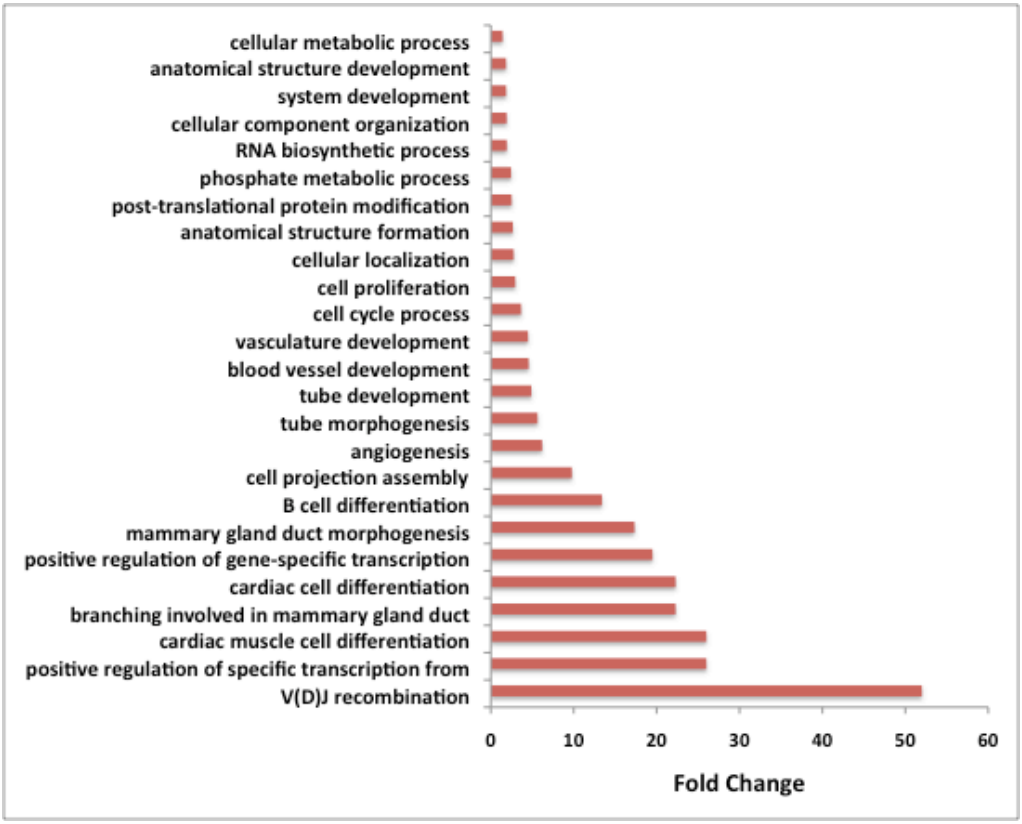

Figure 3-13: Gene ontology (GO) categories showing the most enriched biological processes of down regulated candidate targets between D3.5 and D5 of in vitro differentiation.

All categories displayed are of p-value<0.001 and are sorted according to fold change of the number of genes in the experiment list over the reference list (whole genome) for each biological process.

Although these functional categories are quite broad, they are consistent with the function of Foxa2 in promoting neuronal differentiation and possibly inhibiting the development of alternative cell fates. In order to validate the target genes in these categories we identified the transcription factors together and other genes involved in diverse functions such as, Bmp7 (Bmp signaling), Corin (floor plate marker), Axin2 (Wnt signaling target), Fgr2 (Fgf8 receptor), Slit2 (migration process). Initially we tested the sites bound by Foxa2 *in vitro* through ChIP-qPCR assays performed on chromatin from E12.5 ventral midbrain tissue. A large proportion of the sites (80%) validated by the independent ChIP-qPCR assays (Figure 3-15). The 20% of bound regions that did not validate may be bound at earlier developmental time points. We next assayed the functional relevance of Foxa2 binding to these target genes. For the loss of function model we used the $En1^{Cre/+;}Foxa1^{flox/flox};Foxa2^{flox/flox}$ mutant mice, since using $En1^{Cre/+}$ will affect the mDA cells at the progenitor (E10.5) stage.(Lin et al., 2009). The ventral midbrain was dissected from these mutants and the mRNA expression of candidate genes was compared to their wild type littermates by qPCR. Over 50% of the genes tested were affected in these mutants (Figure 3-14, 3-19). These results gave us the confidence that a significant proportion of the genes described as direct targets of Foxa2 will also be under its direct regulation. Interestingly, genes regarded as intrinsic determinants of mDA neuron specification (Lmx1a, and Lmx1b) are Foxa2 direct targets supporting further a direct role of Foxa2 in mDA specification (Huangfu and Anderson, 2006).

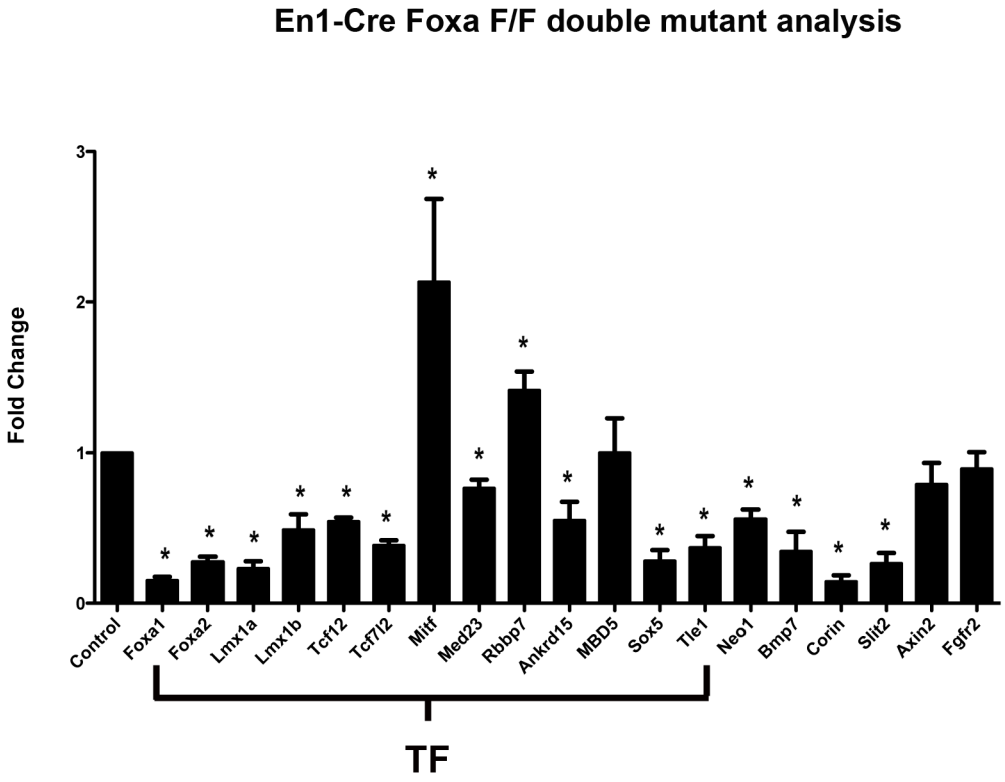

Figure 3-14: Validation of Foxa2 targets in ventral midbrain progenitors of $En1^{Cre/+;}Foxa1^{flox/flox};Foxa2^{flox/flox}$ *mice at E10.5.*

*Expression analysis by qPCR of candidate target transcription factors (TF), and genes involved in other functions. Foxa1 and Foxa2 are used as controls. * Fold change between mutant and its wild type littermate (Control) is statistically significant with p-value<0.05.*

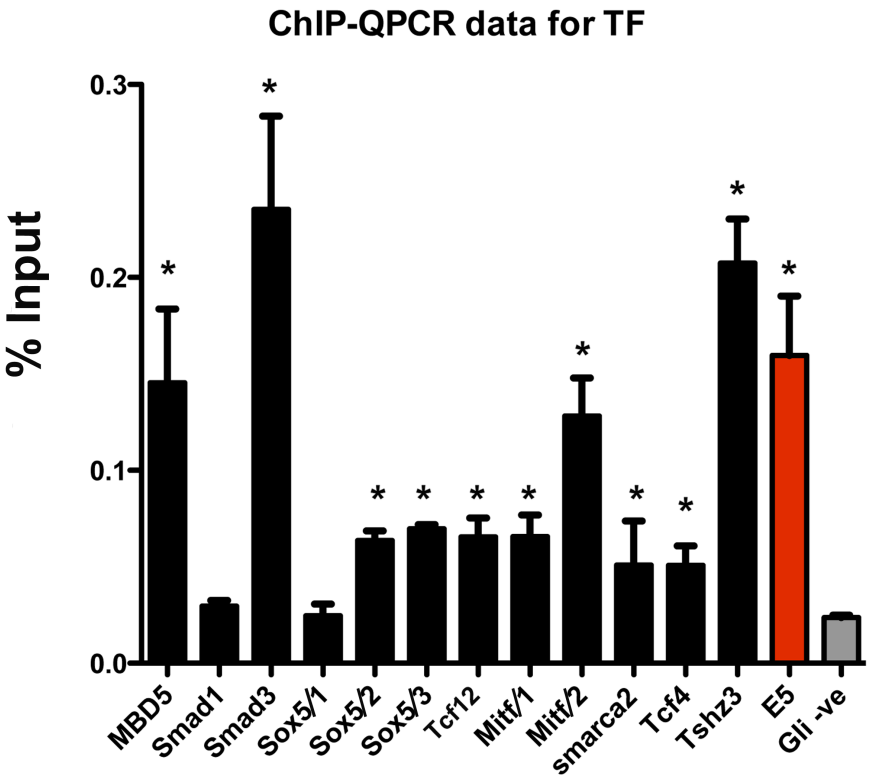
ChIP-QPCR data for TF
% Input
0.3
0.2
0.1
0.0
MBD5
Smad1
Smad3
Sox5/1
Sox5/2
Sox5/3
Tcf12
Mitf/1
Mitf/2
smarca2
Tcf4
Tshz3
E5
Gli -ve

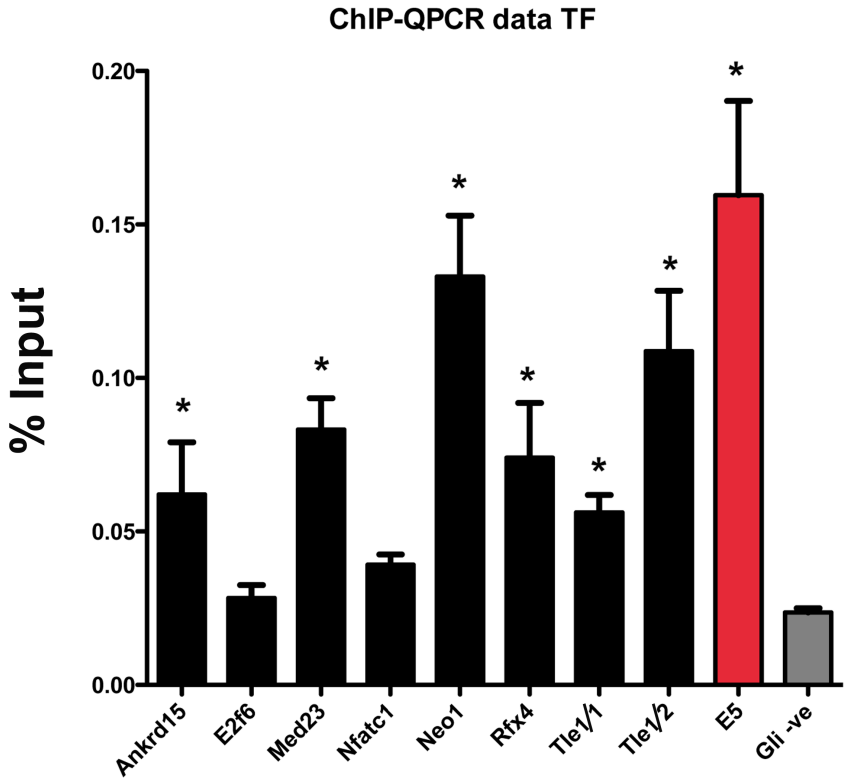
ChIP-QPCR data TF
% Input
0.20
0.15
0.10
0.05
0.00
Ankrd15
E2f6
Med23
Nfatc1
Neo1
Rfx4
Tle1/1
Tle1/2
E5
Gli -ve

Figure 3-15: Validation of ChIP-seq results by independent ChIP-qPCR experiments performed using chromatin from E12.5 mouse ventral midbrain.

*80% of the regions tested are enriched compared to negative control region. Primers amplifying a region in the Gli2 locus were used as negative control. Element 5 (E5) represents Foxa2 bound region in the Gli2 locus used as positive control. Error bars represent SEM. Each ChIP was performed on chromatin samples from three biological replicates. * Enrichment of Foxa2 bound regions over the negative region in the ChIP samples was statistically significant ($P < 0.05$).*

3.1.2.7 E-box motif is enriched in regions associated with up regulated genes involved in neuron development

The E-box motif identified as highly enriched in our ChIP-Seq data has been found in 1065 regions bound by Foxa2. Of these regions, 65 overlapped with up-regulated genes from the in vitro time course microarray expression assay. GO term analysis suggests the involvement of the up regulated genes in biological processes such as axon guidance, neuron maturation and neurogenesis supporting the assumption of an E-box binding protein possibly cooperating with Foxa2 in the induction of these genes (Figure 3-16). Only 14 down-regulated genes were associated with these genomic regions, which imply the correlation of this E-box sequence with transcription activation rather than repression.

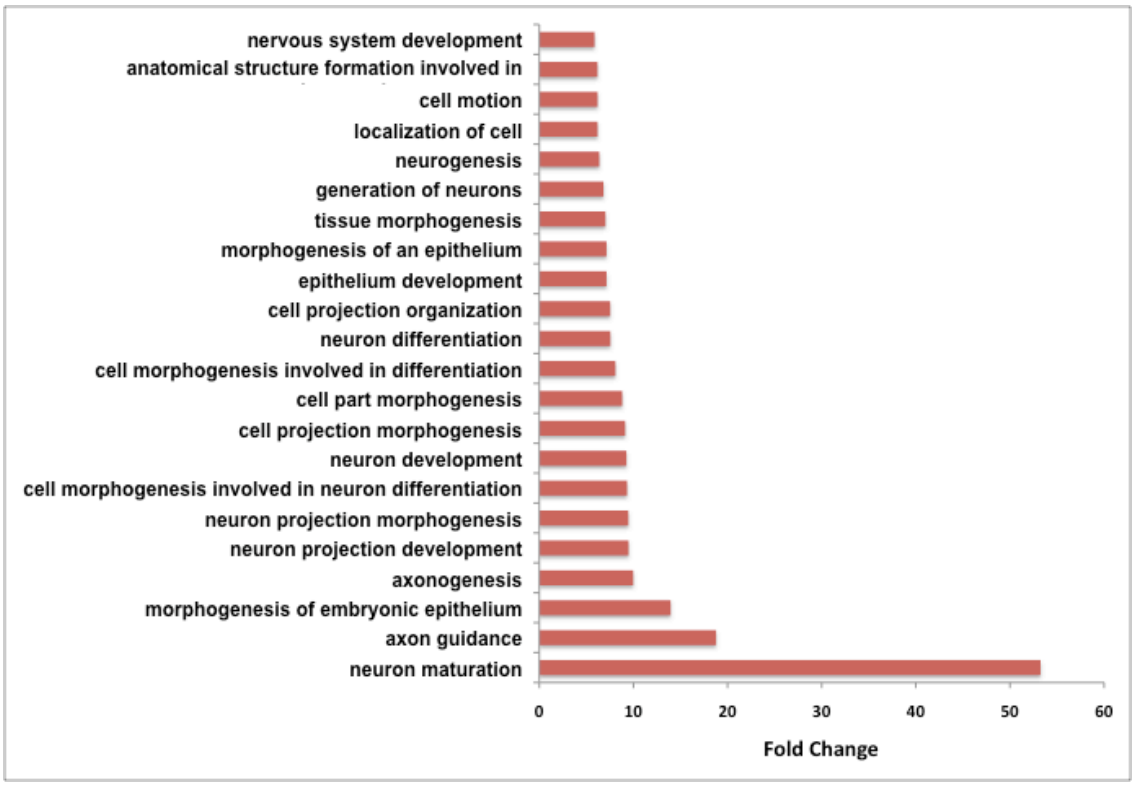

Figure 3-16: Gene ontology (GO) categories showing the most enriched biological processes of up regulated candidate targets between D3.5 and D5 of in vitro differentiation containing the enriched E-box sequence identified from the data set.

All categories displayed are of p-value<0.001 and are sorted according to fold change of the number of genes in the experiment list over the reference list (whole genome) for each biological process.

3.1.2.8 Otx2: a possible cofactor for Foxa2 function in DA progenitor specification

Otx2 has recently been discovered to control the proliferating activity of midbrain DA progenitors and is also required to promote differentiation by activating the expression of Lmx1a either directly or indirectly (Omodei et al., 2008). Furthermore, Otx2 is suggested to regulate Shh expression and positioning in the system. (Omodei et al., 2008). Since Otx2 is also required for regulating Foxa2 direct targets, Shh and

Lmx1a, we chose to test if Otx2 binds directly to the genomic regions identified to be bound by Foxa2. ChIP-qPCR experiments were performed on E12.5 ventral midbrain tissue using Otx2 antiserum to capture Otx2 bound genomic regions. All the regions tested contained an Otx2 DNA binding motif that enhance the possibility of an Otx2 interaction. The selected regions were Lmx1a CR2, Lmx1b CR1, Slit2, and Shh brain enhancer. Interestingly, Otx2 antiserum ChIP enriched for all the regions except for Slit2, and suggests the possible direct involvement of Otx2 in regulating these genes (Figure 3-17).

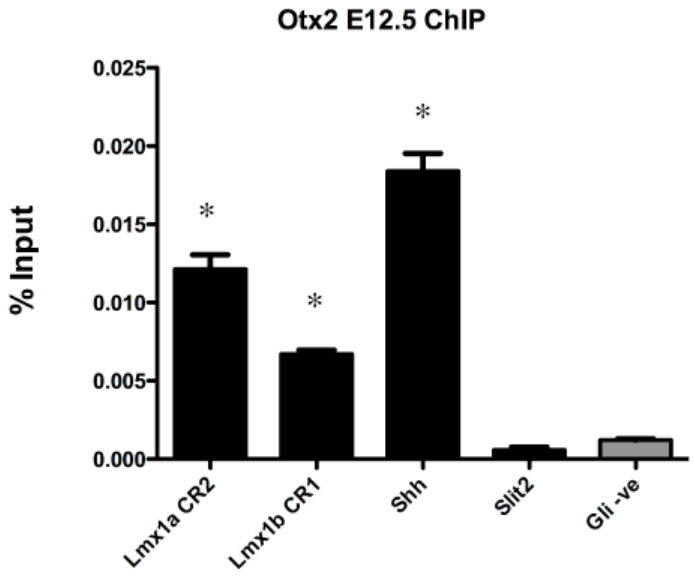

Figure 3-17: ChIP-qPCR experiments performed using chromatin from E12.5 mouse ventral midbrain using Otx2 specific antiserum.

*All regions tested are enriched compared to negative control region except for the Slit2 genomic region. Primers of an Otx2 unbound region in the Gli2 locus was used as negative control.. Error bars represent SEM. Each ChIP was performed on chromatin samples from three biological replicates. * Enrichment of Otx2 bound regions over the negative region in the ChIP samples was statistically significant ($P < 0.05$).*

Otx2 binding to similar regions as Foxa2 lead us to ask the questions: is Otx2 a Foxa2 cofactor and are there more regions bound by both factors leading to more genes being co-regulated? To answer the first question we searched the FANTOM 4 database where data from a large-scale mammalian two-hybrid screen performed using cDNA of transcription factors in human provided a large pool of information for possible physical interactions. Surprisingly, the search identified only a few genes including Otx2 as being co-factors of Foxa2 (Figure 3-18).

A

Gene symbol	Gene name
EN2	Homeobox protein engrailed 2
GSC	Homeobox protein gooscoid
HOXA5	Homeobox protein Hox-A5
NCOA1	Nuclear receptor coactivator 1
ONECUT1	one cut domain, family member 1
OTX2	orthodenticle homeobox 2
TLE1	transducin-like enhancer of split 1

B

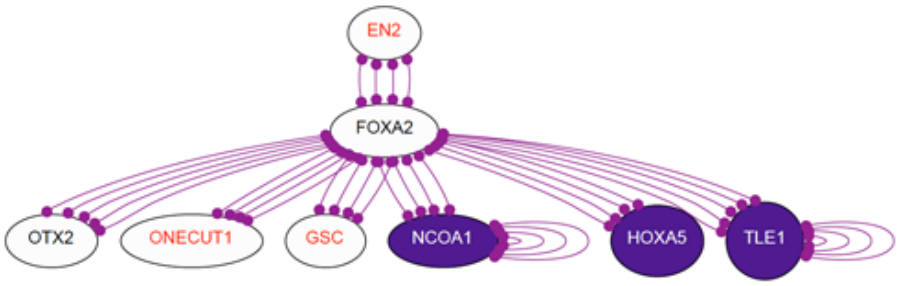

Figure 3-18: Possible Foxa2 cofactors predicted by FANTOM4. (A) Table of candidate Foxa2 cofactors and their respective gene names. (B) In purple, spheres connected by lines indicate the occurrence of physical interactions between the two factors sharing each end of the line.

To answer the second question, we decided to search the ChIP-seq data set for possible enrichment of the Otx2 motif. The position weight matrix from Harvard Uniprobe database was used to search the data set (www.thebrain.bwh.harvard.edu). From this search 629 sequences were found to contain the Otx2 PWM. To establish statistical confidence for the motif search results, 1000 random datasets were generated, each with the same number of sequences as the ChIP-seq dataset, and with the same deoxynucleotide composition. The same parameters were used to search for the Otx2 PWM in these random data sets. We found that the Otx2 PWM was not enriched in the random data sets compared to the Foxa2 ChIP-Seq data with a significance of P value<0.01. Furthermore the TSS of 54 up-regulated genes overlapped with these 629 genomic regions. This data suggests that Foxa2 together with Otx2 may regulate a subset of the genes up regulated in the *in vitro* system.

In order to test this hypothesis, we analyzed the expression of the 54 genes that correlate with an Otx2 binding motif, in the ventral midbrain of both E10.5, $En1^{Cre/+;}Foxa1^{flox/flox};Foxa2^{flox/flox}$ and $En1^{Cre/+;}Otx2^{flox/flox}$ mutant mice. Of the 54 genes tested in the $En1^{Cre/+;}Foxa1^{flox/flox};Foxa2^{flox/flox}$ mice, 24 were differentially regulated (Figure 3-19). Furthermore, 11 out of 24 Foxa2 dependant genes were also differentially expressed in the $En1^{Cre/+;}Otx2^{flox/flox}$ mutant mice (Figure 3-20). These 11 genes are the most likely to require both Foxa2 and Otx2 direct inputs for their proper regulation. ChIP-qPCR experiments need to be performed using Otx2 antiserum to further validate the possible binding of Otx2 to these regions. *(Please note, Slit2, Bmp7, Lmx1a, Lmx1b have been analyzed in Figure 3-14)*

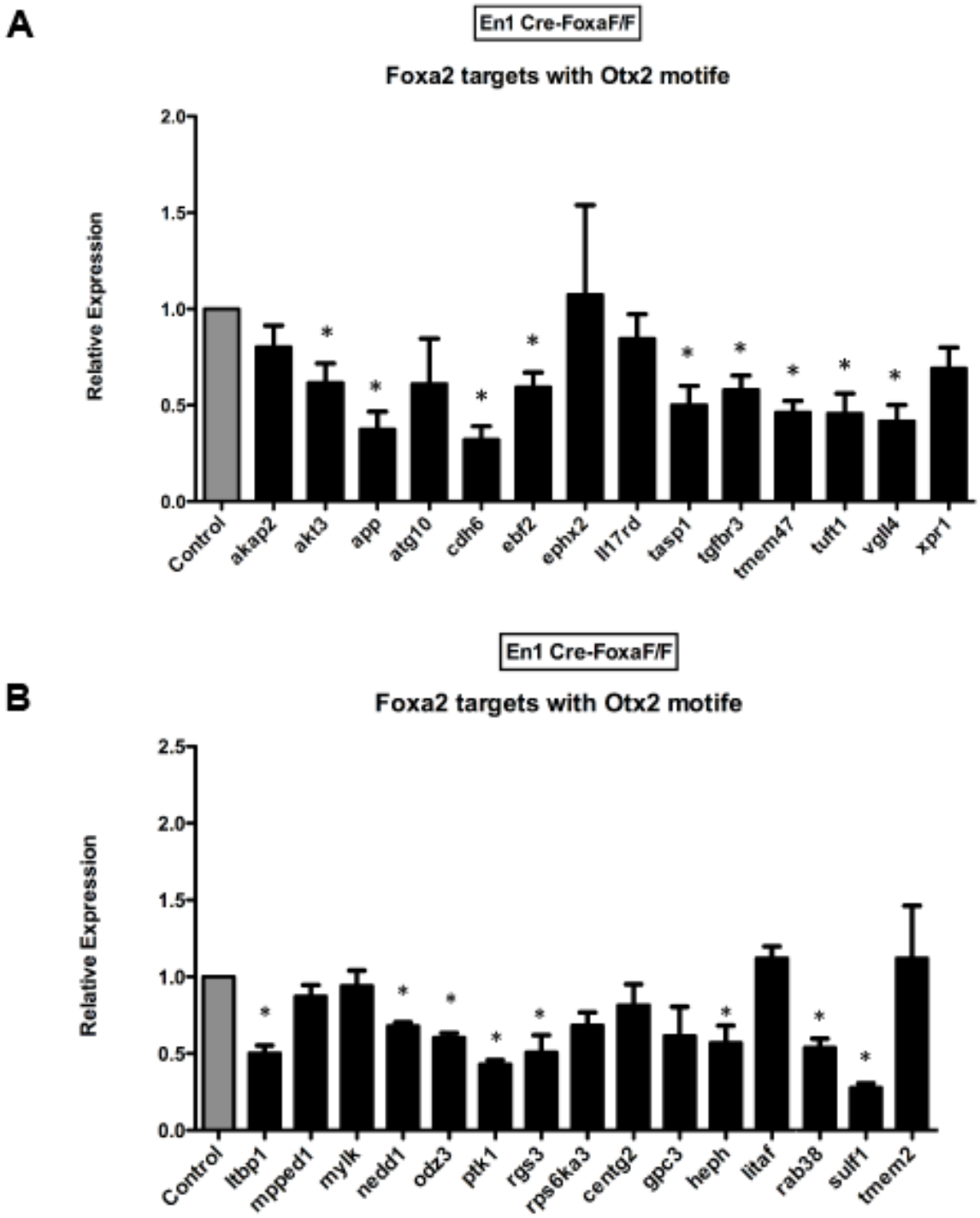
A
En1 Cre-FoxaF/F
Foxa2 targets with Otx2 motife
Relative Expression
2.0
1.5
1.0
0.5
0.0
Control
akap2
akt3
app
atg10
cdh6
ebf2
ephx2
Il17rd
tasp1
tgfbr3
tmem47
tuft1
vgll4
xpr1
B
En1 Cre-FoxaF/F
Foxa2 targets with Otx2 motife
Relative Expression
2.5
2.0
1.5
1.0
0.5
0.0
Control
Itbp1
mpped1
mylk
nedd1
odz3
ptk1
rgs3
rps6ka3
centg2
gpc3
heph
litaf
rab38
sulf1
tmem2

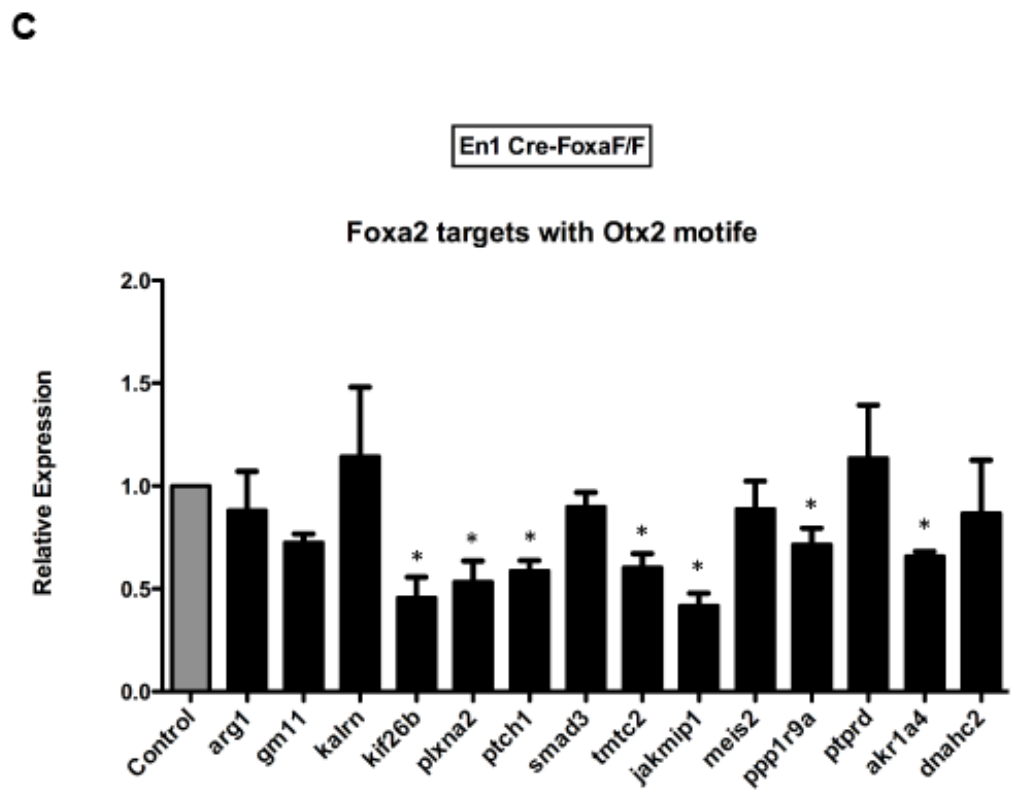

*Figure 3-19: qPCR expression analysis of Foxa2 target genes that may be coregulated by Otx2.in ventral midbrains of $En1^{Cre/+;}Foxa1^{flox/flox};Foxa2^{flox/flox}$ mice at E10.5. (A-C) Of the 54 genes with genomic regions bound by Foxa2, that contains an Otx2 DNA binding motif 24 are differentially expressed within these mutants. * Fold change between mutant and wild type littermate (Control) is statistically significant with p-value<0.05.*

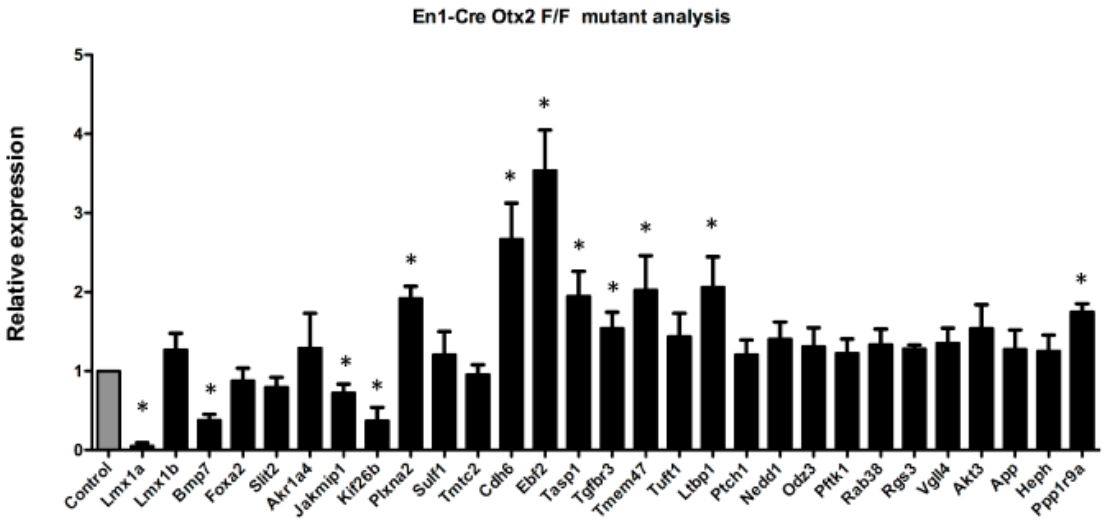

*Figure 3-20: qPCR expression analysis of Foxa2 regulated target genes that may be coregulated by Otx2.in ventral midbrains of $En1^{Cre/+;}Otx2^{flox/flox}$ mice at E10.5. (A-C) Of the 24 genes regulated by Foxa2, that contains an Otx2 DNA binding motif in their candidate regulatory regions, 10 are differentially expressed within these mutants and are likely to require an Otx2 input for their proper expression. In this case Lmx1a is used as control (Omodei et al., 2008) * Fold change between mutant and wild type littermate (Control) is statistically significant with p-value<0.05.*

3.1.2.9 Predictions of physical interaction of transcription factors regulated by Foxa2 *in vitro*

Transcriptional regulatory networks drive tissue specific spatial and temporal patterns of gene expression (Naef and Huelsken, 2005). These networks usually involve the assembly of transcription factors on DNA target promoter sequences of genes they regulate. Often these transcription factors do not act independently but form complexes with other transcription factors and members of the transcription regulation machinery (Ravasi et al., 2010). To test this hypothesis in our system, we used the Foxa2-bound targets whose expression are affected in $En1^{Cre/+;}Foxa1^{flox/flox};Foxa2^{flox/flox}$ mutant embryos together with Foxa2 and Otx2 on FANTOM and searched for possible

interactions. Interestingly, other than Foxa2 interacting with Otx2 we see that Tle1 is a possible cofactor (Figure 3-21). Tle1 is part of the Groucho family of transcriptional repressors that play key roles in developmental processes (Santisteban et al., 2010). It has previously been shown in liver cells that Foxa proteins recruit Tle cofactors to the site of action and repress gene expression (Sekiya and Zaret, 2007). We therefore hypothesize that Foxa2 may act through Tle1 to repress the alternative cell fates. In addition, Foxa2 interacts with Otx2 to induce the DA neuronal cell fate. These predictions also suggest that Foxa2 and Otx2 may be involved in a larger complex including Mitf, a known gene activator involved in melanocyte development, proliferation and survival (Kumasaka et al., 2005). Hence, Mitf may play similar roles in the mDA system during specification.

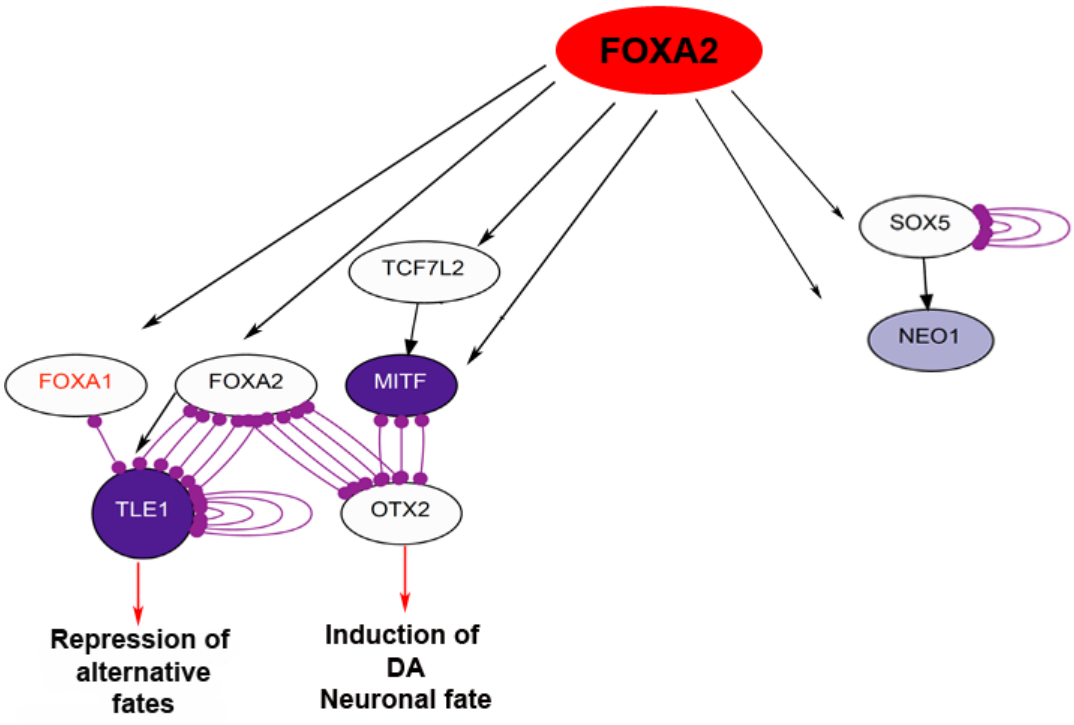

Figure 3-21: Physical interaction identified, using FANTOM4, of Foxa2 regulated transcription factors.

In purple, Circles connected by lines indicate the occurrence of physical interactions between the two factors sharing each end of the line. Black arrows indicate positive regulation of expression. Black Arrows leading from factors other than Foxa2 are predicted by FANTOM4. Foxa2 and Otx2 possibly interact and cooperate to induce the DA neuronal fate. The Tle1/Foxa1/2 interaction is possibly required for the repression of alternative fates.

3.1.2.10 Identification of Lmx1a and Lmx1b regulatory elements

Analysis of the phenotype of Lmx1a and Lmx1b double mutant embryos demonstrated overlapping essential reveals their roles in the specification and proliferation of mDA progenitors, and ensure their proper differentiation (Yan, 2008). In an attempt to further characterize the transcriptional regulators that act upstream of Lmx1a and Lmx1b in the midbrain we used an *in vivo* reporter assay to identify the *cis*-acting sequences that regulate *Lmx1a/b* gene expression (Simmons, 2001). Two well-conserved Foxa2-bound genomic regions identified from the ChIP-Seq data in both gene loci were used for independent ChIP-qPCR analysis (Figure 3-22).

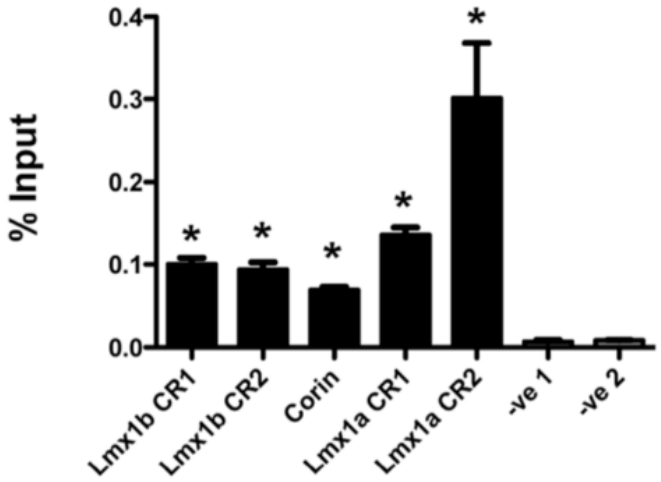

Figure 3-22 ChIP-qPCR experiments performed using chromatin from E12.5 mouse ventral midbrain using Foxa2 specific antiserum.

*Lmx1a/b conserved regions are enriched for Foxa2 binding compared to negative control regions (-ve1, -ve2). The conserved region in the Corin gene locus is used as positive control. Error bars represent SEM. Each ChIP was performed on chromatin samples from three biological replicates. * Enrichment of Foxa2 bound regions over the negative region in the ChIP samples was statistically significant ($P < 0.05$).*

All four regions enriched for Foxa2 binding and confirmed the ChIP-Seq peaks identified for them. To further validate these regions *in vivo*, they were cloned in a LacZ reporter plasmid and injected into fertilized mouse embryos to assess their enhancer activity by X-gal staining at E10.5. Interestingly, three out of the four regions exhibited enhancer activity driving expression of the *lacZ* reporter gene to regions of the ventral CNS in transgenic mice (Figure 3-23). Both Lmx1a genomic regions CR1, and CR2 activated LacZ expression in transgenic embryos. CR1 is 522 bp long and CR2 is 446 bp. Lmx1a CR1 gave reporter expression throughout the ventral neural tube that mimicked the Foxa2 expression pattern, where as Lmx1a CR2 gave an expression pattern similar to rostral domain of the Lmx1a endogenous expression pattern, i.e. in the caudal forebrain and anterior midbrain (Figure 3-23A and C). Identifying two enhancers for Lmx1a suggests the requirement of multiple signaling inputs to multiple cis-regulatory elements for the proper regional expression of this gene. One of the two regions tested for Lmx1b gave reporter expression (Fgure 3-23E). This region was named Lmx1b CR1 and is 206 bp long. The LacZ expression pattern mimics very well the expression of Lmx1b in the ventral neural tube, and the future auditory neural tissue (Yan, 2008; Guo et al., 2007). Coronal sections through the midbrains of the embryos that gave restricted expression

patterns in the ventral midbrain indicate that LacZ expression was restricted to endogenous domains of Lmx1a and Lmx1b expression in the ventral midbrain (Figure 3-25, 3-26).

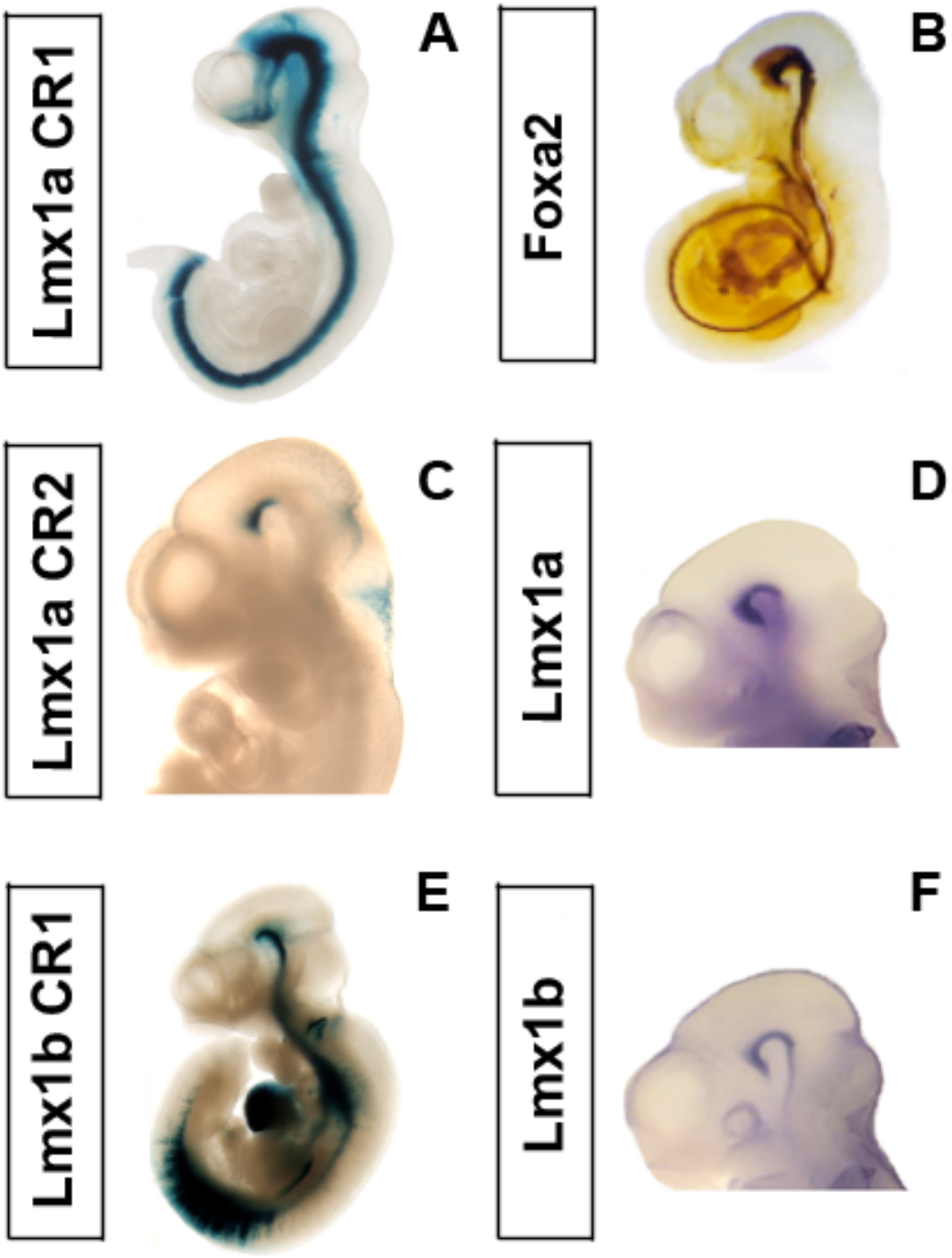

Figure 3-23:LacZ reporter expression driven by the genomic regions identified to be bound by Foxa2 within the Lmx1a and Lmx1b gene loci.

(A-B) Lmx1a CR1 has a broad expression pattern very similar to the Foxa2 expression pattern is the same developmental stage. 2/2 transgenics gave the same expression pattern (C-D) Lmx1a CR2 drives expression in a restricted domain within the rostral midbrain and most caudal forebrain regions similar to the Lmx1a expression pattern in those regions. 1/1 transgenic embryo gave this expression pattern (E-F) Lmx1b CR1 is sufficient to drive expression in the Lmx1b positive domains in the midbrain. 3/4 transgenic embryos gave this expression pattern. (B, D, and F are whole mount ISH of Foxa2, Lmx1a and Lmx1b respectively. Modified from Epstein et al, 1996, and Yan, 2008)

Consensus binding sites for Foxa2 were identified in all enhancers supporting the view that Foxa2-dependent mechanisms exist to activate *Lmx1a/b* gene expression in the midbrain floor plate. Luciferase assays were carried out for all three enhancers to establish if Foxa2 exerts an input on the regulatory activity of these enhancers in P19 cells. Co-transfection of Foxa2 with the Lmx1a CR1 and CR2 luciferase constructs shows a significant but not very high fold change of luciferase activity over the single transfections. This may be due to the presence of another co-activator since these enhancers already posses positive regulatory activity when compared to the empty luciferase vector. The presence of a repressor of Foxa2 activity may be possible, not allowing optimum Foxa2 regulation of these enhancers. Co-transfection of Foxa2 with the Lmx1b CR1 luciferase construct shows a significant and high fold change suggesting a strong Foxa2 input in the regulation of this enhancer. From these results we chose to mutate the Foxa2 binding site (Figure 3-24 B) found within the Lmx1b CR1 and perform the *in vivo* LacZ reporter assay. The LacZ expression of the mutated construct was

generally weaker and the midbrain LacZ expression was reduced to a large extent. These results clearly show the requirement of the Foxa2 site for the proper regulation of this enhancer.

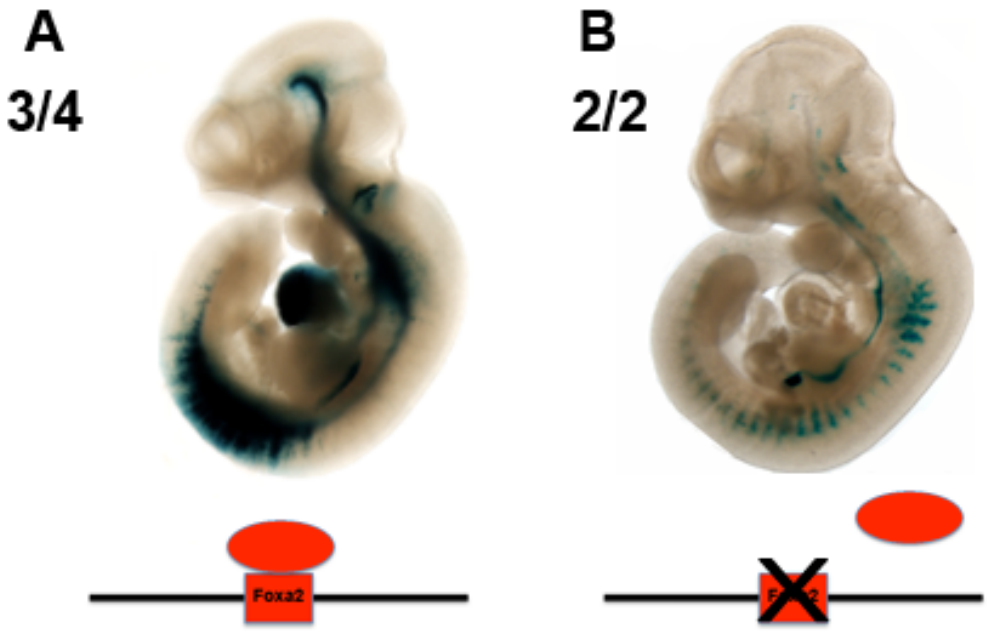

Figure 3-24: The Foxa2 DNA binding motif within the Lmx1b CR1 is required for driving expression to the floor plate of the midbrain and in caudal CNS regions.

(A) Wild type expression pattern. Red box indicates the Foxa2 DNA binding motif. (B) Foxa2 motif mutated construct drives very weak expression and the majority of the midbrain specific expression was lost. 2/2 transgenic embryos gave the same expression pattern.

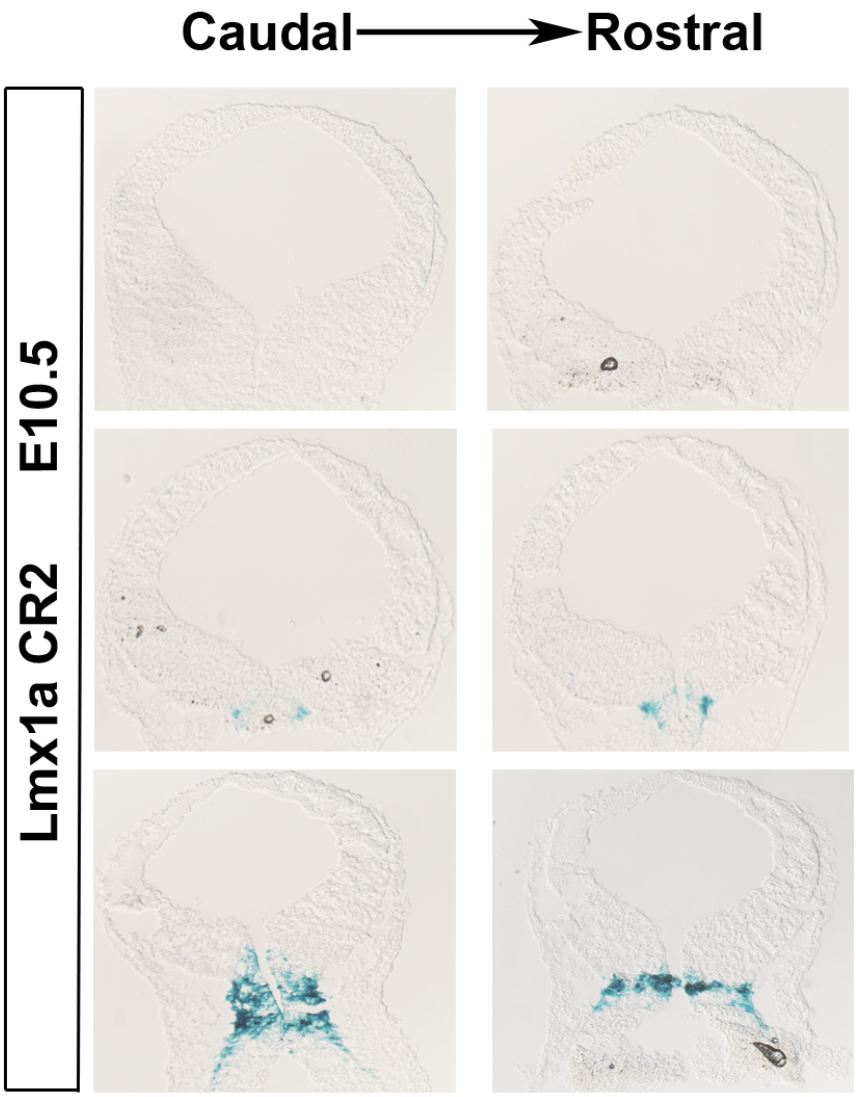

Figure 3-25: Coronal sections through the midbrain of Lmx1a CR2 transgenic mouse at E10.5.

LacZ expression pattern is restricted to the floor plate in the rostral midbrain. It is unclear whether LacZ expression is restricted to the floor plate or is also expressed in more dorsal progenitors in the anteriormost regions based on these sections, however the anteriormost expression mimics Lmx1a expression in wild-type embryos (Fig. 3-23D).

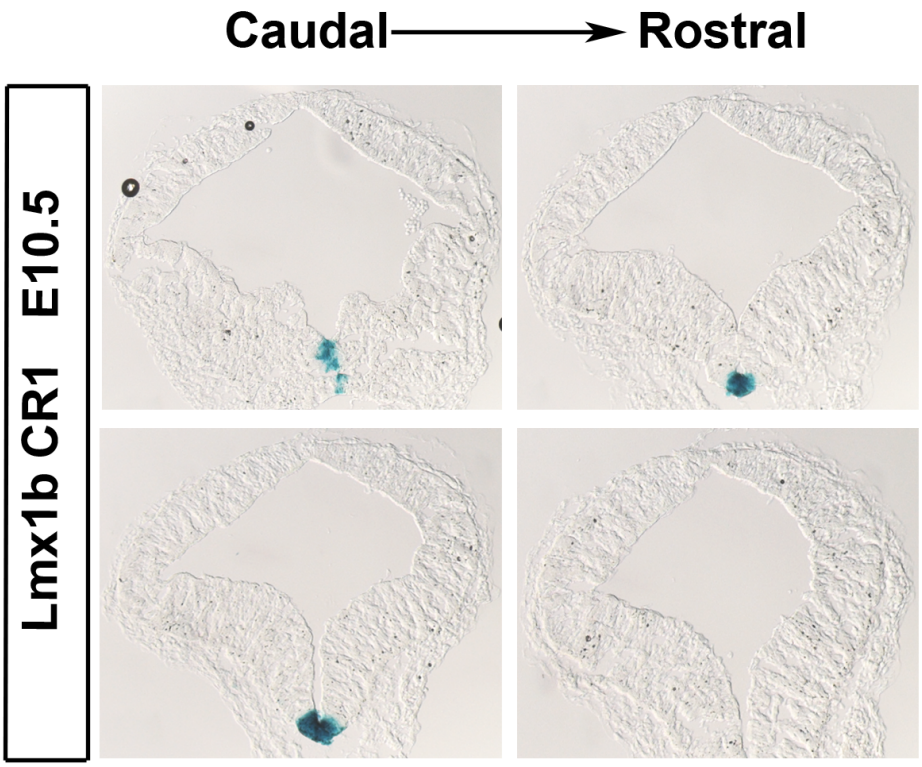

Figure 3-26: Coronal sections through the midbrain of the Lmx1b CR1 transgenic mouse at E10.5.

Expression pattern is restricted to the floor plate region throughout the A-P axis, similar to Lmx1b expression in wild-type embryos at this stage.

3.1.3 Identification and characterization of Foxa2 binding events *in vivo*

In the next chapters we present results generated from Foxa2 ChIP-Seq experiments performed on *in vivo* E12.5 and E14.5 ventral midbrain dissected tissue. For illustrative reasons many of the regions identified as bound by Foxa2 will be identified by black blocks rather than the peaks you have been shown up to this point.

3.1.3.1 Foxa2 ChIP-seq performed on E12.5 and E14.5 ventral midbrain tissue

To identify genes regulated by Foxa2 that are involved in differentiation we chose a different approach than the previous experiment. We dissected ventral midbrain tissue at time points where differentiation is actively taking place. The proneural gene Neurg2 and the orphan nuclear receptor Nurr1, expressed in immature and mature neurons, are key markers of this process. At E12.5 the ventral midbrain stains for Neurog2 in a salt and pepper pattern and an overlap with Nurr1 can clearly be observed (Ferri et al., 2007). Given this pattern of expression, E12.5 is an appropriate time point to model early differentiation and study the role of Foxa2 in this process.

In addition of investigating the role of Foxa2 function in early differentiation we wanted to complement the study with an additional investigation of the role of Foxa2 in late differentiation of mDA neurons. The time point chosen for this study is E14.5 where neurogenesis has largely ceased and only mature neurons can be identified by staining for Nurr1 and TH, where most if not all Nurr1+ cells stain for TH, indicating that not many immature neurons are present.

Figure 3-27 indicates the ventral midbrain regions dissected and harvested for the ChIP-seq analysis. This procedure was performed for both E12 and E14 ChIP-Seq assays.

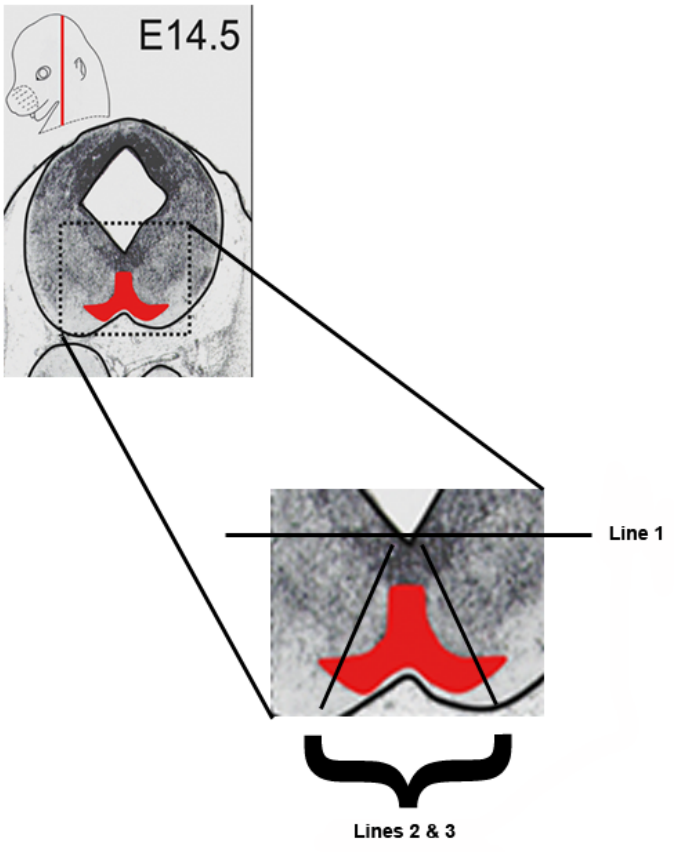

Figure 3-27:Schematic of E14.5 midbrain dissection limits defining the mDA domain.

Line 1 indicates the dorsal limit. Lines 2 and 3 indicate the harvested area, including the mDA domain used for the ChIP experiments. (Modified from Jacobs, 2009)

The quality of the *in vivo* data sets was assessed according to known and newly discovered positive controls from the *in vitro* analysis. Enhancers known to be bound by Foxa2, such as the Shh brain enhancer, the Lmx1a CR2, Lmx1b CR1 and the Aadc neuronal promoter, were detected by our *in vivo* ChIP-Seq assays, and all these bound regions had a FDR well under 5% (Figure 3-29). For the purpose of these studies we assigned 5% FDR as the cut off point for the regions to be included in the analysis.

Furthermore, the Foxa2 motif was enriched in both E12 and E14 ChIP-seq data sets (Figure 3-28B-C). We also observed 1407 (20%) regions in common between the *in vitro* and E12.5 data sets, and 1717 (25%) regions were in common between the E12 and E14 data sets. Of these regions over 40% were in common with the *in vitro* data set, further confirming the high quality of the data in all three ChIP-seq experiments.

.

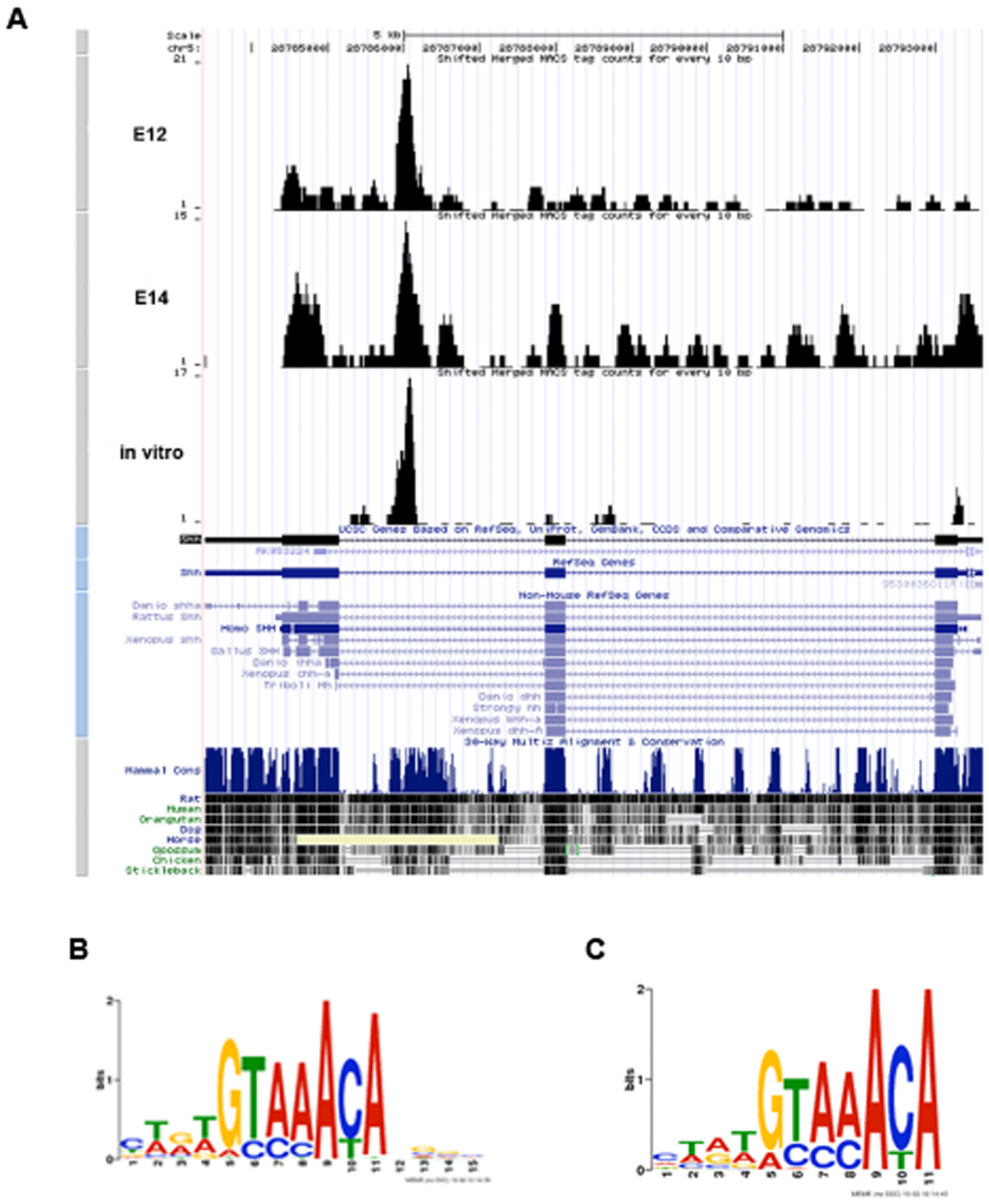

Figure 3-28:. (A) Schematic of the Shh gene locus extracted from the UCSC genome browser. Foxa2 peaks can be observed in the Shh floor plate enhancer region in all three data sets. (B) De novo motif enriched in E12 and E14 ChIP-seq data sets identified using MEME search engine. The motif is identical to the Foxa2 DNA binding motif.

A

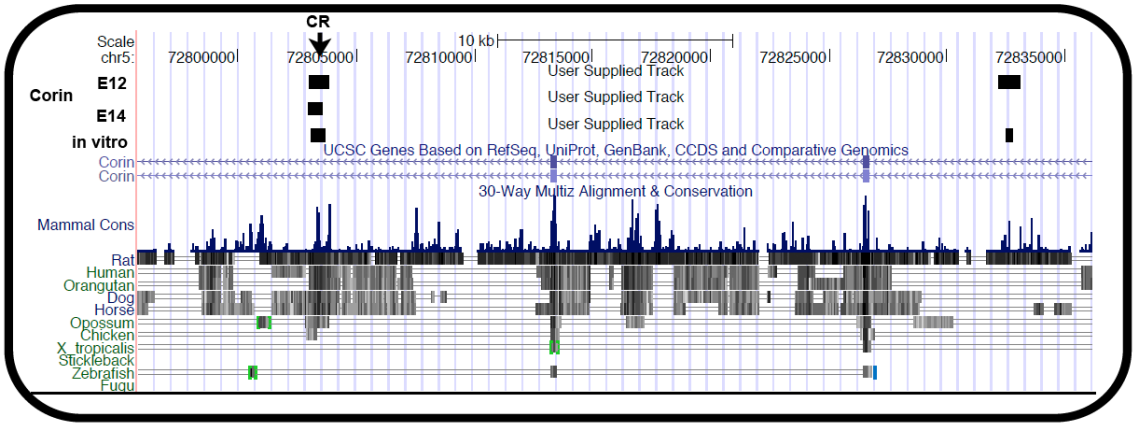
CR
Scale
chr5:
72800000
72805000
72810000
72815000
72820000
72825000
72830000
72835000
10 kb
Corin
E12
E14
in vitro
User Supplied Track
User Supplied Track
User Supplied Track
UCSC Genes Based on RefSeq, UniProt, GenBank, CCDS and Comparative Genomics
Corin
Corin
30-Way Multiz Alignment & Conservation
Mammal Cons
Rat
Human
Orangutan
Dog
Horse
Opossum
Chicken
X_tropicalis
Stickleback
Zebrafish
Fugu

B

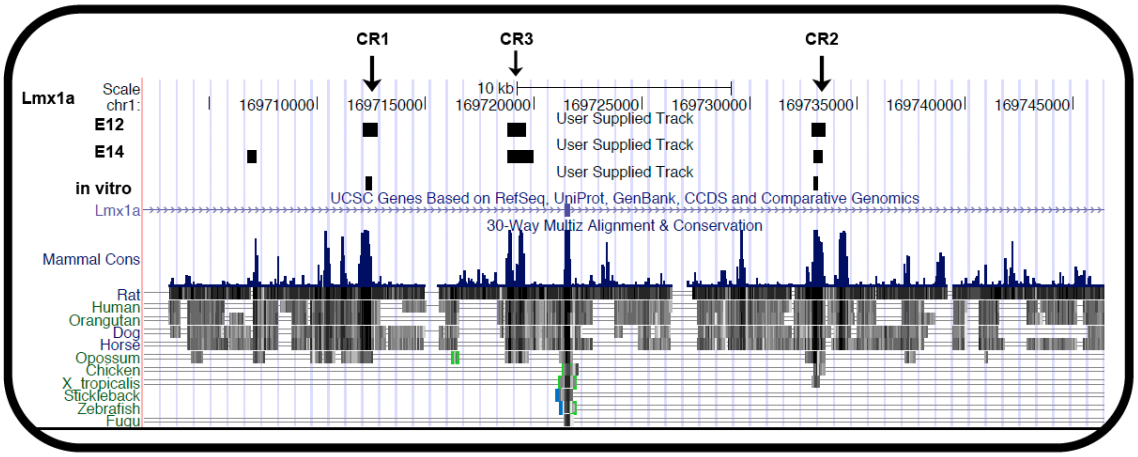
CR1
CR3
CR2
Lmx1a
Scale
chr1:
169710000
169715000
169720000
169725000
169730000
169735000
169740000
169745000
10 kb
E12
E14
in vitro
User Supplied Track
User Supplied Track
User Supplied Track
UCSC Genes Based on RefSeq, UniProt, GenBank, CCDS and Comparative Genomics
Lmx1a
30-Way Multiz Alignment & Conservation
Mammal Cons
Rat
Human
Orangutan
Dog
Horse
Opossum
Chicken
X_tropicalis
Stickleback
Zebrafish
Fugu

C

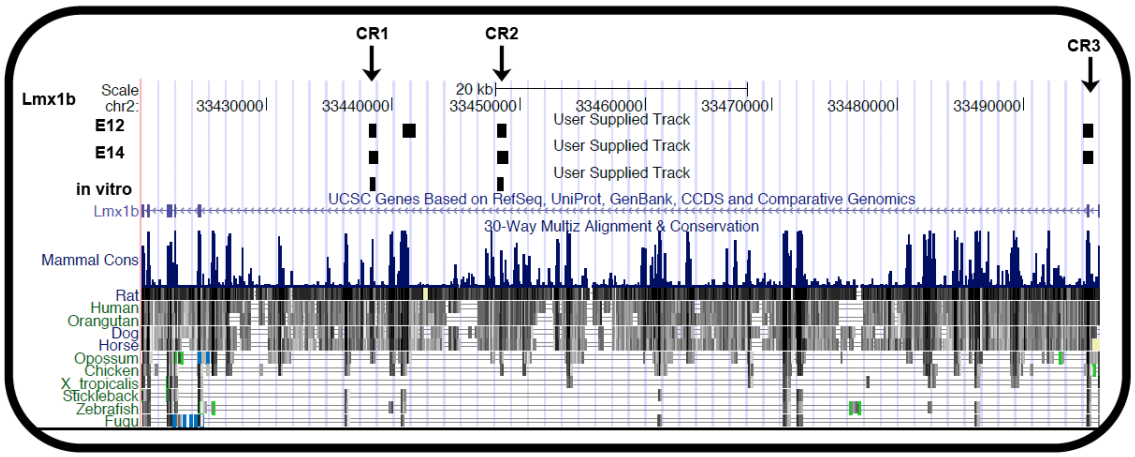
CR1
CR2
CR3
Lmx1b
Scale
chr2:
33430000
33440000
33450000
33460000
33470000
33480000
33490000
20 kb
E12
E14
in vitro
User Supplied Track
User Supplied Track
User Supplied Track
UCSC Genes Based on RefSeq, UniProt, GenBank, CCDS and Comparative Genomics
Lmx1b
30-Way Multiz Alignment & Conservation
Mammal Cons
Rat
Human
Orangutan
Dog
Horse
Opossum
Chicken
X_tropicalis
Stickleback
Zebrafish
Fugu

D

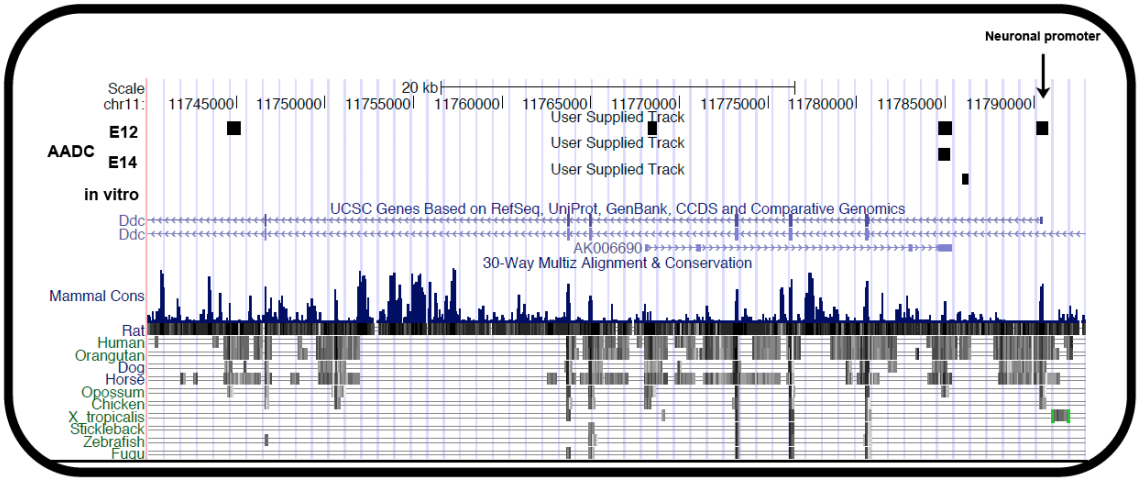

Figure 3-29: Schematic of the genomic regions bound by Foxa2 in all three data sets.

(A-C) Foxa2 peaks can be observed in the gene loci of Corin, Lmx1a, and Lmx1b previously identified in the in vitro data set. (D) Foxa2 peaks can be observed in the AADC locus in all three data sets. At E12 a Foxa2 peak is observed in the AADC neuronal promoter described by (Aguanno et al., 1995). (Each black block indicates the area covered by the detected peak)

3.1.3.2 Characterization of ChIP-Seq peaks identified using E12.5 ventral midbrain tissue

From the E12.5 ChIP-seq analysis we identified 7008 high confidence peaks. Interestingly, 54% of peaks were located within an annotated gene region. Only 18% of the peaks were located within 2 kb upstream or downstream of the TSS of annotated genes, while 34% of the peaks were located within 10 kb of the TSS (Figure 3-30). Out of peaks overlapping genes 24% were localized within the first intron (Figure 3-31 A). We also observed that over 30% of all peaks were more than 100 kb from the closest down stream gene (Figure 3-31 B). Surprisingly, 45% overlapped conserved genomic regions, identical to the *in vitro* data, suggesting that Foxa2 binding to conserved sequences is a key characteristic of its binding to the genome. Similar to the *in vitro* data Foxa2-binding sites are observed at a range of locations across the mouse genome.

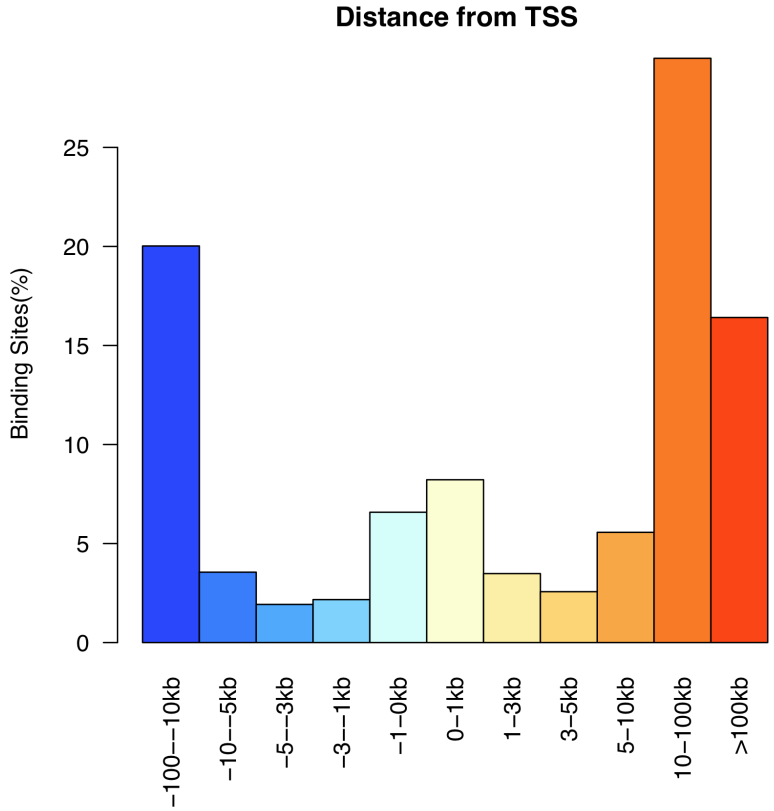

Figure 3-30: Percentage of binding sites located at various distances from TSS. Recruitment at distal regions from the TSS is a general characteristic of Foxa2 genomic recruitment

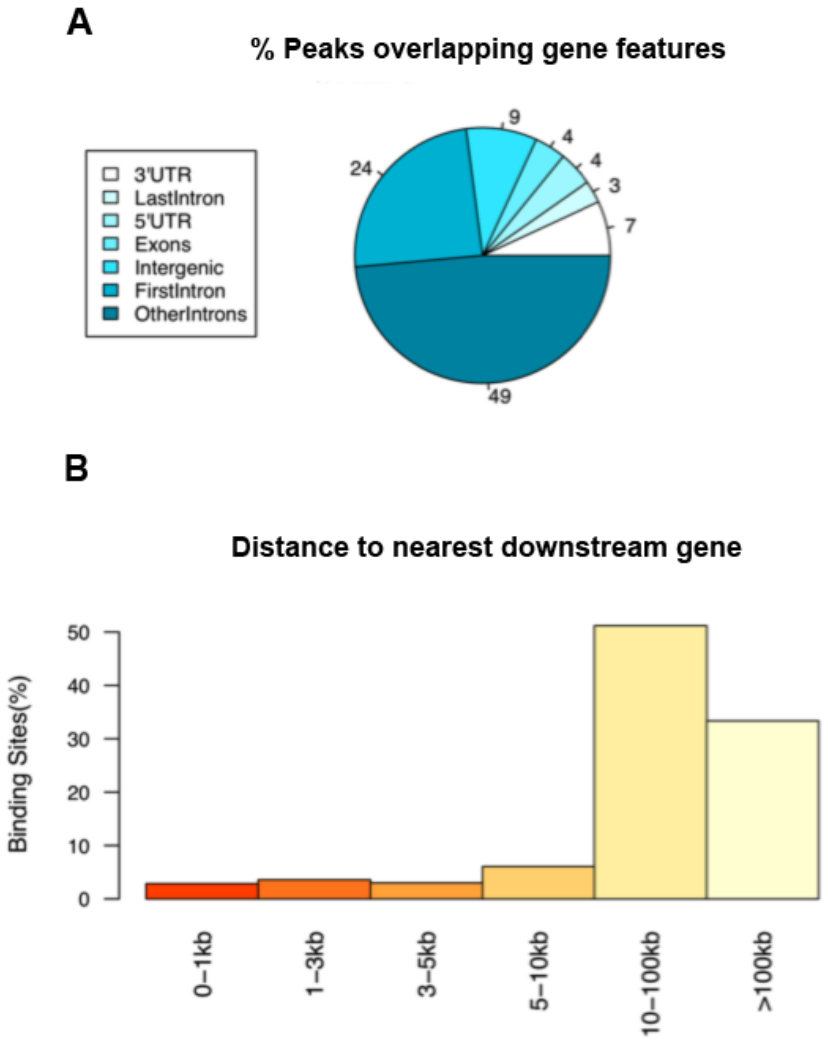

Figure 3-31. (A) Distribution of peaks within genes. Majority of peaks are distributed within intronic regions with 24% identified within the first intron. (B) Distribution of the peaks from the nearest downstream gene. Most of the peaks are found between 10 and 100 kb away from the nearest downstream gene.

3.1.3.3 Characterization of ChIP-seq peaks identified using E14.5 ventral midbrain tissue

CHIP-seq performed on E14.5 ventral midbrain tissue identified 8346 high confidence peaks. Of these peaks 57.5% overlapped a gene region. Peaks identified within 2kb of the TSS of annotated genes represent 21% of the total number of peaks, and 38% were located within 10 kb (Figure 3-32). 20% of peaks within genes were located within the first intronic region (Figure 3-33 A). Around 30% of the peaks were over 100kb away from the closest downstream gene (Figure 3-33 B). Out of all peaks 41% overlapped with conserved genomic regions further confirming Foxa2 binding to conserved sequences as a key characteristic.

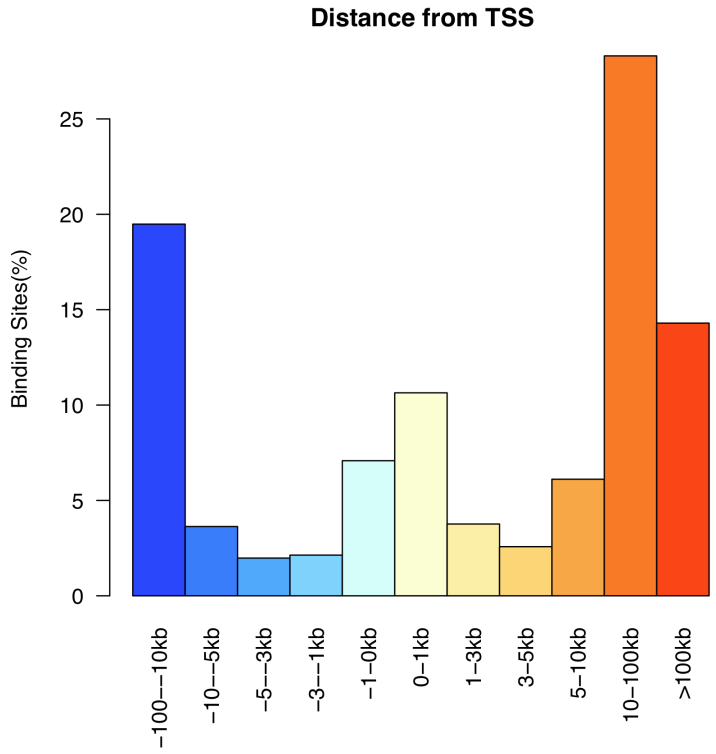

Figure 3-32: Percentage of binding sites located at various distances from TSS. Recruitment at distal regions from the TSS is a general characteristic of Foxa2 genomic recruitment. An increase in recruitment of Foxa2 closer to TSS of annotated genes is observed.

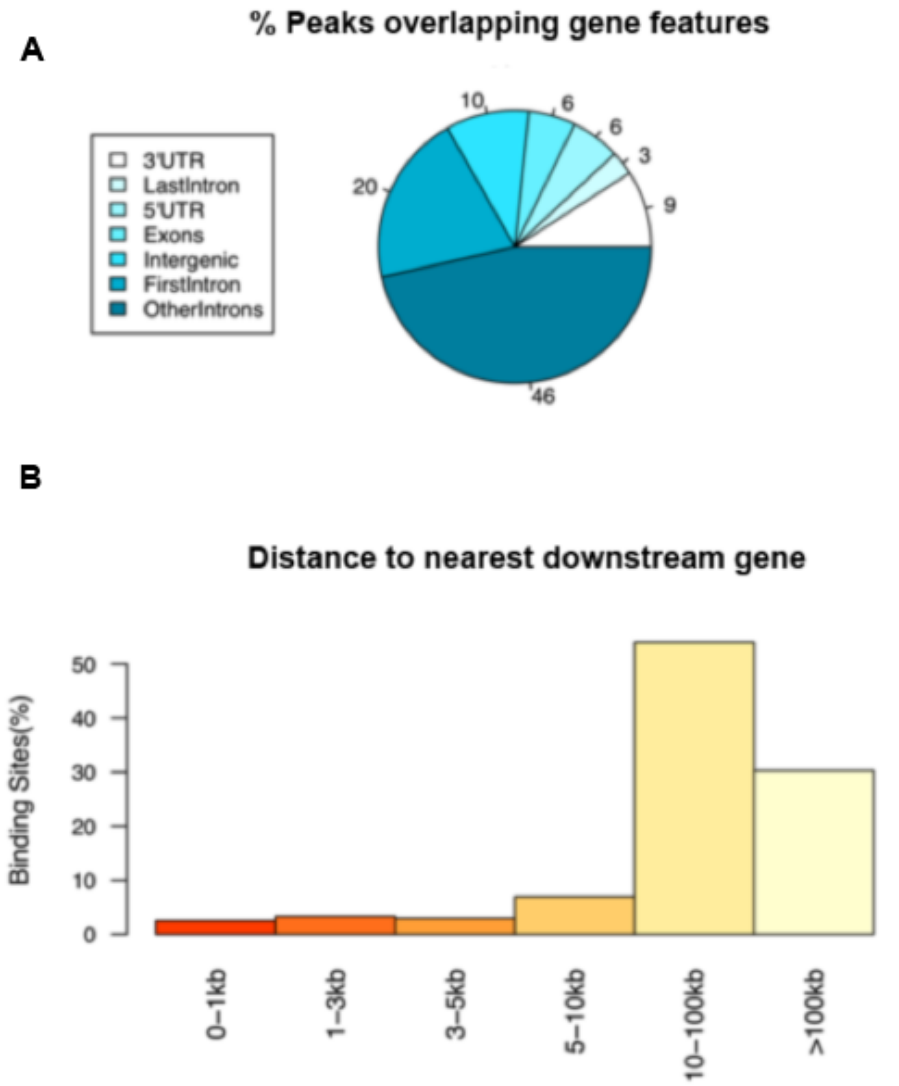

Figure 3-33: (A) Distribution of peaks within genes. Majority of peaks are distributed within intronic regions with 2o% identified within the first intron. A reduction compared to the other two data sets. (B) Distribution of the peaks from the nearest downstream gene. Most of the peaks are found between 10 and 100 kb away from the nearest downstream gene.

3.1.3.4 Overlap of ChIP-Seq lists with microarray time course expression assays

To identify functionally relevant genes, we chose to overlap the Foxa2-bound targets with expression profiling data of floor plate regions of the midbrain where the mDA cells reside. In the lab, a former postdoctoral fellow dissected midbrain floor plate regions from E10.5, E11.5, E12.5 and E14.5 embryos and analyzed the expression profile of these cells by microarray experiments using Illumina MouseRef-8 v 2.0 expression beadchip platforms. These expression data was then analyzed using Gene Spring (Agilent technologies) to study the temporal dynamics of gene expression in this tissue (Figure 3-35, 3-36). We identified 5549 genes that were differentially expressed (DE) between the time points described. Of these genes 24% mapped with at least one peak from the *in vitro* ChIP-seq data set. Similarly, 22% of DE genes mapped with peaks from the E12 ChIP-seq data set, and 26% mapped with the E14 ChIP-seq data set. Interestingly, the distribution of the Foxa2 peaks from the TSS of the DE genes indicate a 10% increase of peaks identified within 2kb of the TSS when comparing the *in vitro* ChIP-seq data with the E12.5 ChIP-seq data, and a 15% increase was observed when comparing the *in vitro* data with the E14.5 data set (Figure 3-34). This observation is not surprising since a similar distribution can be observed on the genome wide level as well. This data suggests that Foxa2 binding shifts slightly closer to promoter regions during differentiation of mDA neurons. This is comparable with adult liver genome wide studies of Foxa2, where many binding events can be identified close to the TSS, unfortunately these studies did not compare different developmental stages (Wederell et al., 2008).

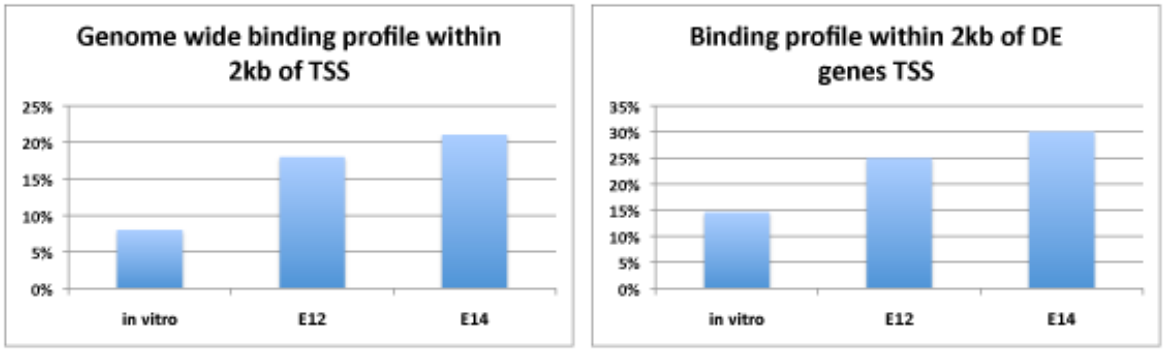

Figure 3-34:Comparison of genome wide Foxa2 binding profile with DE candidate targets. Distribution of peaks within 2 kb of TSS of all annotated genes (Genomic binding) and of DE targets reveals that the shift of Foxa2 binding towards the TSS of genes in the in vivo data sets is a general characteristic of Foxa2 genomic distribution.

3.1.3.5 Foxa2 binding profile of peaks associated with early and late onset genes

We next decided to look at the distribution of Foxa2 binding sites of genes with specific expression trends. DE genes from the *in vivo* microarray time course experiment were clustered into 12 sub-clusters according to Pearson correlation with P-value < 0.001. This allowed us to choose groups of genes with specific expression patterns of biological importance for the development of midbrain DA neurons. Two groups of genes were chosen according to their co-clustering with known progenitor and mature DA neuronal markers. A group of 342 genes that included progenitor markers such as Lmx1a, Foxa2, Slit2, and Corin are described as early onset genes, and the group of 1605 genes that includes mature neuronal markers such as Th, Pitx3, and Ddc are described as late onset genes (Figures 3-35, 3-36).

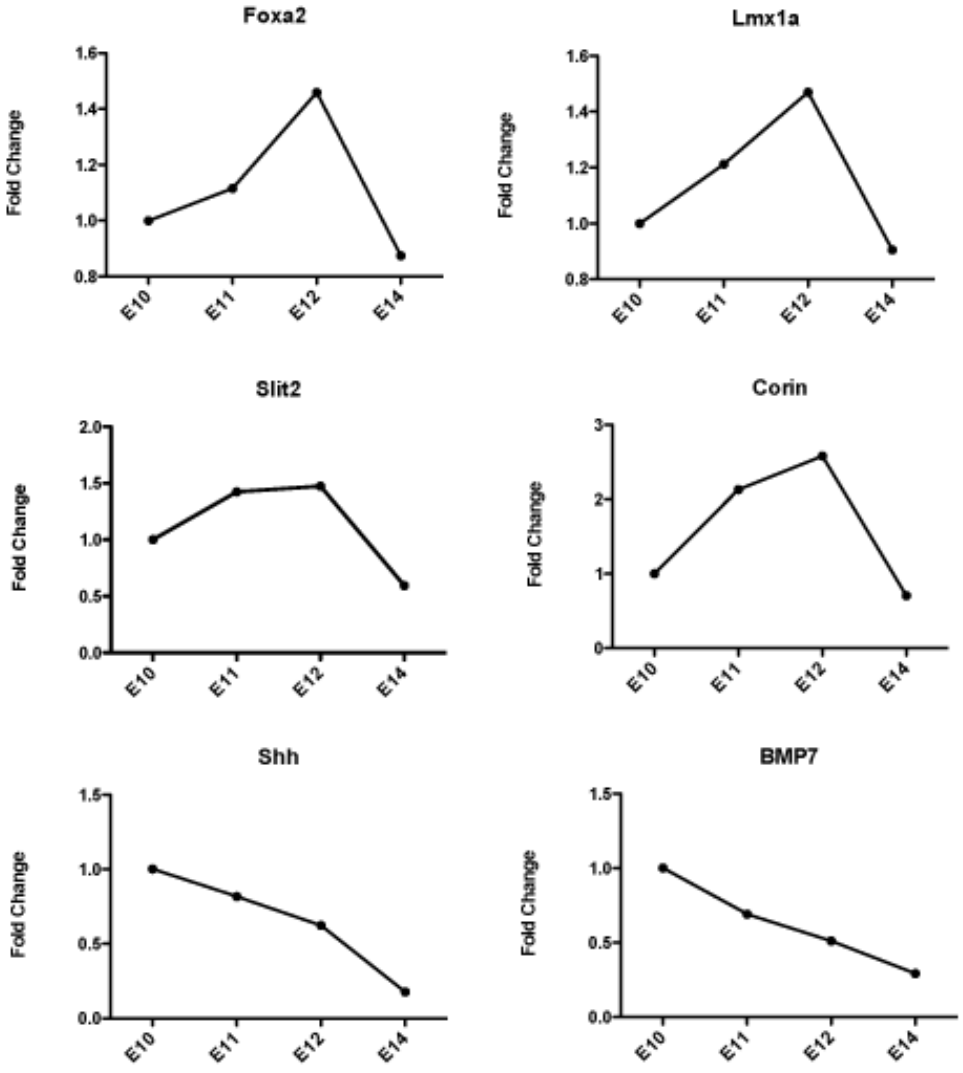

Figure 3-35: Gene expression time course assay of in vivo early onset genes (E10-E14). Genes presented: Foxa2, Lmx1a, Slit2, Corin, Shh, and Bmp7.

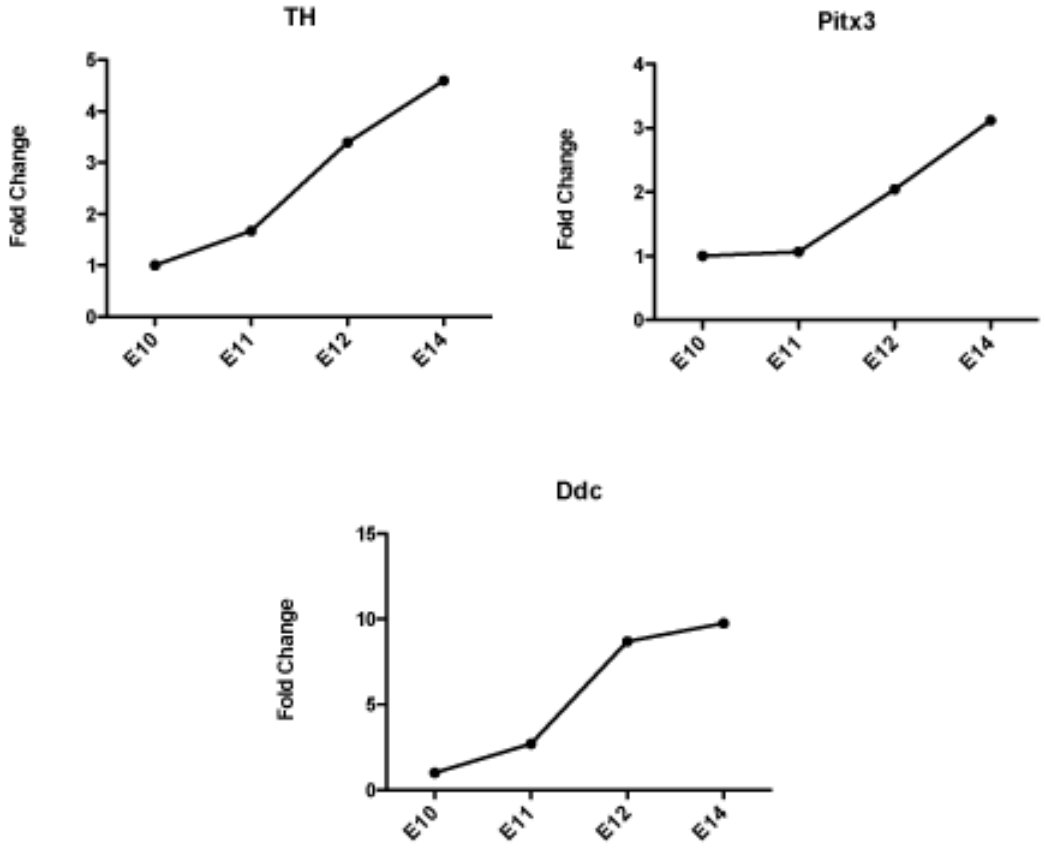

Figure 3-36: Gene expression time course assay of in vivo late onset genes (E10-E14). Genes presented: TH, Pitx3, and Ddc.

For the purpose of this study we carried out the analysis of peaks from the *in vivo* ChIP-seq data sets that mapped with early and late onset genes. Of the early onset genes 121 overlapped with the E12 ChIP-seq data set and 132 with the E14 ChIP-seq data set. Also, 489 of the late onset genes overlapped with the E12 data set and 588 genes overlapped with the E14 data set. The distribution of the Foxa2 binding sites from the TSS of these genes is similar to the genome wide observed distribution (Table 2 and 3).

Early onset genes

Within	*In vitro* ChIP	E12 ChIP	E14 ChIP
2kb	11%	17%	27%
5kb	20%	20%	34%
10kb	28%	26%	42%
50kb	55%	60%	71%
100kb	75%	78%	84%

Late onset genes

Within	*In vitro* ChIP	E12 ChIP	E14 ChIP
2kb	10%	17%	28%
5kb	17%	23%	31%
10kb	26%	32%	42%
50kb	65%	69%	73%
100kb	83%	84%	87%

Table 2: Distribution of peaks identified in all three data sets (E12, E14, in vitro) from the TSS of early and late onset genes expressed in vivo. The majority of the peaks can be identified within 100 kb of the TSS of annotated genes. An increase can be detected in the number of peaks within 2kb of the TSS between in vitro and in vivo ChIP-seq assays.

Within	*In vitro* ChIP	E12 ChIP	E14 ChIP
2kb	8%	18%	21%
5kb	18%	25%	28%
10kb	27%	34%	38%
50kb	65%	69%	72%
100kb	72%	85%	86%

Table 3: Distribution of peaks identified in all three data sets (E12, E14, in vitro) from the TSS of all annotated genes. The majority of the peaks can be identified within 100 kb of the TSS of annotated genes. An increase can be detected in the number of peaks within 2kb of the TSS between in vitro and in vivo ChIP-seq assays.

3.1.3.6 GO term analysis reflects Foxa2 possible functions during mDA neuron differentiation

In order to establish which biological processes may be regulated by Foxa2 at E12 and E14 involved in midbrain DA neuronal development, GO term analysis was performed on the early and late onset genes that overlapped with the E12 ChIP-seq data set, and on the late onset genes that overlapped with the E14 ChIP-seq data set. As expected, early onset genes bound by Foxa2 at E12 when neurogenesis is actively taking place are enriched for terms involved in neuron fate commitment, regulation of neurogenesis, and axon guidance (Figure 3-37). It was interesting to observe in the late onset genes bound at E12 to be enriched for terms involved in regulation of synaptic transmission and neuron projection development, processes which are usually active at late stages of neuronal development, suggesting the involvement of Foxa2 in later neuronal processes during differentiation (Figure 3-38) (Cowan M W et al., 1997).

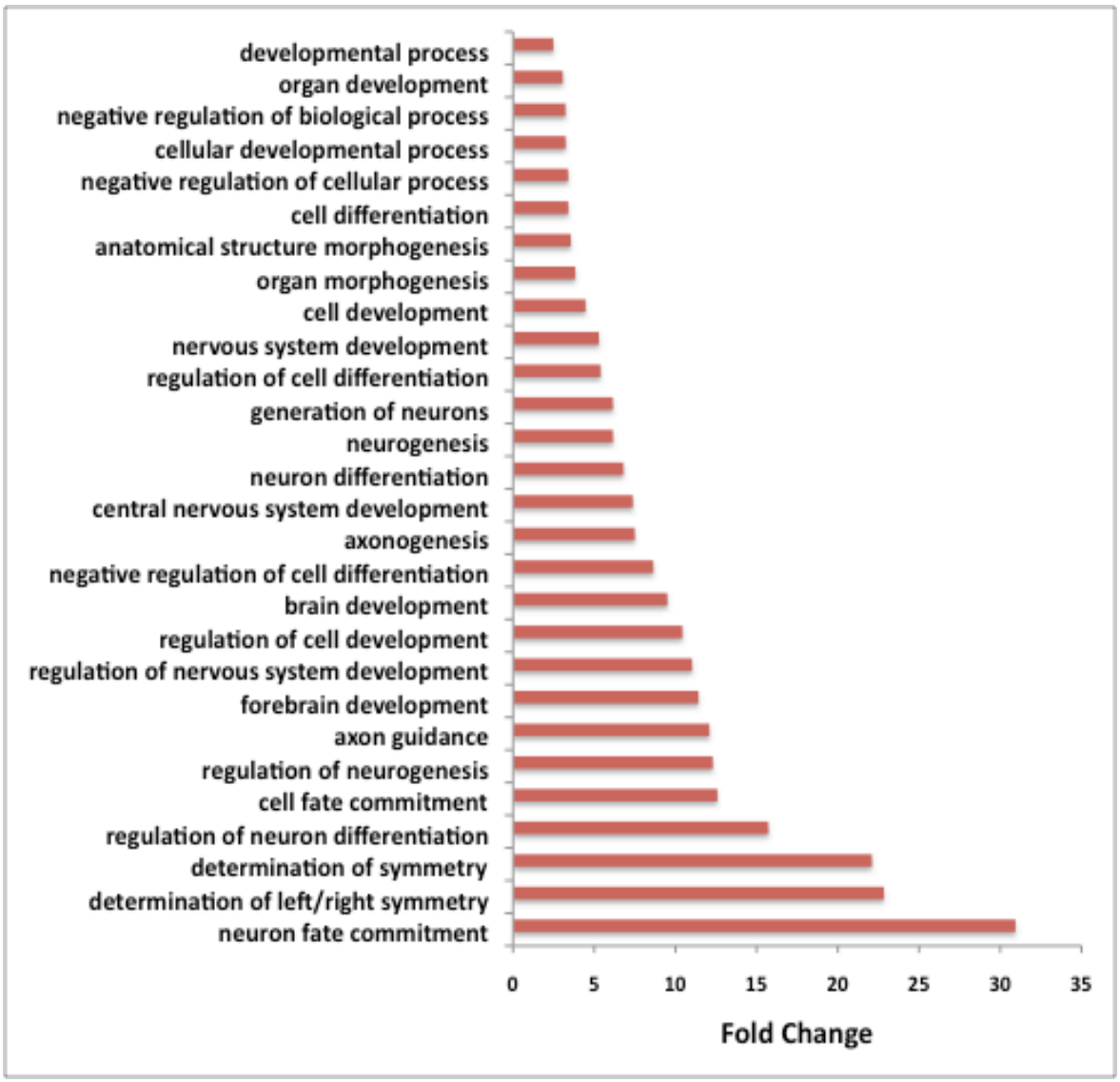

Figure 3-37: Gene ontology (GO) categories showing the most enriched biological processes of early onset candidate targets identified from the E12 ChIP-seq data set.

All categories displayed are of p-value<0.001 and are sorted according to fold change of the number of genes in each biological process in the experiment list over the reference list (whole genome).

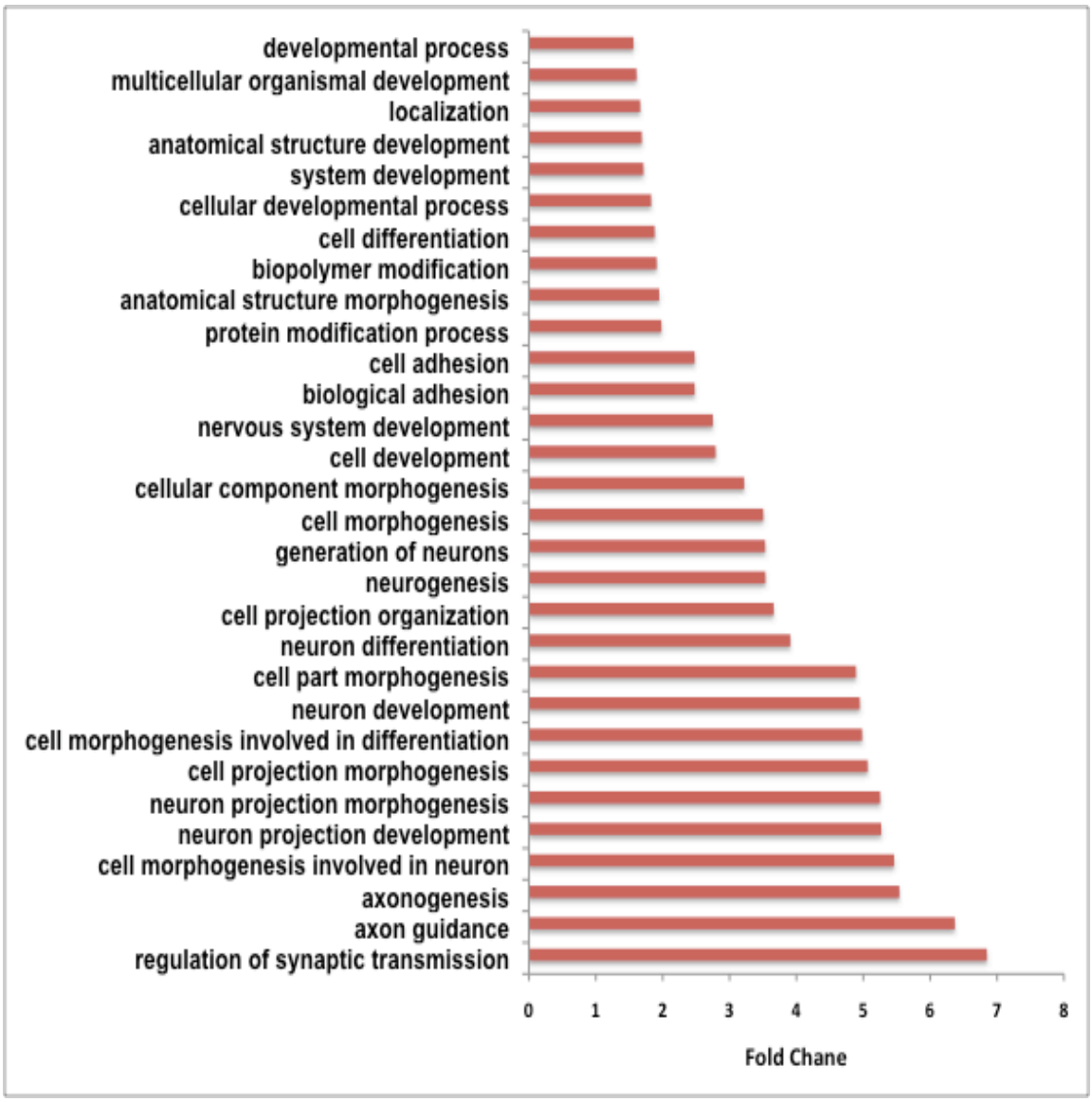

Figure 3-38:Gene ontology (GO) categories showing the most enriched biological processes of late onset candidate targets identified from the E12 ChIP-seq data set.

All categories displayed are of p-value<0.001 and are sorted according to fold change of the number of genes in each biological process in the experiment list over the reference list (whole genome).

Late onset genes bound at E14.5 by Foxa2 reveal terms enriched for ATP hydrolysis coupled with proton transport, dendrite morphogenesis, and regulation of neuronal synaptic plasticity (3-40). This suggests later roles of Foxa2 in the regulation of energy utilization in the cell coupled with late neuron differentiation processes. Since many of these genes bound at E14.5 are also bound and may be regulated at E12, we perform the GO term analysis on genes uniquely bound at E14.5 (Figure 3-42). The regions bound only at E14.5 were obtained by subtracting from the E14.5 ChIP-Seq candidate gene list all the candidate target genes bound at E12. This should produce a list enriched in candidate genes uniquely bound at E14.5. To further confirm this, independent ChIP-qPCR assays with Foxa2 antiserum were performed on regions uniquely bound at E14.5, E12.5 and on regions shared at both stages (Figure 3-39). The results suggest that the E14.5 unique Foxa2 bound gene list is truly enriched with regions only bound at E14.5 and the genes mapped to these regions are likely not bound and consequently not regulated at E12.5. Interestingly, the GO terms enriched for Foxa2 candidate targets unique for the E14.5 list are involved in transmission of a nerve impulse (Figure 3-41). This result suggests the possible requirement of Foxa2 at E14.5 for the late functions of a neuron in transmitting its signals.

A

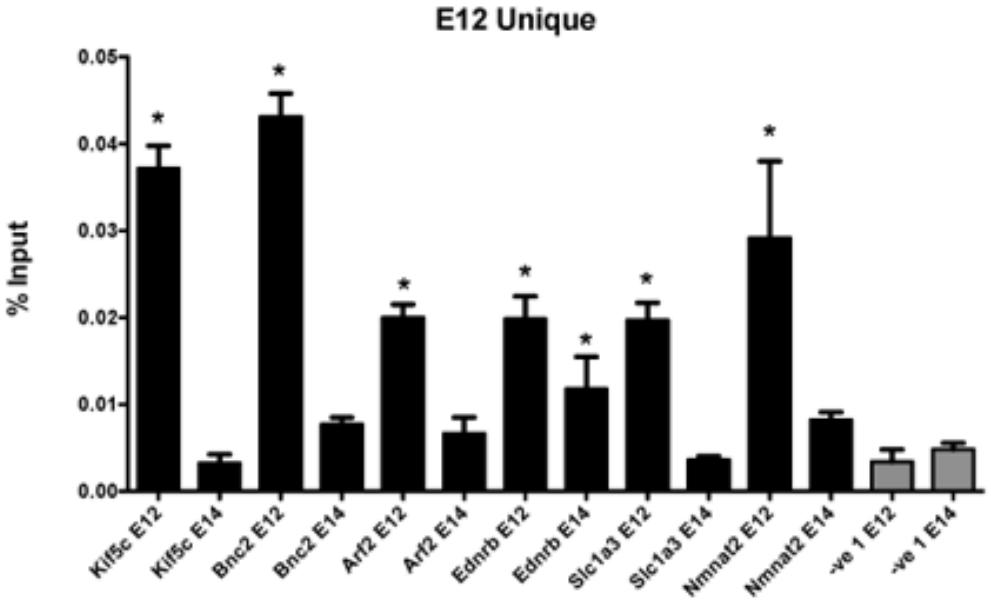
E12 Unique
% Input
0.05
0.04
0.03
0.02
0.01
0.00
Klf5c E12
Klf5c E14
Bnc2 E12
Bnc2 E14
Arf2 E12
Arf2 E14
Ednrb E12
Ednrb E14
Slc1a3 E12
Slc1a3 E14
Nmnat2 E12
Nmnat2 E14
-ve 1 E12
-ve 1 E14

B

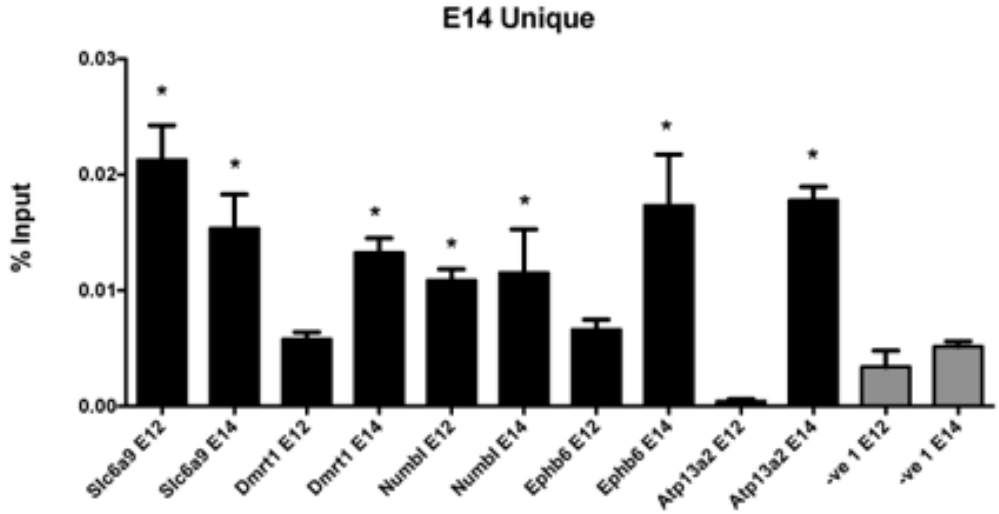
E14 Unique
% Input
0.03
0.02
0.01
0.00
Slc6a9 E12
Slc6a9 E14
Dmrt1 E12
Dmrt1 E14
Numbl E12
Numbl E14
Ephb6 E12
Ephb6 E14
Atp13a2 E12
Atp13a2 E14
-ve 1 E12
-ve 1 E14

C

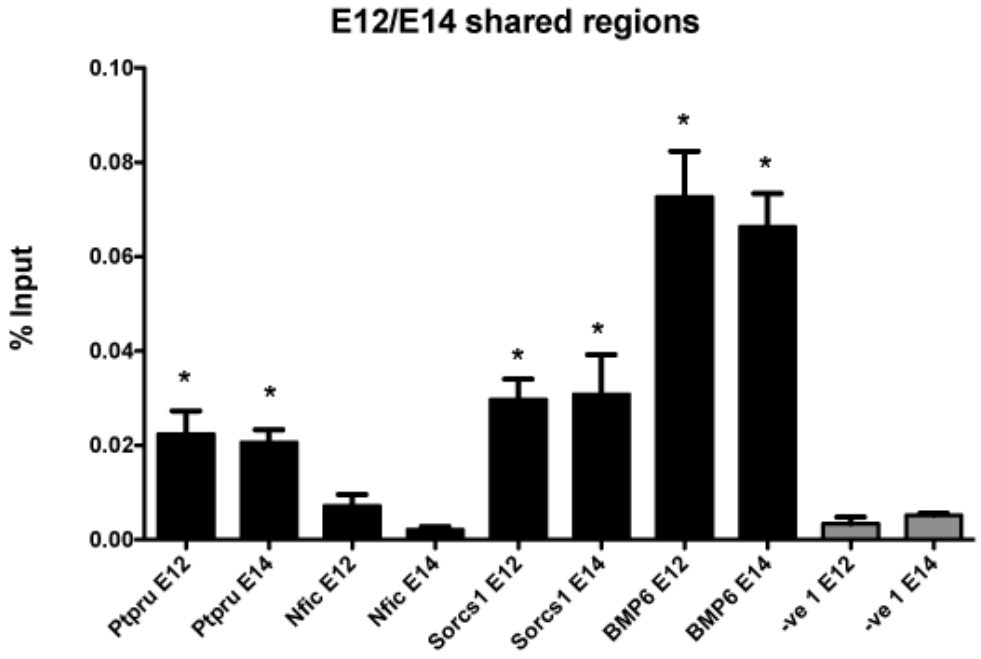

*Figure 3-39 ChIP-qPCR assays performed on chromatin from E12.5 and E14.5 mouse ventral midbrain using Foxa2 specific antiserum. (A) Foxa2 binding to regions unique to the E12.5 ChIP-seq list. (B) Foxa2 binding to regions unique to the E14.5 ChIP-Seq list. (C) Foxa2 binding to regions shared between both the E12.5 and E14.5 ChIP-Seq lists. Error bars represent SEM. Each ChIP was performed on chromatin samples from three biological replicates. * Enrichment of Foxa2 bound regions over the negative region in the ChIP samples was statistically significant ($P < 0.05$).*

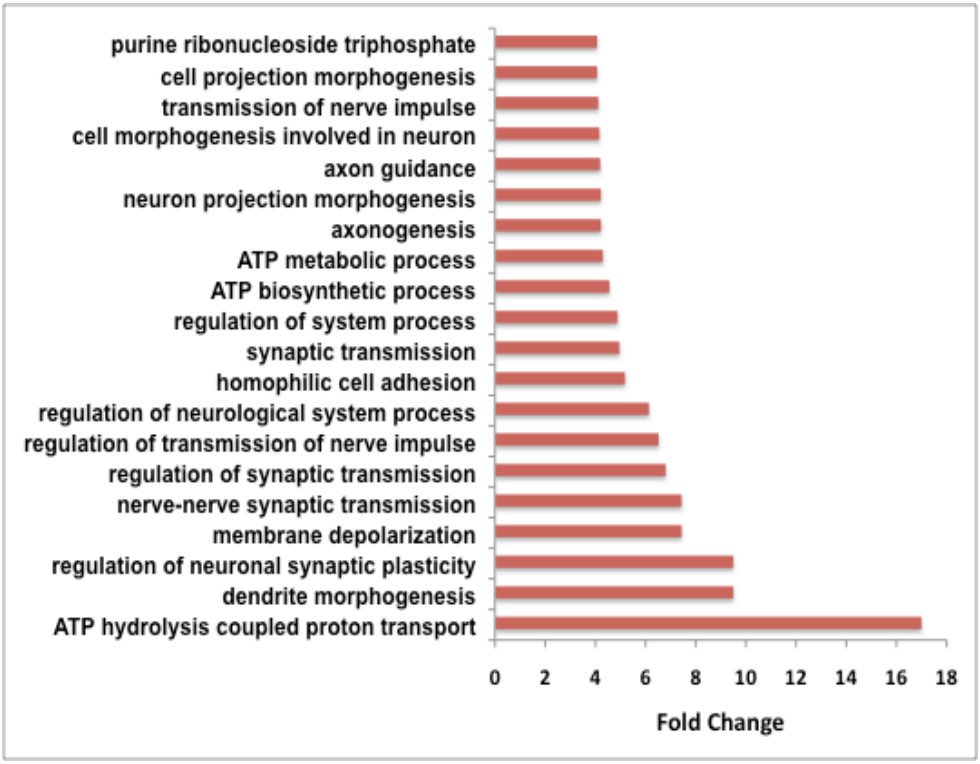

Figure 3-40:Gene ontology (GO) categories showing the most enriched biological processes of late onset candidate targets identified from the E14 ChIP-seq data set.

All categories displayed are of p-value<0.001 and are sorted according to fold change of the number of genes in each biological process in the experiment list over the reference list (whole genome).

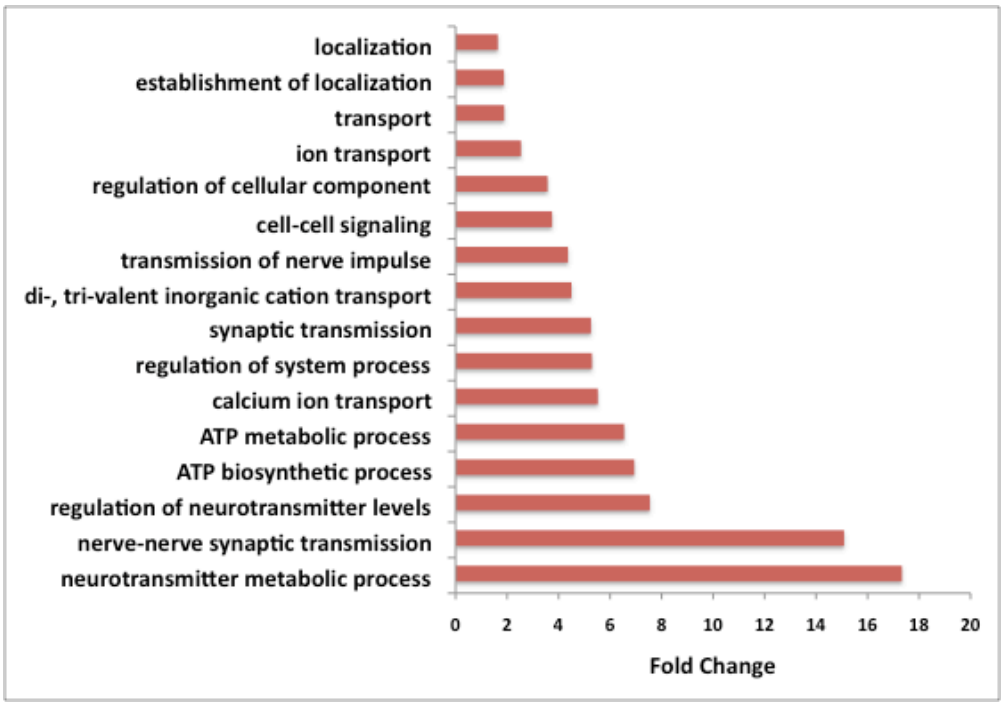

Figure 3-41: Gene ontology (GO) categories showing the most enriched biological processes of late onset candidate targets unique to the E14 ChIP-seq data set.

All categories displayed are of p-value<0.001 and are sorted according to fold change of the number of genes in each biological process in the experiment list over the reference list (whole genome).

3.1.3.7 Validation of late onset gene targets in Nestin-Cre Foxa1/2 flox mutant mice

For validation purposes of the functional relevance of Foxa2 binding to its target genes, 30 late onset genes, including transcription factors, bound by Foxa2 at both E12 and E14 were selected for testing in the *Nestin*$^{Cre/+;}$*Foxa1*$^{flox/flox}$*;Foxa2*$^{flox/flox}$ conditional mutant mouse model. In this model the midbrain DA progenitors are specified but do not fully differentiate (Kele et al., 2006). Thus, the main genes that are affected in these mutants are late onset genes that are likely activated during differentiation. From RT-qPCR expression assays we can observe that 50% of the genes analyzed are affected in the mutants compared to their wild type littermates (Figure 3-42). This data provides further confidence for the quality of the lists for predicting Foxa2 regulated genes.

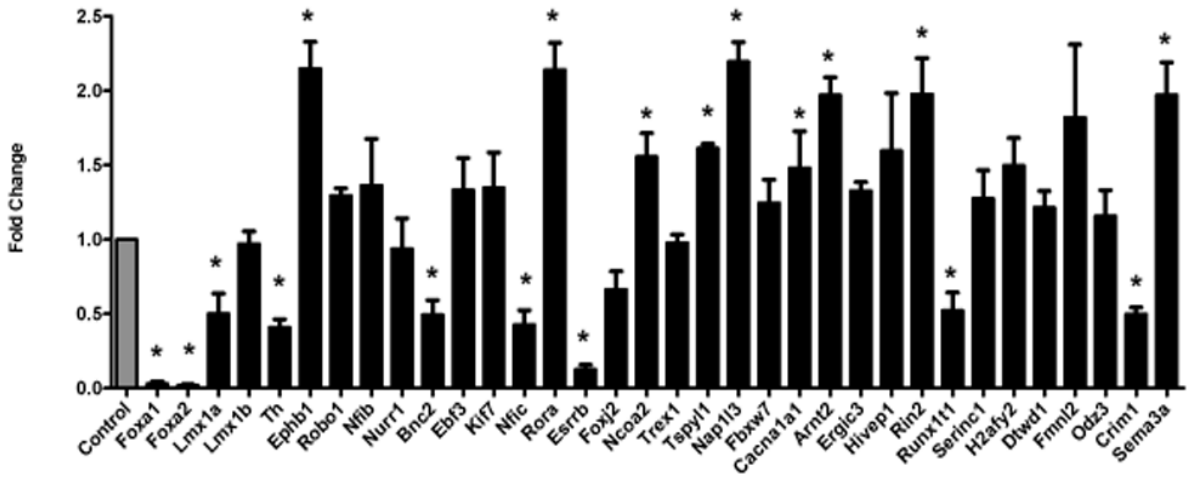

Figure 3-42: RT-qPCR validation of Foxa2 targets in ventral midbrain tissue of *Nestin*$^{Cre/+;}$*Foxa1*$^{flox/flox}$*;Foxa2*$^{flox/flox}$ *mice at E12.5. Expression analysis by qPCR of candidate target transcription factors, and genes involved in other functions. * Fold change between mutant and wild type littermate (Control) is statistically significant with p-value<0.05.*

3.1.3.8 Prediction of physical interaction of transcription factors regulated by Foxa2 *in vivo*

From the previous assay we identified late onset transcription factors regulated by Foxa2 and bound at both stages E12 and E14. It is very interesting to discover transcription factors that require Foxa2 input at multiple developmental time points. This suggests that these factors may be of much importance for the regulation of differentiation. To further classify these transcription factors, we used FANTOM 4 to identify any possible interactions these transcription factors may have between them (Figure 3-43). Notably, two interaction clusters were identified. The first involves the interaction of nuclear receptors Esrrb, Ncoa2 (Src-2), and Rora. It has previously been shown that Foxa2 interacts with nuclear receptors to induce its target genes (Carroll et al., 2005). The second cluster identified involves the interaction of nuclear factors Nfib and Nfic. These factors are very interesting since they seem to play important roles in regulating neurogenesis (Kumbasar et al., 2009). Also the BHLH-PAS member Arnt2 is predicted to be upstream of these nuclear factors and may be involved in mDA neuron development in mouse since it has such a role in Zebrafish DA neuron development (Löhr et al., 2009).

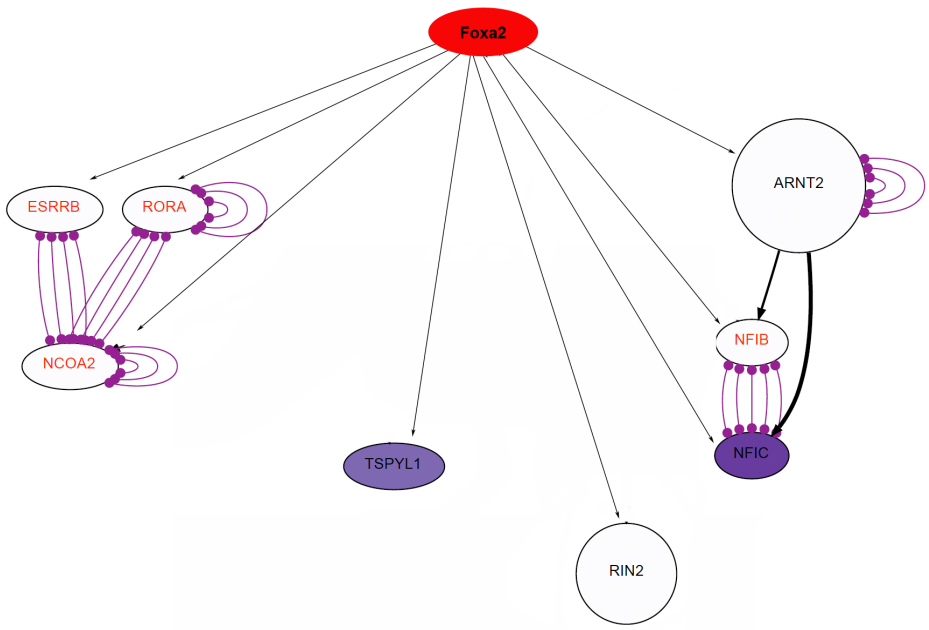

Figure 3-43: Physical interaction predicted by FANTOM4, of Foxa2 regulated transcription factors.

In purple, Circles connected by lines indicate the occurrence of physical interactions between the two factors sharing each end of the line. Black arrows indicate positive regulation of expression. Black Arrows leading from factors other than Foxa2 are predicted by FANTOM4. Nuclear receptors (Essrb, Rora, and Ncoa2) regulated by Foxa2 possibly interact and cooperate to induce downstream target genes.

3.1.3.9 Close correlation of Foxa2 binding events with Gli1 bound regions

The zinc finger transcription regulators Gli1-3 mediate Shh morphogen activity through binding to their consensus sequence and controlling the transcription of their target genes (Hooper and Scott, 2005). A recent ChIP-on-chip study has identified multiple genomic regions bound by Gli1 (Vokes et al., 2007), where many of the associated transcripts are components of Shh signaling. Also, many of these regions have already been published as enhancers regulated by Gli activity (Sasaki, 1997; Agren,

2004; Hallikas, 2006; Dai, 1999; Santagati, 2003). Notably, Foxa2 bound regions identified in our ChIP-seq data sets are observed within the Gli1 ChIP-on-chip peaks from the mentioned study, suggesting a tight regulatory loop between Foxa2 and Shh signaling (Table 4). Further more, Foxa2 binding events have been identified in both Gli1 and Gli2 loci (Element1-5), whereas Gli1 only regulates its own enhancer (Figure 3-44). This data is supported by genetic analysis of the *Wnt1*$^{Cre/+}$;*Foxa2*$^{flox/flox}$ mouse embryos performed by a former student in the lab (Appendix D: Figure 4-13). It was observed that Foxa2 acts by repressing Gli1 and Gli2 as well as Ptch1 in the mDA system. Together with results from our ChIP-seq data we suggest that Foxa2 repression of these genes is direct.

Gene	Gli1 Peaks	Foxa2 Peaks	ChIP-seq Data Set
Ptch1	TSS -1.1kb	TSS -0.84kb	In vitro
Ptch1	TSS -3.7kb	TSS -3.85kb	In vitro
Ptch1	TSS -7.9kb	TSS -8kb	In vitro and in vivo
Ptch1	Intron 2	TSS +8.9kb (Intron 2)	In vitro
Ptch1	TSS -61.9kb	TSS -61.9kb	In vitro and in vivo
Ptch2	Intron 1,2	TSS +3.9kb (Intron 2)	In vivo
Nkx2.2	TSS -1.9kb	TSS -1kb	In vivo
Nkx2.9	TSS -8.7kb	TSS -8.1kb	In vitro
Gli1	Promoter, intron 1,2	TSS +1.3kb (Intron 2)	In vitro
Hhip	Intron 1	TSS +3.6kb (Intron 1)	In vitro and in vivo
Foxa2	TSS +5.8kb	TSS +4.9kb	In vitro and in vivo

Table 4:Foxa2 binding to genomic regions identified in a Gli1 ChIP-on-chip study (Vokes et al., 2007).

Regions are described as base pairs away from the TSS. The Foxa2 ChIP-Seq data sets that present the binding events in each case are mentioned. Foxa2 is shown to bind directly to enhancer regions regulating components of the Shh signaling pathway.

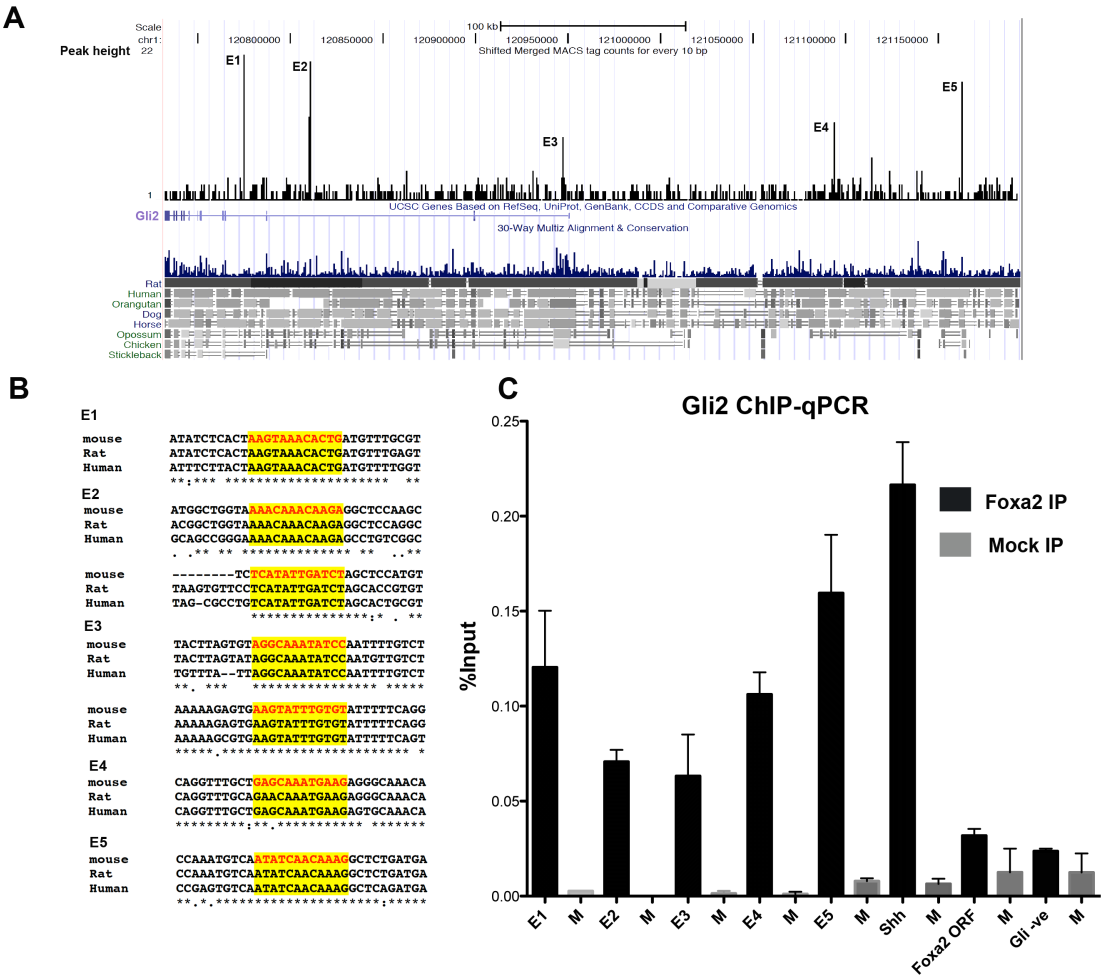

Figure 3-44: Occupancy of Gli2 gene conserved elements by Foxa2. (A) Schematic diagram of the Gli2 locus indicating peaks generated by Foxa2 in vitro ChIP-Seq experiment (E1-E5). (B) Foxa2 binding sites (in yellow) identified by the Jaspar database and their conservation.(C) ChIP experiments using chromatin from E12.5 ventral midbrain tissue validating the ChIP-Seq results using Foxa2 anti serum or anti-IgG antibody (M: Mock IP). Error bars represent SEM. Each ChIP was performed on chromatin samples from three biological replicates, and enrichment of all Gli2 elements in the Foxa2 ChIP samples compared with the mock ChIP was statistically significant ($P < 0.05$).

3.1.3.10 Differential binding of Foxa2 on promoters driving the expression of the DA synthesis enzymes TH and AADC

The possible role of Foxa2 in inducing TH and AADC (also known as Ddc) has previously been described (Bae et al., 2009; Raynal et al., 1998 2006). Interestingly, AADC expression precedes that of TH in midbrain DA neurons. AADC can already be detected in these cells at E10.5 whereas the first TH+ cells can be detected at E11.5 (Castelo-Branco and Arenas, 2006; Mavromatakis, 2006). Identifying the mechanism responsible for this differential expression of TH and AADC will provide useful information regarding the control of the developmental timing of gene expression. Lee et al, have described the efficient binding of Foxa2 to the TH promoter through ChIP assays only in the presence of Nurr1, suggesting that Nurr1 acts as a recruitment factor for Foxa2 on this region. The authors have also identified the Foxa2 DNA binding sequence within the TH promoter that is required for the Foxa2 specific induction of luciferase activity. Raynal et al. identified the Foxa2 DNA binding motif within the AADC neuronal promoter and have shown Foxa2 binding to this region through electrophoretic mobility gel shift assays. Luciferase assays of AADC neuronal promoter in the context of P19 cells show a Foxa2 specific induction that further strengthens the argument of the presence of a Foxa2 input (Table 5).

We performed ChIP assays and quantified with qPCR to assess Foxa2 binding to these regions at both stages E10.5 and E12.5 of ventral midbrain (VM) development (Figure 3-46). We observe clear Foxa2 binding to the AADC neuronal promoter at E10.5 but this is not the case for the TH promoter at this stage. Foxa2 binding is observed at both promoters in ChIP assays performed on E12.5 VM (Figure 3-46). This result can be partially explained by comparing the Foxa2 DNA binding motifs of both promoters. The

Foxa2 motif in the AADC neuronal promoter is identical to the known Foxa2 motif (high affinity) providing the possibility of strong protein/DNA interaction (Figure 3-45). Whereas the motif identified in the TH promoter by Lee et al. is not a perfect match for the Foxa2 DNA binding motif (low affinity), indicating that Foxa2 may not interact strongly at this sequence. These results suggest that Foxa2 requires another transcription factor or higher concentration of Foxa2 are required for binding to the low affinity Foxa2 motif in the TH promoter.

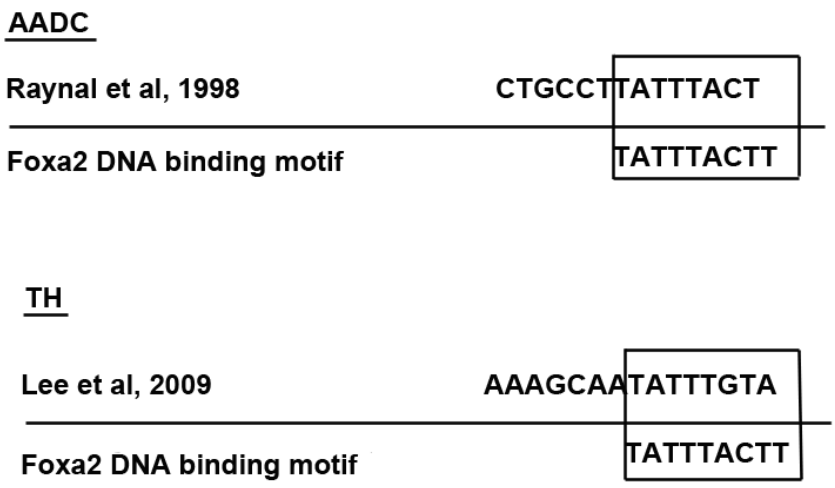

Figure 3-45: Comparison of the Foxa2 DNA binding domain defined by the Jaspar base with Foxa2 bound sequences in the AADC neuronal promoter and the TH promoter.

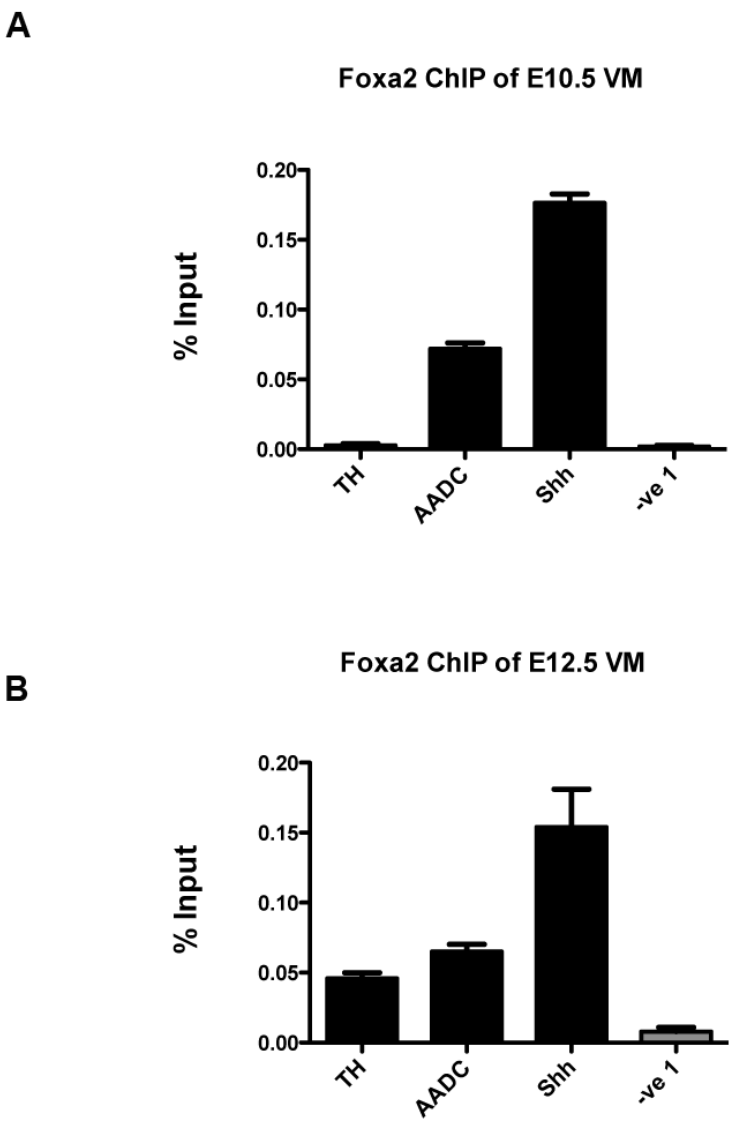

*Figure 3-46: ChIP-qPCR assays performed on chromatin from E10.5 and E12.5 mouse ventral midbrain using Foxa2 specific antiserum. (A) Foxa2 binding to promoter regions of the AADC neuronal promoter and the TH promoter at E10.5 (B) Foxa2 binding to promoter regions of the AADC neuronal promoter and the TH promoter at E12.5. Foxa2 binds to both promoter regions only at E12.5 compared to binding only to the AADC promoter at E10.5. Error bars represent SEM. Each ChIP was performed on chromatin samples from three biological replicates. * Enrichment of Foxa2 bound regions over the negative region in the ChIP samples was statistically significant ($P < 0.05$).*

3.1.3.11 Luciferase enhancer analysis of Foxa2 bound regions suggests the requirement of co-factors

To further analyze the mechanisms governing the regulation of Foxa2 function we performed luciferase enhancer reporter assays on genomic regions bound by Foxa2 that also contain, Lmx1a, Otx2 and/or Nurr1 binding motifs, since genetic data predicts that these factors cooperate with Foxa2 to perform their function (Yan, 2008; Perez-Balaguer et al., 2009; Lee et al., 2010; Rascle et al., 2008; Uniprobe, Jaspar database). These regions were divided into two groups according to the transcripts they are predicted to regulate, progenitor markers (First nine) and mature neuron markers (Last 4) (Table). The genomic regions of mature neuron markers are tested for Foxa2, Lmx1a and Nurr1 induction, whereas the progenitor markers are tested for Foxa2, Lmx1a and Otx2 induction. Interestingly, Foxa2-mediated effect was observed on 70% (9/13) of the regions suggesting Foxa2 may require other factors to induce a subgroup of its targets. Otx2 can induce only 3 of the nine regions it was tested on and only one region (Bmp7) show cooperative interaction with Foxa2 (Table 5). This may imply that not many targets co-regulated by Foxa2 and Otx2 were tested, or that Otx2 interacts with Foxa2 to induce a very specific subset of genes. Surprisingly, Lmx1a had an effect on the enhancer activity of 90% of the regions (9/10) tested. Lmx1a and Foxa2 had a synergistic effect on the enhancer activity of four of these regions. Furthermore, Foxa2 and Lmx1a together but neither of the single factors alone stimulated the enhancer activity of genomic regions of Slit2 and Pitx3 (Figure 3-47). These results strongly suggest that Foxa2 and Lmx1a cooperate in inducing this subset of regulatory elements. Out of the four regions tested with Nurr1, three show combinatorial effect with Foxa2. This indicates a possible

interaction of Foxa2 with Nurr1 to affect these regulatory elements. Further studies need to be performed to dissect these interactions.

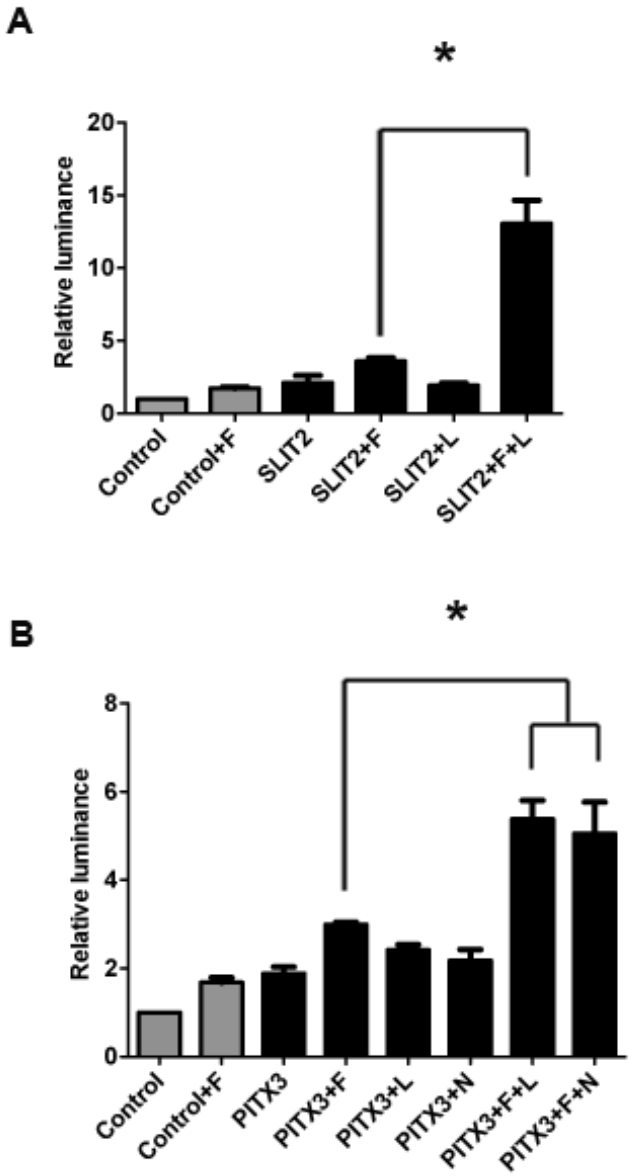

Figure 3-47: Synergistic relationship of Foxa2 with Lmx1a and Nurr1.

(A) Synergistic activation of the Slit2 enhancer by Foxa2 and Lmx1a. (B) Synergistic activation of the Pitx3 enhancer by Foxa2 and Lmx1a or Nurr1.

Coordinates	Gene	F	L	O	N	F+L	F+O	F+N
chr5:72,803,018-72,803,822	Corin	+	+	●		+	●	
chr5:48,399,872-48,400,686	Slit2	●	●	●		++	●	
chr9:71,865,663-71,865,906	Tcf12	+	+	●		+	●	
chr7:137,401,646-137,402,500	Fgfr2	●	+	●		+	●	
chr2:172,760,380-172,760,946	Bmp7	+	+	●		++	++	
chr11:108,784,270-108,784,469	Axin2	+	+	+		+	●	
chr1:169,711,978-169,712,499	Lmx1a CR1	+		●		●	●	
chr1:169,732,970-169,733,415	Lmx1a CR2	●		+			●	
chr2:33,438,286-33,438,491	Lmx1b CR1	+		●			-	
chr16:72,687,986-72,688,222	Robo1	+	●		+	+		++
chr19:46,210,180-46,211,110	Pitx3	●	●		●	++		++
chr11:11,790,324-11,791,073	Ddc	+	+		●	+		+
chr9:102,113,800-102,114,335	EphB1	-	-		-	--	-	--

Table 5: Summary of the luciferase assays performed on regions bound by Foxa2 in vitro and in vivo. F: Foxa2, L: Lmx1a, O: Otx2, N: Nurr1, F+L: Cotransfection of Foxa2 and Lmx1a, F+O: Cotransfection of Foxa2 and Otx2, F+N: Cotransfection of Foxa2 and Nurr1. +: Significant Fold change of cotransfections of Luciferase construct with transcription factors compared to transfection of the Luciferase construct alone but does not illustrate combinatorial effect. (Inductive effect). ++: Significant fold change of cotransfections of the Luciferase constructs with transcription factors compared to transfection of the Luciferase construct alone and also illustrates synergistic effect. (Inductive effect). - : Significant fold change of cotransfections of Luciferase constructs with transcription factors compared to transfection of the Luciferase construct alone but does not illustrate synergistic effect. (Repressive effect). -- : Significant fold change of cotransfections of Luciferase constructs with transcription factors compared to transfection of the Luciferase construct alone and also illustrates synergistic effect. (Repressive effect). Red dot indicates no effect.

3.1.3.12 Corin and Slit2 are affected in the Shh-Cre *Lmx1a* (*dreher*)/*Lmx1b* Flox double mutant mice

We have shown previously that Foxa2 binds to genomic regions close to the TSS of many genes expressed in the ventral midbrain. Corin and Slit2 show a restricted expression within the mDA progenitor domain. The luciferase assays performed on genomic regions close to the TSS of these genes indicates that both Foxa2 and Lmx1a have an input in regulating these regions. Expression analysis of these genes through ISH indicates that these genes are lost in the $Shh^{Cre/+}$ $Lmx1a^{drdr}/Lmx1b^{floxflox}$ mutant mouse embryos compared to their wild type littermates (Figure 3-49). Moreover, ChIP-qPCR assays with Lmx1b antiserum suggest the direct binding of Lmx1b to the Corin and Slit2 genomic regions identified from the Foxa2 ChIP-Seq analysis (Figure 3-48). This result confirms further the requirement of both Foxa2 and Lmx1a for the proper expression of these genes and the mechanism by which this occurs is through binding and regulating the identified Corin and Slit2 enhancers. *In vivo* LacZ reporter analysis of these enhancers is required to further confirm this observation.

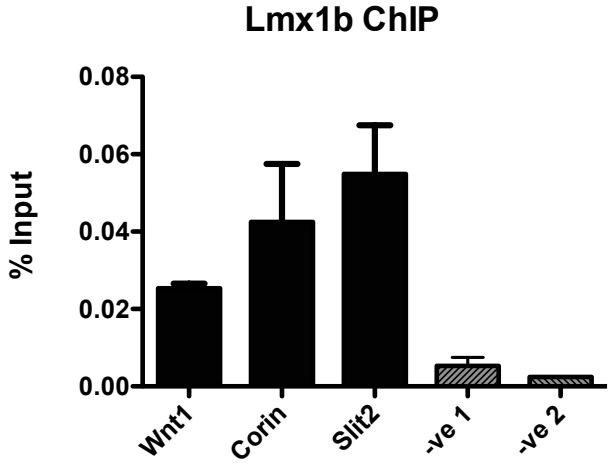

*Figure 3-48: ChIP-qPCR assays performed on chromatin from E12.5 mouse ventral midbrain using Lmx1b specific antiserum. Lmx1b binding to Enhancer regions close to the Corin ans Slit2 TSS. Wnt1 promoter region was used as positive control (Chung et al., 2009). Error bars represent SEM. Each ChIP was performed on chromatin samples from three biological replicates. * Enrichment of Lmx1b bound regions over the negative region in the ChIP samples was statistically significant (P < 0.05).*

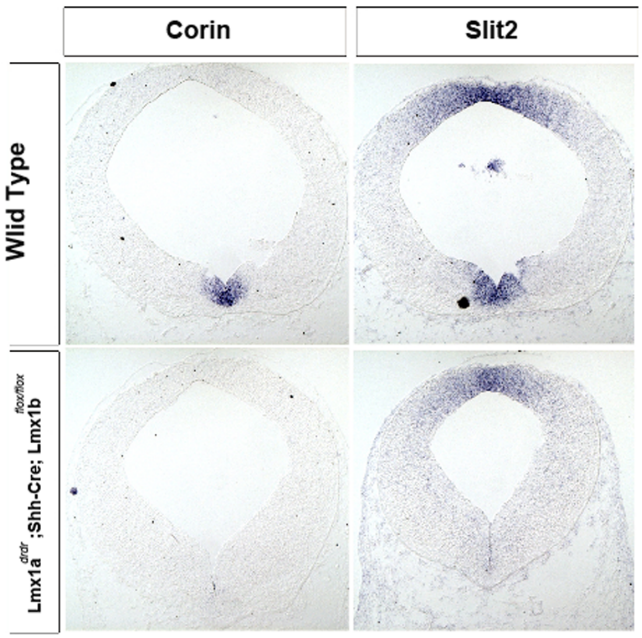

Figure 3-48: Foxa2 targets Corin, and Slit2 are affected in the $Shh^{Cre/+}$ $Lmx1a^{drdr}$/$Lmx1b^{floxflox}$ mouse embryos.

Slit2 and Corin are lost in these mutants indicating that Lmx1a and lmx1b are required for their proper expression. (Kind contribution by Dr. Martin Levesque)

4. Discussion

Degeneration of midbrain DA neurons is observed at the onset of Parkinson's disease. The detailed study of the transcriptional network involved in the development of these neurons will assist in future treatment of this disease. Genetic data for the Forkhead transcription factor Foxa2 has shown it to play an important role in the development of midbrain DA. The recent advances in microarray and sequencing technologies have made it possible to map the genome wide recruitment sites of transcription factors in living cells. This has allowed the identification of gene regulatory circuitry associated with developmental processes. This thesis presents genome wide DNA binding analysis of Foxa2 at two important time points of midbrain DA neuron development: Specification (*in vitro* progenitors), and differentiation (E12.5, and E14.5 ventral midbrain tissue).

4.1 Foxa2 genomic recruitment at distant regions from the TSS

To identify the target genes regulated by Foxa2 we applied ChIP combined with massively parallel sequencing. Characterizing the position of the DNA interaction sites relative to TSS of genes in three ChIP-Seq data sets reveals that only a small fraction of the Foxa2 bound regions are found within promoters, whereas the majority are found at large distances from annotated genes or within introns. This data is in line with previous ChIP-Seq studies performed on Foxa2 (Wallerman et al., 2009). A large proportion of these sites are conserved throughout many species suggesting that many of these regions are cis-regulatory elements exerting their regulation on promoters from a distance, or they may be regulating genes that have not yet been annotated. The wide distribution of the Foxa2 binding sites indicates that studies on the transcription factor activity of Foxa2

should not be limited to promoter regions as was previously carried out in ChIP-chip studies since this may lead to conclusions that may not be entirely accurate (Odom et al., 2007).

Further experimentation is required to establish a detailed map of the distal cis-regulatory elements that are bound and regulated by Foxa2 and identifying the effected transcription. This could be achieved by a large-scale enhancer reporter analysis, where the Foxa2 bound regions are isolated and amplified with subsequent cloning into reporter constructs (Luciferase or LacZ). This way producing a library containing the possible Foxa2 bound cis-regulatory elements. These constructs would then be used for screening in appropriate cell lines. Finally, sequencing of the genomic regions that pass the screening will reveal their genomic coordinates. Although this method will not overcome the difficulty of associating the cis regulatory elements with their preferred regulated transcripts, since any gene from any direction is a possible candidate, nonetheless, it does provide important data for which of the Foxa2 bound regions also demonstrate enhancer activity. This approach will be very difficult to perform since our data sets suggests that Foxa2 is bound to many thousands of distal regions that differ depending on the developmental stage the experiment is performed at. Also, enhancer analysis in cell lines is very context dependant and thus cell lines need to be chosen carefully.

4.2 Possible functions of Foxa2 during the specification, and differentiation of midbrain DA neurons revealed by GO term analysis

GO term analysis has been widely used for the association of genes identified in large-scale experiments with known biological processes (Koudritsky and Domany, 2008). In this study with the aid of GO term analysis we identified possible global functions of Foxa2 during the specification, and differentiation of midbrain DA neurons. Foxa2 direct targets identified at the DA progenitor stage were associated with DE genes during the specification process of the DA progenitor fate. We observed that Foxa2 was bound to genes up regulated and down regulated during this process suggesting a possible dual role of Foxa2 as an inhibitor and activator of gene expression. The up regulated genes bound by Foxa2 were highly enriched with terms involved in early neuronal development whereas the genes that were down regulated were highly enriched for terms involved in the development of alternative fates such as cardiac muscle. These data suggest potential roles for Foxa2 in inducing the neural fate and inhibiting the alternative fates. It is important to investigate the mechanisms that help Foxa2 distinguish between its roles as an activator or repressor. Co-factors such as Tle1 (Groucho1) have been shown to be recruited by Foxa2 on the regulatory elements of genes that are destined to be repressed (Santisteban et al., 2010). It will be very interesting to see if the same model applies for the repression of genes identified in our system since Tle1 is expressed and may perform similar roles.

The Foxa2 target genes identified at E12.5 are enriched with terms involved in neural fate commitment, neuron development and neurogenesis. Finally, terms enriched at E14.5 indicate the subsequent roles of Foxa2 in regulating genes involved in synaptic

and nerve impulse transmission. These results suggest that Foxa2 may play very important roles during DA neuron differentiation and their mature functional aspects.

The study of the regulatory elements controlling the expression of these genes will provide insightful information for the mechanisms involved in the distinct regulation of the developmentally early and late genes. The first step will involve the careful grouping of the elements according to the timing of expression of the associated genes and analysis of the DNA sequence for transcription factor motifs, in the attempt to identify common signaling inputs involved in their regulation.

4.3 Foxa2 function regulated by co-factors

Gene expression is controlled by regulatory elements bound by combinations of transcription factors. Foxa2 expression is much broader than the domain where mDA neurons reside and this suggests that there may be another co-factor regulating Foxa2 DA specific functions. Hence, the identification of co-factors that function together with Foxa2 in regulating DA neuron development is crucial for understanding this process. ChIP-seq is quickly proving to be a very efficient way to identify such cofactors for your gene of interest (Motallebipour et al., 2009; Wallerman et al., 2009).

4.3.1 E-box binding proteins may cooperate with Foxa2 in early specification and neurogenesis of midbrain DA neurons

In our study we identified an E-box motif (CAGCTG) that is enriched in the *in vitro* data set. This motif is very similar to the DNA binding motifs of two basic-helix-loop-helix transcription factors Mash1 (Ascl1), and AP-4 (Castro et al., 2006; Jung and Hermeking, 2009). Mash1 is usually an activator whereas AP-4 is usually an inhibitor of transcription (Kim et al., 2006). This motif is highly enriched in genomic regions

associated with genes that are up regulated in the *in vitro* DA progenitor model, thus supporting the possibility that this motif may be bound by Mash1 or another E-box binding protein that functions as an activator. This sequence was not enriched in the *in vivo* data sets suggesting the E-box binding co-factor may be part of an early DA specification transcription factor combinatorial code.

It has recently been shown that midbrain DA neurons in Ngn2 mutant mice fail to develop normally mainly due to a block in generation of Nurr1+ precursors. This is observed by a 66% reduction in TH+ neurons at the end of the neurogenic period (E14.5) (Kele et al., 2006). Interestingly, Mash1 was also reduced in the DA progenitor domain suggesting a possible contribution to this dramatic phenotype. Furthermore, substitution of Ngn2 expression Mash1 knock-in at the Ngn2 locus partially rescued the phenotype indicating the requirement of Ngn2 for the proper development of mDA neurons (Kele et al., 2006). This work also suggests redundancy between Ngn2 and Mash1 functions. This notion is further supported by a recent study of the Delta-like 3 (Dll3) promoter, where it is shown that Mash1 and Ngn2 bind to the same regulatory elements of this promoter in a single complex. They also indicate that Mash1 and Ngn2 interaction with the specific E-box sequence (CACATG) may require other unknown factors (Henke et al., 2009). In our study, we have identified Foxa2 binding events *in vivo* in the Nurr1 promoter 118 bp upstream of the TSS (Figure 4-5). It will be very interesting to investigate if the Mash1/Ngn2 complex is involved in regulating the Nurr1 promoter and if Foxa2 is required for this function. This data would give Foxa2 a direct role in promoting the maturation of mDA neurons by directly inducing Nurr1. In support of this model, analysis of the Nestin-Cre Foxa1/2 double mutants by Ferri et al. show that the cells are

blocked at neurogenesis, since by E12.5, Neurog2 expression can be identified albeit reduced and there is a clear block in Nurr1 expression. Conversely, work performed by Simon Stott in the lab where he analyzed the effect of a developmentally later Cre recombination of *Foxa1;Foxa2* $^{flox/flox}$ mice driven by the DAT promoter has demonstrated that by E14.5 there are no more TH+ cells where deletion of *Foxa1;Foxa2* has occurred with the maintenance of Nurr1 expression indicating a requirement of Foxa protein to maintain TH expression (Zhuang et al., 2005). It is worth mentioning that the Foxa2 peaks in the Nurr1 promoter has been identified only in the E12.5 data set but not E14.5 where neurogenesis has ended and the expression of Ngn2 and Mash1 is essentially absent in the DA domain. This provides an explanation for the maintenance of Nurr1 expression in the DAT-Cre Foxa1/2 F/F mice since Foxa2 is not required to maintain its expression. Further investigation is required to confirm these interpretations.

4.3.2 Otx2 co-regulates a subset of Foxa2 target genes

Genetic data have shown that Otx2 and Foxa2 may directly or indirectly regulate common targets involved in mDA neuron differentiation such as Shh, lmx1a, and Lmx1b (Omodei et al., 2008 2009). In this thesis ChIP-analysis has shown that Foxa2 and Otx2 binds to the regulatory regions of the affected genes and indicates that this regulation is direct. Furthermore, a large-scale mammalian two-hybrid screen predicts a Foxa2/Otx2 interaction. In our *in vitro* ChIP-Seq data set, we identified an enrichment of the Otx2 DNA binding motif, which strongly suggests that Otx2 may co-regulate a subset of Foxa2 direct targets. In this study, the ChIP-Seq data together with analysis of loss of function models for Foxa2 and Otx2, we identified 11 genes that require both Otx2 and Foxa2 inputs for their proper expression. Among these genes, the most interesting ones are

Ltbp1 (latent transforming growth factor beta binding protein), Tgf-β receptor 3, and Bmp7, which are components of Tgf-β superfamily of signaling molecules (Fuchshofer et al., 2009; Zhou et al., 2009). Tgf-β signaling has been previously shown to play important roles in mDA neuron development (Farkas et al., 2003). Moreover, Foxa2 and Otx2 synergistically activated the enhancer activity of the Foxa2-bound genomic region of BMP7 in luciferase assays. These results indicate that Otx2 may co-regulate a small subset of the Foxa2 direct target genes, and the Tgf-β signaling pathway may depend on both factors for its proper regulation.

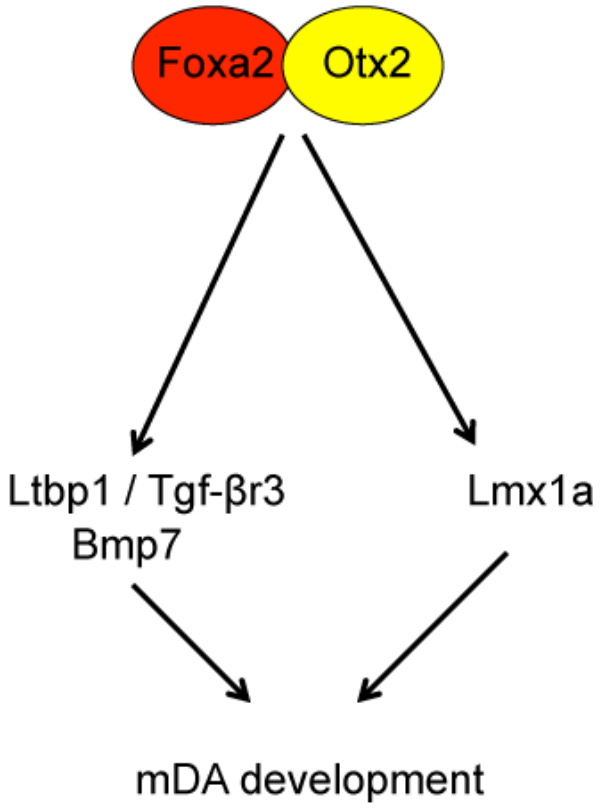

Figure 4-1: Model of possible Foxa2/Otx2 interaction in mDA development. Foxa2 and Otx2 may be required to modulate Tgf-beta signaling by regulating it's components Ltbp1, Tgf-βr3, and Bmp7. Furthermore, Foxa2 and Otx2 are required for the induction of Lmx1a.

Loss of function studies in mice suggests that Foxa2 together with Otx2 are required for the proper expression of Lmx1a. Furthermore, ChIP-qPCR analysis using Otx2 antiserum together with luciferase assays of Lmx1a CR2 indicates a direct Otx2 input in regulating this enhancer.

The regulatory input of Otx2 on Lmx1b expression is different from that of Lmx1a. Analysis of En1-Cre *Otx2* Flox mutant mice indicates an expansion of the Lmx1b domain to more dorsal regions, suggesting a possible inhibitory role of Otx2, which restricts Lmx1b to the mDA domain (Puelles et al., 2004). Luciferase assays of the Lmx1b CR1 support the presence of an inhibitory effect of Otx2 when co-transfected with the luciferase construct. Moreover, ChIP-qPCR analysis with Otx2 antiserum of the Lmx1b CR1 suggests that this effect is direct. Mutation analysis of the Otx2 DNA binding motif within these constructs is required to confirm these observations. These results indicate the possible presence of an Otx2/Foxa2 code for the proper specification of mDA neurons through the induction of Lmx1a, and restricting the expression domain of Lmx1b, and also possibly through modulating the Tgf-βsignaling pathway. Further analysis is required to confirm the extent of disruption of the Tgf-beta signaling pathway by evaluating the activity of smad proteins, which are the pathway downstream effectors.

4.3.3 Lmx1a cooperates with Foxa2 to regulate the specification and development of midbrain DA neurons

We have investigated the possibility of a Foxa2 and Lmx1a combinatorial relationship in regulating gene expression. Intensive genetic analysis of mutant mice have strongly suggested this interaction for the proper specification of midbrain DA neurons (Lin et al., 2009; Nakatani et al., 2010). Luciferase reporter analysis demonstrates the possible occurrence of a Foxa2/Lmx1a combinatorial induction of novel enhancer regions regulating early and late developmental genes (Table 5). Genetic data indicates that Foxa2 does not function independently to induce midbrain DA properties, but requires Lmx1a as well. Moreover, Lmx1a can induce the complete midbrain DA phenotype only in the Foxa2+ domains (Nakatani et al., 2010). Furthermore, data from Nakatani et al. have suggested that Foxa2 and Lmx1a are required for the induction of Neurog2 either directly by regulating its promoter or indirectly by repressing Helt, a BHLH transcription factor which acts mainly as a repressor. Our ChIP-Seq data has identified a Foxa2 binding event on a conserved region very close to the known Neurog2 enhancer on the 3' end of the gene (Figure 4-4). Strikingly, an Lmx1a DNA binding motif was identified near the predicted Foxa2 binding site (Rascle et al., 2009). Further analysis is required to establish if this region demonstrates enhancer activity and the presence of a Foxa2/Lmx1a input for its regulation. If this model is confirmed it will place Foxa2 as a direct regulator of Neurog2 further expanding a feed forward loop driving the DA progenitors towards differentiation (Figure 4-6).

4.4 Conclusions from of Lmx1a and Lmx1b regulatory elements

In this study we identified the genomic regions that govern the expression pattern of Lmx1b and in part the expression pattern of Lmx1a. Since the Lmx1b CR1 enhancer was the smallest (200 bp) of the three analyzed it made it easier to identify the possible Foxa2 binding site by DNA mutations and subsequent LacZ reporter assays. This analysis demonstrated a direct role for Foxa2 in the regulation of Lmx1b expression. This remains to be established for the Lmx1a enhancers.

The LacZ expression pattern of Lmx1b CR1 enhancer is restricted to the floor plate where mDA neurons are born. Co-labeling analysis with floor plate markers should be performed to confirm this finding. We are very hopeful that this enhancer will serve as a good tool for lineage tracing analysis and mutant analysis specific to the floor plate by driving Cre expression to this region.

Furthermore, the Lmx1a CR2 enhancer seems to drive LacZ expression to the rostral half of the Lmx1a+ mDA progenitor domain. Co-staining of β-gal and Lmx1a will be performed to confirm this interpretation. It would be very interesting to identify which mDA neuron subpopulation this enhancer labels at later developmental stages. It has been proposed that subpopulation can already be identified at E12.5. This is shown by Otx2 expression patterns where Otx2+ labels only a subset of mDA neurons at this stage (Di Salvio et al., 2009). Lmx1a CR2 labeling one of these Otx2+/- subpopulations will allow us to speculate that these cells are specified to their subpopulations very early in development (E10.5). Identifying the factors involved in this early specification process would provide novel mechanistic insights for mDA development.

4.5 Foxa2 roles in coordinating Shh signaling pathway

Foxa2 is known to induce Shh expression within the notochord and floor plate (Echelard et al., 1993; Hynes et al., 1995). Recent papers have demonstrated that Foxa2 can also act as a repressor of Shh downstream targets such as Nkx2.2 (Lin et al., 2009). A recent study in the lab of the Wnt1-Cre Foxa2-flox mutant mice by Mavromatakis, 2006 have demonstrated that Foxa2 is involved in modulating Shh signaling by inhibiting the expression of its intracellular transducer, Gli2. The ChIP-Seq data indicate that this effect may be direct, since Foxa2 is binding on five candidate regulatory elements on the Gli2 locus and promoter. Furthermore, these genetic studies have demonstrated that Foxa2 is required for the expression of Foxa1, and the repression of other Shh signaling components, Ptch1 and Gli1. Notably, Foxa2 binding sites were identified on the Gli1 and Ptch1 regulatory regions, which correlated very well with the Gli1 binding sites identified from a Gli1 ChIP-on-chip analysis by Vokes et al. This data suggests a direct role of Foxa2 in controlling the expression of Shh components and downstream targets (Figure 4-2).

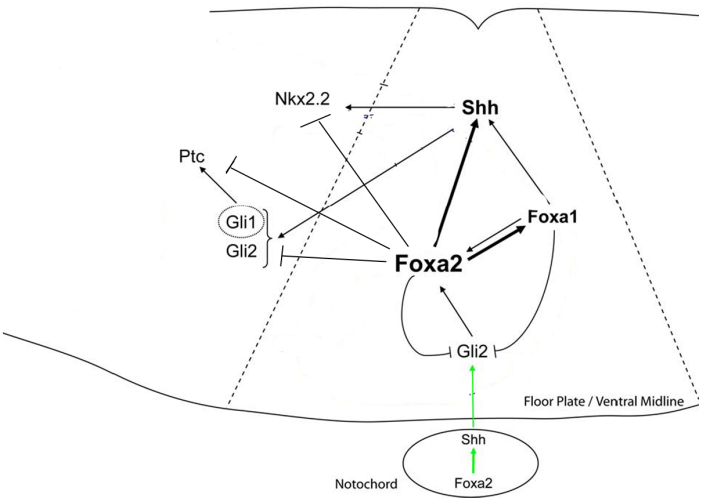

Figure 4-2:Foxa2 coordinates Shh signaling. (1) Foxa2 gene activity induces the transcription of Shh within the notochord and subsequent diffusion of the morphogenetic Shh protein induces the expression of genes involved in specifying the floor plate region in the overlying neural plate (green arrows). Gli2, which is known to mediate the primary response of Shh signalling, induces the expression of Foxa2 within the presumptive floor plate region. (2) Foxa2 protein induces the transcriptional activation of Shh and Foxa1 in this region. Foxa2 and possibly Foxa1 are involved in the down-regulation of Gli2 gene expression from the ventral midline. (3) Shh signaling induces target genes such as Nkx2.2 and also induces the transcription of mediators of the Shh signalling cascade including Ptc, the membrane bound Shh receptor. Through this activation of mediators, Foxa2 gene expression is induced, therefore creating a positive feedback loop in which both Foxa2 and Shh maintain their gene expression within this midline tissue. (3) Foxa2 may directly regulate the ventral limit of Nkx2.2, Gli1, Gli2, and Ptc.(Modified from Mavromatakis, 2006)

4.6 Concluding ideas

Gene expression patterns are mainly controlled by transcription factors (Wilson et al., 2009). Foxa2 has been shown to play critical roles in the specification and development of various tissues in mouse and C elegans (Gaudet and Mango, 2002; Li et al., 2009; Santisteban et al., 2010; Xu et al., 2009). This observation suggests that Foxa2 is involved in the regulation of gene expression patterns in a highly complex manner. Numerous models have been generated for the possible mechanisms of Foxa2 function. From our data a number of possible model mechanisms of Foxa2 function have emerged in DA neuron development. These observations and interpretation need to be investigated further.

4.6.1 The affinity model

The affinity model has been previously described in C elegans where high affinity binding sites lead to the early expression of Foxa2 target genes and lower affinity binding sites lead to the delay in gene expression (Gaudet and Mango, 2002). Also, the affinity of the Foxa2 binding sites may play a role in the expression profile of cells of specific tissue depending on the expression levels of Foxa2 (Figure 4-3)(Kele et al., 2006). For example, in the liver it has been shown that it is more likely to find Foxa2 target genes with lower affinity binding sites where Foxa2 expression levels are high (Tuteja et al., 2008). From our study the expression of two genes TH and AADC seem to fit this model. TH and AADC are both required in late neuronal function for DA synthesis but their expression is initiated at two different time points. The early expression (E10.5) of AADC correlates

with the presence of a high affinity (according to sequence compatibility) Foxa2 binding site within its neuronal promoter. Moreover, the later expression (E11.5) of TH correlates with the presence of a low affinity Foxa2 binding site within its promoter region. Given the large number of targets genes identified in this study at different time points of midbrain DA neuron development it would be interesting to further validate the affinity model for the temporal regulation of genes by Foxa2.

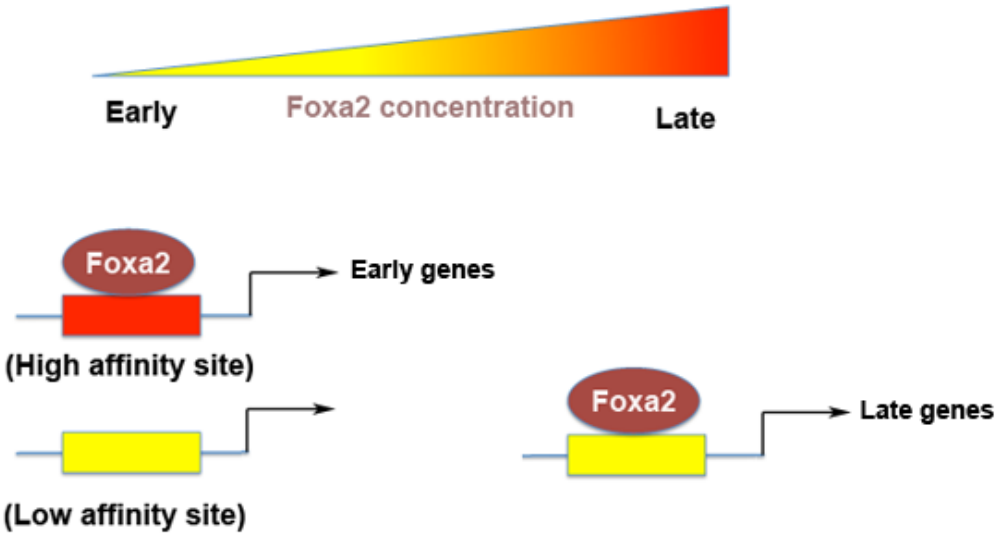

Figure 4-3: The affinity model suggests that Foxa2 regulation of transcription may depend on the DNA binding motif it identifies on regulatory regions, as well as on its concentration in the cell. Lower concentrations are required to induce genes with high affinity motifs compared to genes with low affinity motifs within their regulatory regions. (Modified from Mango, 2009)

4.6.2 Combinatorial control and feed-forward loops

A key mechanism that may provide progression of development with stable commitment to the mDA neuronal fate is the combinatorial control of transcription by multiple factors interacting with Foxa2. Furthermore, Foxa2 involvement has been suggested in feed forward loops where Foxa2 induces a target gene and together they co-induce target genes involved in regulating developmental progression (Ang, 2006; Mango, 2009). Notably, in our study we have identified Foxa2 binding events on possible regulatory regions of candidate target genes that are regulators of key events in midbrain DA development (Lmx1a, Lmx1b, Neurog2, Nr4a2, and Pitx3). We have previously suggest that Otx2 and Foxa2 together induce the expression of Lmx1a, and both induce and restrict the expression of Lmx1b, the key specification factors of DA neurons. Gain of function analysis of Lmx1a in chick and loss of function analysis of Foxa2 in mouse demonstrate the regulation of expression of the proneural gene Neurog2, which is required for differentiation of mDA neurons (Huangfu and Anderson, 2006; Kele et al., 2006), The Foxa2 peak identified close to the Neurog2 locus and the possible (well conserved) Lmx1a DNA binding motif within this region suggests this regulation may be direct (Figure 4-4). As suggested previously, Foxa2 together with Neurog2 may be directly required to induce Nurr1 (Nr4a2) since a peak was identified within its promoter and an E box motif was observed. Finally Nurr1 and Foxa2 co-regulate the Pitx3 element identified and all three regulate the expression of TH the mature DA neuronal marker (Figure 4-6). This is a complex network of interaction that requires further investigation.

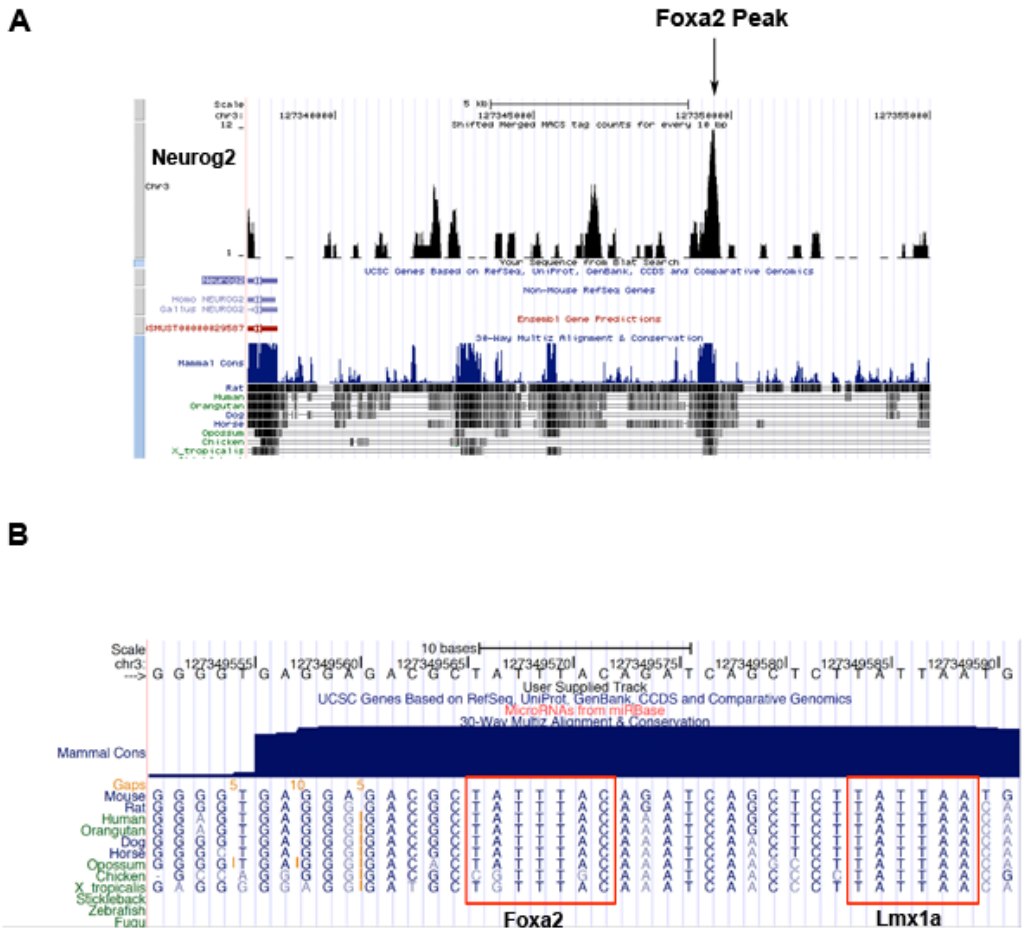

Figure 4-4: Occupancy of Neurog2 conserved genomic element by Foxa2. (A) Schematic diagram of genomic region occupied by Foxa2 down stream of the Neurog2 gene, from data obtained by Foxa2 ChIP-Seq experiments on E12.5 ventral midbrain tissue. Arrow indicate peak called by peak calling algorithm MACS. (B) Schematic diagram indicating the position of the predicted Foxa2 and Lmx1a DNA binding sites.

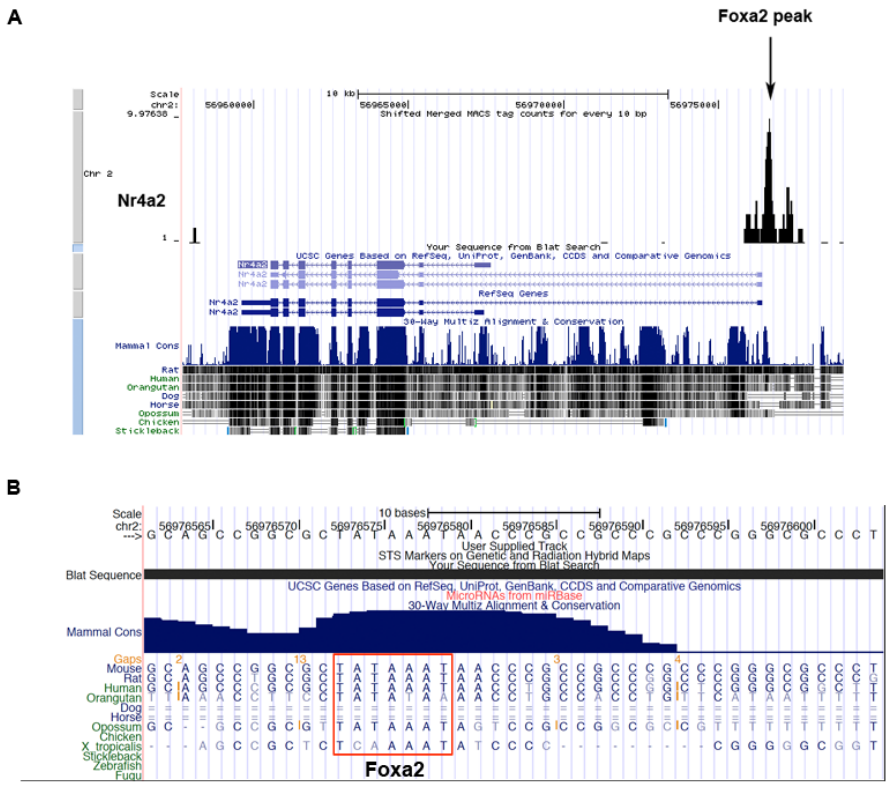

Figure 4-5: Occupancy of the Nurr1 (Nr4a2) promoter by Foxa2. (A) Schematic diagram of the genomic region occupied by Foxa2, from data obtained by Foxa2 ChIP-Seq experiments on E12.5 ventral midbrain tissue. Arrow indicates peak called by peak calling algorithm MACS. (B) Schematic diagram of mouse Nurr1promotes indicates the presence of predicted Foxa2.

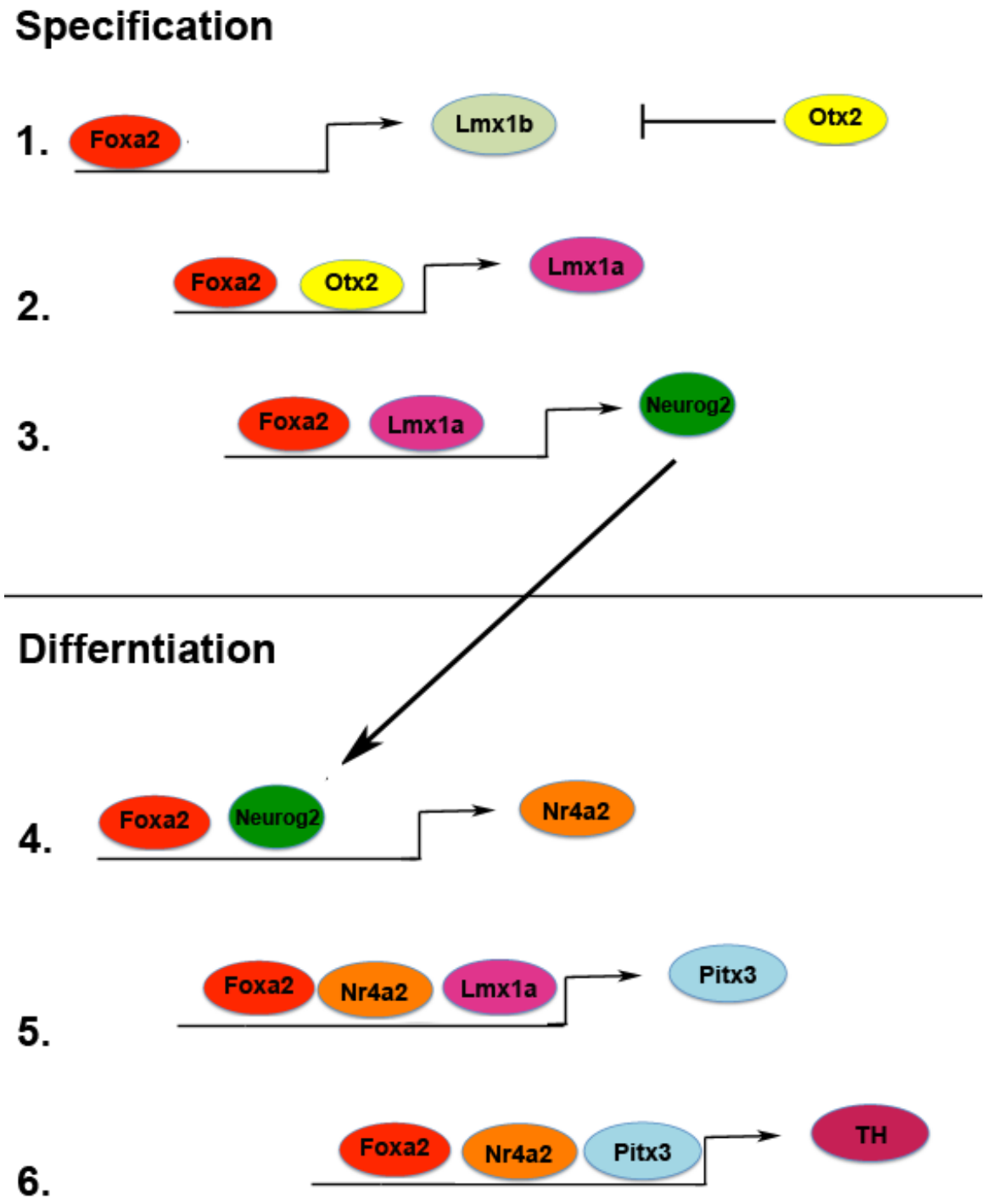
Specification
1.
Foxa2
Lmx1b
Otx2
2.
Foxa2
Otx2
Lmx1a
3.
Foxa2
Lmx1a
Neurog2
Differntiation
4.
Foxa2
Neurog2
Nr4a2
5.
Foxa2
Nr4a2
Lmx1a
Pitx3
6.
Foxa2
Nr4a2
Pitx3
TH

Figure 4-6: Combinatorial regulation of mDA specific genes through feed forward loops. (1) During specification, Foxa2 induces directly Lmx1b while Otx2 regulates its dorsal limit. (2) Foxa2 and Otx2 possibly regulate directly the expression of Lmx1a within the floor plate region. (3) Foxa2 in combination with Lmx1a may induce directly Neurog2 (Ngn2) and promote differentiation. (4) Foxa2 together with Neurog2 may regulate Nurr1 (Nr4a2) by binding to its promoter. (5) Foxa2 and possibly in combination with Lmx1a and Nurr1 positively regulate Pitx3. (6) Finally, Foxa2, Nurr1 and Pitx3 are required for the induction of TH by regulating directly it's promoter. (This is a hypothetical series of events during the specification and differentiation of mDA neurons that requires further analysis and validation).

All together, our work provides extensive information regarding possible Foxa2 functions during the development of mDA neurons through the identification of Foxa2 direct targts. This data suggests that Foxa2 is required at multiple points in the development of mDA neurons: specification, and differentiation. Further analysis is required to confirm these results, but nonetheless; we provide insights on the diverse range of functions Foxa2 may performs for the proper development of mDA neurons.

4.7 Appendix A

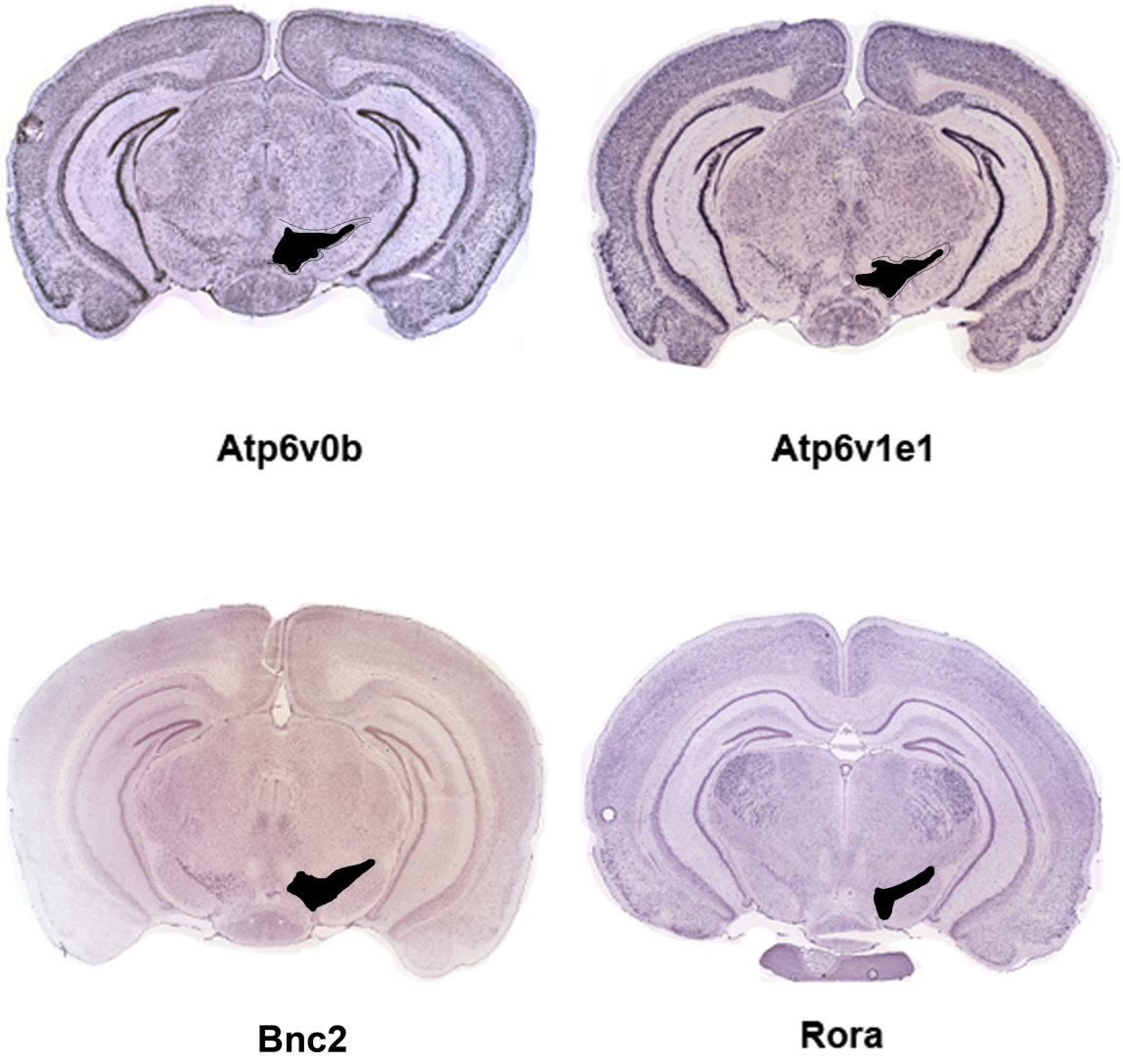

Figure 4-7: Coronal sections through adult mouse midbrain. In situ hybridization analysis of genes identified from the in vivo ChIP-Seq assays. Black area indicates expression within the DA area. Look at atlas next. (Modified from the Allen brain atlas)

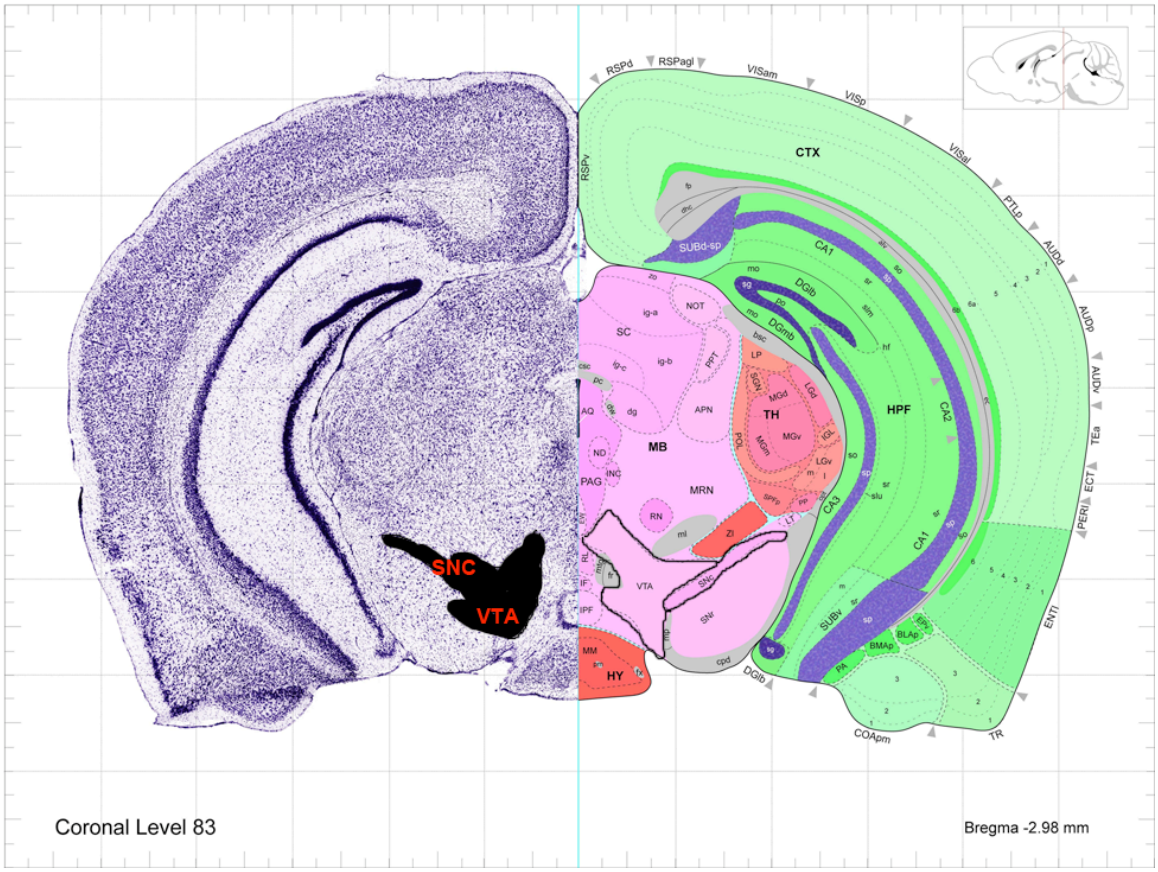

Figure 4-8: Coronal sections through adult mouse midbrain. Anatomy atlas of the adult mouse midbrain. Black region indicates DA population area (SNc, and VTA). (Modified from the Allen brain atlas)

4.8 Appendix B

Gene	MGI Gene/Marker ID	Name
Akap2	MGI:1306795	A kinase (PRKA) anchor protein 2
Akr1a4	MGI:1929955	aldo-keto reductase family 1, member A4 (aldehyde reductase)
Akt3	MGI:1345147	thymoma viral proto-oncogene 3
ankrd15	MGI:2147707	KN motif and ankyrin repeat domains 1
App	MGI:88059	amyloid beta (A4) precursor protein
Arg1	MGI:88070	arginase, liver
Atg10	MGI:1914045	autophagy-related 10 (yeast)
axin2	MGI:1270862	axin2
bmp7	MGI:103302	bone morphogenetic protein 7
Cdh6	MGI:107435	cadherin 6
Centg2	MGI:2653690	ArfGAP with GTPase domain, ankyrin repeat and PH domain 1
cobl	MGI:105056	cordon-bleu
corin	MGI:1349451	corin
Corin	MGI:1349451	corin
Dnahc2	MGI:107731	dynein, axonemal, heavy chain 2
e2f6	MGI:1354159	E2F transcription factor 6
Ebf2	MGI:894332	early B-cell factor 2
ephb1	MGI:1096337	Eph receptor B1
Ephb1	MGI:1096337	Eph receptor B1
Ephx2	MGI:99500	epoxide hydrolase 2, cytoplasmic
fgfr2	MGI:95523	fibroblast growth factor receptor 2
foxa1	MGI:1347472	forkhead box A1
foxa2	MGI:1347476	forkhead box A2
Gm114	MGI:2684960	polo-like kinase 1 substrate 1
Gpc3	MGI:104903	glypican 3
Heph	MGI:1332240	hephaestin
Il17rd	MGI:2159727	interleukin 17 receptor D
Itpr2	MGI:99418	inositol 1,4,5-triphosphate receptor 2
Jakmip1	MGI:1923321	janus kinase and microtubule interacting protein 1
Kalrn	MGI:2685385	kalirin, RhoGEF kinase
Kif26b	MGI:2447076	kinesin family member 26B
Litaf	MGI:1929512	LPS-induced TN factor
lmx1a	MGI:1888519	LIM homeobox transcription factor 1 alpha
lmx1b	MGI:1100513	LIM homeobox transcription factor 1 beta
Ltbp1	MGI:109151	latent transforming growth factor beta binding protein 1
mbd5	MGI:2138934	methyl-CpG binding domain protein 5
med23	MGI:1917458	mediator complex subunit 23
Meis2	MGI:108564	Meis homeobox 2
mitf	MGI:104554	microphthalmia-associated transcription factor
Mpped1	MGI:106316	metallophosphoesterase domain containing 1
msx2	MGI:97169	homeobox, msh-like 2
Mylk	MGI:894806	myosin, light polypeptide kinase
Ncald	MGI:1196326	neurocalcin delta
Nedd1	MGI:97293	neural precursor cell expressed, developmentally down-regulated gene 1
neo1	MGI:1097159	neogenin
nfatc1	MGI:102469	nuclear factor of activated T-cells, cytoplasmic, calcineurin-dependent 1
nrp2	MGI:1100492	neuropilin 2
Odz3	MGI:1345183	odd Oz/ten-m homolog 3 (Drosophila)
Pdzrn3	MGI:1933157	PDZ domain containing RING finger 3
Pftk1	MGI:894318	cyclin-dependent kinase 14
Plxna2	MGI:107684	plexin A2
Ppp1r9a	MGI:2442401	protein phosphatase 1, regulatory (inhibitor) subunit 9A
Ptch1	MGI:105373	patched homolog 1
Ptprd	MGI:97812	protein tyrosine phosphatase, receptor type, D
Rab38	MGI:1919683	RAB38, member of RAS oncogene family
rbbp7	MGI:1194910	retinoblastoma binding protein 7
Rbbp7	MGI:1194910	retinoblastoma binding protein 7
rfx4	MGI:1918387	regulatory factor X, 4 (influences HLA class II expression)
Rgs3	MGI:1354734	regulator of G-protein signaling 3
robo1	MGI:1274781	roundabout homolog 1 (Drosophila)
Rps6ka3	MGI:104557	ribosomal protein S6 kinase polypeptide 3
slit1	MGI:1315203	slit homolog 1 (Drosophila)
slit2	MGI:1315205	slit homolog 2 (Drosophila)
smad1	MGI:109452	MAD homolog 1 (Drosophila)
smad3	MGI:1201674	MAD homolog 3 (Drosophila)
Smad3	MGI:1201674	MAD homolog 3 (Drosophila)
smarca2	MGI:99603	SWI/SNF related, matrix associated, actin dependent regulator of chromatin, subfamily a, member 2
Sort1	MGI:1338015	sortilin 1
sox5	MGI:98367	SRY-box containing gene 5
Sulf1	MGI:2138563	sulfatase 1
Tasp1	MGI:1923062	taspase, threonine aspartase 1
tcf12	MGI:101877	transcription factor 12
Tcf12	MGI:101877	transcription factor 12
tcf7l2	MGI:1202879	transcription factor 7-like 2, T-cell specific, HMG-box
Tgfbr3	MGI:104637	transforming growth factor, beta receptor III
tle1	MGI:104636	transducin-like enhancer of split 1, homolog of Drosophila E(spl)
Tmem2	MGI:1890373	transmembrane protein 2
Tmem47	MGI:2177570	transmembrane protein 47
Tmtc2	MGI:1914057	transmembrane and tetratricopeptide repeat containing 2
tshz3	MGI:2442819	teashirt zinc finger family member 3
Tuft1	MGI:109572	tuftelin 1
Vgll4	MGI:2652840	vestigial like 4 (Drosophila)
Xpr1	MGI:97932	xenotropic and polytropic retrovirus receptor 1

Figure 4-9: Gene symbol, names and MGI IDs of genes mentioned in the in vitro ChIP-Seq analysis.

Gene symbol	Genomic coordinates										
ankrd15	chr19:25305058-25305582										
axin2	chr11:108784279-108784497										
bmp7	chr2:172760362-172760740										
cobl	chr11:12440478-12440797										
corin	chr5:72803060-72803677										
e2f6	chr12:16825215-16825515										
ephb1	chr9:102113704-102113963										
fgfr2	chr7:137402117-137402369										
foxa1	chr12:58647168-58647323										
foxa2	chr2:147865841-147866623										
lmx1a	chr1:169712276-169712508	chr1:169732998-169733196									
lmx1b	chr2:33438208-33438620	chr2:33448354-33448744									
mbd5	chr2:48806132-48806340										
med23	chr10:24554402-24554636										
mitf	chr6:97704553-97705048										
msx2	chr13:53825921-53826363										
neo1	chr9:58883041-58883402										
nfatc1	chr18:80845645-80845888										
nrp2	chr1:62799648-62799883										
rbbp7	chrX:159202022-159202208										
rfx4	chr10:84173663-84174050										
robo1	chr16:72677689-72678122										
Shh	chr5:28785783-28786314										
slit1	chr19:41741350-41741655										
slit2	chr5:48,395,011-48,395,347	chr5:48400259-48400621									
smad1	chr8:81885085-81885376										
smad3	chr9:63598095-63598682										
smarca2	chr19:26713431-26713665	chr19:26821902-26822242									
sox5	chr6:143991375-143991740	chr6:144052405-144052667	chr6:144052849-144053171	chr6:144233579-144233886	chr6:144309957-144310237						
tcf12	chr9:71865577-71865943										
tcf7l2	chr19:55971137-55971387										
tle1	chr4:71783321-71783770	chr4:71837034-71837499									
tshz3	chr7:37552555-37552886										
Gli2	chr1:120774789-120775202	chr1:120810300-120810966	chr1:120946997-120947307	chr1:121093398-121093720	chr1:121114012-121114309	chr1:121201879-121202551					

Figure 4-10: Genomic regions identified from the in vitro data set and used in ChIP-qPCR validation analysis using chromatin from E12.5 dissected ventral midbrain.

GO terms of genes up regulated between D3.5 and D5 of in vitro differentiation

GO_ID	LEVEL(S)	TERM	NB_IN_REF	FREQ_IN_REF	NB_IN_SET	FREQ_IN_SET	P_VALUE	ENRICHMENT/	GENES_IN_SET	Fold Change
GO:0030509	8	BMP signaling pathway	27	0.0019	5	0.0439	1.97E-06	E	Bmp7,Cer1,Twsg1,Smad1,Gpc3	23.1052632
GO:0007411	8,11,5,9,10,1	axon guidance	79	0.0055	8	0.0702	1.90E-07	E	Ephb1,Bmp7,Lmx1a,Slit3,Tgfb2,Sema3f,Shh,Slit2	12.7636364
GO:0001822	5,6	kidney development	69	0.0048	6	0.0526	1.64E-05	E	Bmp7,Kif3a,Ret,Shh,Slit2,Gpc3	10.9583333
GO:0030705	7,5,6	cytoskeleton-dependent intracellular transport	100	0.007	7	0.0614	1.32E-05	E	Wipf1,Kif3a,Zfp282,Dnahc2,Klc1,Tubb2b,Gata6	8.77142857
GO:0031175	8,5,7,10,9	neurite development	188	0.0131	11	0.0965	2.58E-07	E	Abi2,Ephb1,Bmp7,Lmx1a,Slit3,Tgfb2,Mtap2,Sema3f,MBD5,Shh,Slit2	7.36641221
GO:0048666	7,4,9,6	neuron development	211	0.0147	12	0.1053	9.83E-08	E	Abi2,Ephb1,Bmp7,Lmx1a,Slit3,Tgfb2,Mtap2,Sema3f,Ret,MBD5,Shh,Slit2	7.16326531

GO terms of predicetd genes up regulated between D3.5 and D5 of in vitro differentiation (E-box motif identified within Foxa2 bound regions)

GO_ID	LEVEL(S)	TERM	NB_IN_REF	FREQ_IN_REF	NB_IN_SET	FREQ_IN_SET	P_VALUE	ENRICHMENT/	GENES_IN_SET	Fold Change
GO:0042551	6,9,7,10,5	neuron maturation	12	0.0008	2	0.0426	0.000644	E	Cdkn1c,Ret	53.25
GO:0007411	7,9,8,4,12,10,	axon guidance	100	0.0068	6	0.1277	7.14E-07	E	Bmp7,Tgfb2,Epha7,Slit2,Mnx1,Efna5	18.7794118
GO:0016331	6,8,7,9,5	morphogenesis of embryonic epithelium	90	0.0061	4	0.0851	0.0001839	E	Ptch1,Bmp7,Cobl,Ret	13.9508197
GO:0007409	6,8,7,11,9,12,	axonogenesis	187	0.0128	6	0.1277	2.56E-05	E	Bmp7,Tgfb2,Epha7,Slit2,Mnx1,Efna5	9.9765625
GO:0031175	4,9,6,10,7	neuron projection development	230	0.0157	7	0.1489	7.27E-06	E	Bmp7,Tgfb2,Epha7,Ppp1r9a,Slit2,Mnx1,Efna5	9.48407643
GO:0048812	5,7,6,10,8,11,	neuron projection morphogenesis	198	0.0135	6	0.1277	3.52E-05	E	Bmp7,Tgfb2,Epha7,Slit2,Mnx1,Efna5	9.45925926
GO:0048667	6,9,7,10,8	cell morphogenesis involved in neuron differentiation	201	0.0137	6	0.1277	3.82E-05	E	Bmp7,Tgfb2,Epha7,Slit2,Mnx1,Efna5	9.32116788
GO:0048666	8,5,9,6	neuron development	303	0.0207	9	0.1915	3.86E-07	E	Cdkn1c,Bmp7,Tgfb2,Epha7,Ppp1r9a,Slit2,Mnx1,Ret,Efna5	9.25120773

GO terms of genes down regulated between D3.5 and D5 of in vitro differentiation

GO_ID	LEVEL(S)	TERM	NB_IN_REF	FREQ_IN_REF	NB_IN_SET	FREQ_IN_SET	P_VALUE	ENRICHMENT/	GENES_IN_SET	Fold Change
GO:0033151	10,9,8,6,5	V(D)J recombination	9	0.0006	2	0.0312	0.0006558	E	Foxp1,Tcf3	52
GO:0010552	11,10,12,9,8	positive regulation of specific transcription from RNA polymerase II promoter	17	0.0012	2	0.0312	0.0023947	E	Tcf3,Rarg	26
GO:0055007	6,7,9,8,10	cardiac muscle cell differentiation	18	0.0012	2	0.0312	0.0026826	E	Foxp1,Tsc1	26
GO:0060444	8,7,9,10,11,6	branching involved in mammary gland duct morphogenesis	20	0.0014	2	0.0312	0.0033032	E	Etv5,Pml	22.2857143
GO:0035051	5,6,7	cardiac cell differentiation	21	0.0014	2	0.0312	0.0036355	E	Foxp1,Tsc1	22.2857143
GO:0043193	10,9,11,8,7	positive regulation of gene-specific transcription	24	0.0016	2	0.0312	0.0047176	E	Tcf3,Rarg	19.5
GO:0060603	7,9,8,10,6	mammary gland duct morphogenesis	26	0.0018	2	0.0312	0.0055082	E	Etv5,Pml	17.3333333
GO:0030183	7,9,10,8,6	B cell differentiation	52	0.0035	3	0.0469	0.0014295	E	Foxp1,Plcg2,Bcl11a	13.4
GO:0030031	4	cell projection assembly	71	0.0048	3	0.0469	0.0034142	E	Mtss1,Pcnt,Capg	9.77083333
GO:0001525	4,6,7,8,9,5	angiogenesis	148	0.0101	4	0.0625	0.0035015	E	Arhgap22,Col18a1,Pitx2,Pml	6.18811881
GO:0035239	5,4	tube morphogenesis	163	0.0111	4	0.0625	0.0048596	E	Tsc1,Pitx2,Etv5,Pml	5.63063063
GO:0048514	6,7,8,5	blood vessel morphogenesis	206	0.0141	5	0.0781	0.0017599	E	Arhgap22,Col18a1,Pitx2,Ntrk2,Pml	5.53900709

4.9 Appendix C

Gene symbol	MGI Gene/Marker ID	Name
th	MGI:98735	tyrosine hydroxylase
ephb1	MGI:1096337	Eph receptor B1
nfib	MGI:103188	nuclear factor I/B
nurr1	MGI:1352456	nuclear receptor subfamily 4, group A, member 2
bnc2	MGI:2443805	basonuclin 2
ebf3	MGI:894289	early B-cell factor 3
kif7	MGI:1098239	kinesin family member 7
nfic	MGI:109591	nuclear factor I/C
rora	MGI:104661	RAR-related orphan receptor alpha
esrrb	MGI:1346832	estrogen related receptor, beta
foxj2	MGI:1926805	forkhead box J2
ncoa2	MGI:1276533	nuclear receptor coactivator 2
trex1	MGI:1328317	three prime repair exonuclease 1
tspyl1	MGI:1298395	testis-specific protein, Y-encoded-like 1
nap1l3	MGI:1859565	nucleosome assembly protein 1-like 3
fbxw7	MGI:1354695	F-box and WD-40 domain protein 7
cacna1a1	MGI:109482	calcium channel, voltage-dependent, P/Q type, alpha 1A subunit
arnt2	MGI:107188	aryl hydrocarbon receptor nuclear translocator 2
ergic3	MGI:1913616	ERGIC and golgi 3
hivep1	MGI:96100	human immunodeficiency virus type I enhancer binding protein 1
rin2	MGI:1921280	Ras and Rab interactor 2
runx1t1	MGI:104793	runt-related transcription factor 1; translocated to, 1 (cyclin D-related)
serinc1	MGI:1926228	serine incorporator 1
h2afy2	MGI:3037658	H2A histone family, member Y2
dtwd1	MGI:1916435	DTW domain containing 1
fmnl2	MGI:1918659	formin-like 2
odz3	MGI:1345183	odd Oz/ten-m homolog 3 (Drosophila)
crim1	MGI:1354756	cysteine rich transmembrane BMP regulator 1 (chordin like)
sema3a	MGI:107558	sema domain, immunoglobulin domain (Ig), short basic domain, secreted, (semaphorin) 3A
gli2	MGI:95728	GLI-Kruppel family member GLI2
wnt1	MGI:98953	wingless-related MMTV integration site 1

Figure 4-11: Gene symbol, names and MGI IDs of genes mentioned in the in vivo ChIP-Seq analysis.

Gene	genomic coordinates
Aadc	chr11:11790115-11790718
Arf2	chr11:103831790-103832456
Atp13a2	chr4:140542517-140543196
Bmp6	chr13:38436486-38437392
Bnc2	chr4:84002209-84002830
Dmrt1	chr19:25591527-25591708
Ednrb	chr14:104241965-104242968
Ephb6	chr6:41565779-41566415
Kif5c	chr2:49483626-49484290
Nfic	chr10:80926503-80927557
Nmnat2	chr1:154812761-154813809
Numbl	chr7:28045593-28047092
Ptpru	chr4:131393718-131394534
Slc1a3	chr15:8609313-8610271
Slc6a9	chr4:117529391-117530236
Sorcs	chr19:50562284-50562929
TH	chr7:150,087,596-150,088,586

Figure 4-12: Genomic regions used in ChIP-qPCR analisys using E12.5, and E14.5 chromatin from dissected ventral midbrain

GO terms of early onset genes (E12.5 ChIP-Seq data)

GO_ID	LEVEL(S)	TERM	NB_IN_REF	FREQ_IN_REF	NB_IN_SET	FREQ_IN_SET	P_VALUE	ENRICHMENT/	GENES_IN_SET	Fold Change
GO:0048663	8,9,6,5	neuron fate commitment	46	0.0031	7	0.0959	2.54E-09	E	Dll1,Foxa1,Notch1,Foxa2,Isl1,Wnt1,Notch3	30.9354839
GO:0007368	7,6	determination of left/right symmetry	44	0.003	5	0.0685	2.41E-06	E	Dll1,Notch1,Pitx2,Pcsk6,Acvr1	22.8333333
GO:0009799	5,4	determination of symmetry	45	0.0031	5	0.0685	2.70E-06	E	Dll1,Notch1,Pitx2,Pcsk6,Acvr1	22.0967742
GO:0045664	8,7,9,6	regulation of neuron differentiation	89	0.0061	7	0.0959	2.69E-07	E	Dll1,Lmx1a,Foxa1,Notch1,Foxa2,Isl1,Notch3	15.7213115
GO:0045165	5,4	cell fate commitment	144	0.0098	9	0.1233	3.55E-08	E	Dll1,Foxa1,Notch1,Sox6,Foxa2,Isl1,Wnt1,Neurog2,Notch3	12.5816327
GO:0050767	7,6,8,5	regulation of neurogenesis	114	0.0078	7	0.0959	1.43E-06	E	Dll1,Lmx1a,Foxa1,Notch1,Foxa2,Isl1,Notch3	12.2948718
GO:0007411	7,9,8,4,12,10,	axon guidance	100	0.0068	6	0.0822	9.57E-06	E	Slit1,Lmx1a,Isl1,Neurog2,Slit2,Efna5	12.0882353

GO terms of Late onset genes (E12.5 ChIP-Seq data)

GO_ID	LEVEL(S)	TERM	NB_IN_REF	FREQ_IN_REF	NB_IN_SET	FREQ_IN_SET	P_VALUE	ENRICHMENT/	GENES_IN_SET	Fold Change
GO:0050804	7,8,6	regulation of synaptic transmission	68	0.0046	8	0.0315	1.95E-05	E	Rasgrf1,Rims1,Pink1,Slc1a3,Ctnnd2,Ppp3ca,Drd1a,Cacna2d2	6.84782609
GO:0007411	7,9,8,4,12,10,	axon guidance	100	0.0068	11	0.0433	1.08E-06	E	Kif5c,Robo1,Gap43,App,Klf7,Ank3,Dpysl5,Ablim1,Chl1,Sema6a,Mapk8ip3	6.36764706
GO:0007409	6,8,7,11,9,12,	axonogenesis	187	0.0128	18	0.0709	3.58E-09	E	Ntrk3,Celsr3,Kif5c,Rtn4rl1,Stmn1,Robo1,Gap43,Uchl1,App,Cck,Klf7,Ank3,Dpysl5,Ablim1,Bcl11b,Chl1,Sema6a,Mapk8ip3	5.5390625
GO:0048667	6,9,7,10,8	cell morphogenesis involved in neuron differen	201	0.0137	19	0.0748	1.77E-09	E	Ntrk3,Celsr3,Kif5c,Rtn4rl1,Stmn1,Slc1a3,Robo1,Gap43,Uchl1,App,Cck,Klf7,Ank3,Dpysl5,Ablim1,Bcl11b,Chl1,Sema6a,Mapk8ip3	5.45985401
GO:0031175	4,9,6,10,7	neuron projection development	230	0.0157	21	0.0827	4.60E-10	E	Ntrk3,Celsr3,Mtap2,Kif5c,Rtn4rl1,Stmn1,Robo1,Gap43,Atg7,Uchl1,App,Cck,Klf7,Ank3,Dpysl5,Ablim1,Bcl11b,Mtap1b,Chl1,Sema6a,Mapk8ip3	5.26751592
GO:0048812	5,7,6,10,8,11,	neuron projection morphogenesis	198	0.0135	18	0.0709	8.78E-09	E	Ntrk3,Celsr3,Kif5c,Rtn4rl1,Stmn1,Robo1,Gap43,Uchl1,App,Cck,Klf7,Ank3,Dpysl5,Ablim1,Bcl11b,Chl1,Sema6a,Mapk8ip3	5.25185185
GO:0048858	4,5,6,7	cell projection morphogenesis	205	0.014	18	0.0709	1.50E-08	E	Ntrk3,Celsr3,Kif5c,Rtn4rl1,Stmn1,Robo1,Gap43,Uchl1,App,Cck,Klf7,Ank3,Dpysl5,Ablim1,Bcl11b,Chl1,Sema6a,Mapk8ip3	5.06428571
GO:0000904	5,6,7	cell morphogenesis involved in differentiation	231	0.0158	20	0.0787	3.00E-09	E	Ntrk3,Celsr3,Kif5c,Rtn4rl1,Stmn1,Slc1a3,Robo1,Gap43,Uchl1,App,Esrrb,Cck,Klf7,Ank3,Dpysl5,Ablim1,Bcl11b,Chl1,Sema6a,Mapk8ip3	4.98101266
GO:0048666	8,5,9,6	neuron development	303	0.0207	26	0.1024	1.47E-11	E	Ntrk3,Celsr3,Mtap2,Kif5c,Rtn4rl1,Ret,Stmn1,En1,Slc1a3,Robo1,Gap43,Atg7,Uchl1,App,Cck,Klf7,Ank3,Dpysl5,Drd1a,Ablim1,Bcl11b,Mtap1b,Chl1,Sema6a,Gnaq,Mapk8ip3	4.9468599

GO terms of Late onset genes (E14.5 ChIP-Seq data)

GO_ID	LEVEL(S)	TERM	NB_IN_REF	FREQ_IN_REF	NB_IN_SET	FREQ_IN_SET	P_VALUE	ENRICHMENT/	GENES_IN_SET	Fold Change
GO:0015991	7,9,8,10	ATP hydrolysis coupled proton transport	8	0.0005	3	0.0085	0.000676	E	Atp6v1e1,Atp6v0b,Atp4a	17
GO:0048813	6,8,7,11,9,12,	dendrite morphogenesis	18	0.0012	4	0.0114	0.0007071	E	Dscam,Dclk1,Cacna1a,Klf7	9.5
GO:0048168	9,10,8	regulation of neuronal synaptic plasticity	18	0.0012	4	0.0114	0.0007071	E	Rasgrf1,Rims1,Grik2,Dlg4	9.5
GO:0051899	9,7	membrane depolarization	33	0.0023	6	0.0171	0.0001051	E	Grik2,Chrna4,Cacna1a,Ppp3ca,Cacna1g,Atxn1	7.43478261
GO:0007270	6,7	nerve-nerve synaptic transmission	34	0.0023	6	0.0171	0.0001246	E	Grik2,Cacna1a,Kif1b,Stxbp1,Pink1,Th	7.43478261
GO:0050804	7,8,6	regulation of synaptic transmission	68	0.0046	11	0.0313	5.10E-07	E	Rasgrf1,Rims1,Grik2,Cacna1a,Dlg4,Ctnnd2,Ppp3ca,Stxbp1,Cspg5,Pink1,Cacna2d2	6.80434783
GO:0051969	6,7,5	regulation of transmission of nerve impulse	71	0.0048	11	0.0313	7.93E-07	E	Rasgrf1,Rims1,Grik2,Cacna1a,Dlg4,Ctnnd2,Ppp3ca,Stxbp1,Cspg5,Pink1,Cacna2d2	6.52083333
GO:0031644	6,5	regulation of neurological system process	75	0.0051	11	0.0313	1.38E-06	E	Rasgrf1,Rims1,Grik2,Cacna1a,Dlg4,Ctnnd2,Ppp3ca,Stxbp1,Cspg5,Pink1,Cacna2d2	6.1372549
GO:0007156	5	homophilic cell adhesion	64	0.0044	8	0.0228	0.000117	E	Ret,Pcdh10,Cdh22,Cadm3,Chl1,Celsr3,Clstn1,Cdh13	5.18181818
GO:0007268	5,6	synaptic transmission	194	0.0132	23	0.0655	2.15E-10	E	Rasgrf1,Abat,Rims1,Grik2,Chrna4,Cacna1a,Pclo,Dlg4,Ctnnd2,Ppp3ca,Kif1b,Apba2,Gjd2,Stxbp1,Cspg5,Clstn1,Pink1,Th,Stx1a,Ncan,Gria2,Cacna2d2,Atxn1	4.96212121
GO:0044057	5,4	regulation of system process	154	0.0105	18	0.0513	2.47E-08	E	Rasgrf1,Rims1,Grik2,Cacna1a,Dlg4,Nkx2-5,Ctnnd2,Ppp3ca,Gnao1,Stxbp1,Cacna1g,Cspg5,Pink1,Th,Ryr1,Slc8a1,Ptprm,Cacna2d2	4.88571429
GO:0006754	12	ATP biosynthetic process	73	0.005	8	0.0228	0.0002869	E	Atp8a2,Atp6v1e1,Atp13a2,Atp2c1,Atp6v0b,Atp8a1,Atp4a,Atp1b1	4.56
GO:0046034	11	ATP metabolic process	78	0.0053	8	0.0228	0.0004444	E	Atp8a2,Atp6v1e1,Atp13a2,Atp2c1,Atp6v0b,Atp8a1,Atp4a,Atp1b1	4.30188679
GO:0007409	6,8,7,11,9,12,	axonogenesis	187	0.0128	19	0.0541	9.55E-08	E	Ntrk3,Sema4f,Dclk1,Cacna1a,Ank3,Dpysl5,Ablim1,Ulk2,Chl1,Sema6a,Mapk8ip3,Stxbp1,Celsr3,Robo1,Gap43,Numbl,Cck,Klf7,Bcl11b	4.2265625

GO terms of Late onset genes (Unique to E14.5 ChIP-Seq data)

GO_ID	LEVEL(S)	TERM	NB_IN_REF	FREQ_IN_REF	NB_IN_SET	FREQ_IN_SET	P_VALUE	ENRICHMENT/	GENES_IN_SET	Fold Change
GO:0042133	5,7,8,4	neurotransmitter metabolic process	18	0.0012	3	0.0208	0.0006553	E	Abat,Th,Cacna1a	17.3333333
GO:0007270	6,7	nerve-nerve synaptic transmission	34	0.0023	5	0.0347	1.80E-05	E	Stxbp1,Th,Cacna1a,Grik5,Kif1b	15.0869565
GO:0001505	4,6,7	regulation of neurotransmitter levels	67	0.0046	5	0.0347	0.0004558	E	Abat,Th,Cacna1a,Pclo,Grik5	7.54347826
GO:0006754	12	ATP biosynthetic process	73	0.005	5	0.0347	0.0006694	E	Atp8a2,Atp2c1,Atp6v1e1,Atp8a1,Atp13a2	6.94
GO:0046034	11	ATP metabolic process	78	0.0053	5	0.0347	0.0008968	E	Atp8a2,Atp2c1,Atp6v1e1,Atp8a1,Atp13a2	6.54716981
GO:0006816	7,8	calcium ion transport	129	0.0088	7	0.0486	0.000241	E	Cacna1g,Cacna1a,Atp2c1,Trpm2,Nkx2-5,Slc8a1,Cacng7	5.52272727
GO:0044057	5,4	regulation of system process	154	0.0105	8	0.0556	0.0001183	E	Stxbp1,Cacna1g,Th,Cacna1a,Nkx2-5,Slc8a1,Grik5,Gnao1	5.2952381
GO:0007268	5,6	synaptic transmission	194	0.0132	10	0.0694	1.83E-05	E	Stxbp1,Abat,Clstn1,Th,Cacna1a,Pclo,Stx1a,Grik5,Kif1b,Gria2	5.25757576
GO:0015674	6,7	di-, tri-valent inorganic cation transport	159	0.0108	7	0.0486	0.000809	E	Cacna1g,Cacna1a,Atp2c1,Trpm2,Nkx2-5,Slc8a1,Cacng7	4.5
GO:0019226	5	transmission of nerve impulse	233	0.0159	10	0.0694	8.26E-05	E	Stxbp1,Abat,Clstn1,Th,Cacna1a,Pclo,Stx1a,Grik5,Kif1b,Gria2	4.36477987
GO:0007267	4	cell-cell signaling	353	0.0241	13	0.0903	3.52E-05	E	Stxbp1,Abat,Clstn1,Pfkm,Ntrk2,Th,Cacna1a,Pclo,Dlgap3,Stx1a,Grik5,Kif1b,Gria2	3.74688797
GO:0051128	4,3	regulation of cellular component organizatio	256	0.0175	9	0.0625	0.0007442	E	Mapt,Cdc42ep3,Cacna1a,Nkx2-5,Herc2,Grik5,Capza3,Ulk2,C3	3.57142857
GO:0006811	4,5	ion transport	682	0.0465	17	0.1181	0.000255	E	Cacna1g,Chrna2,Cacna1a,Atp2c1,Trpm2,Grik4,Nkx2-5,Slc8a1,Atp6v1e1,Cacng7,Grik5,Atp13a2,Gria2,Kctd7,Slc10a4,Slc39a3,Svop	2.53978495

4.10 Appendix D

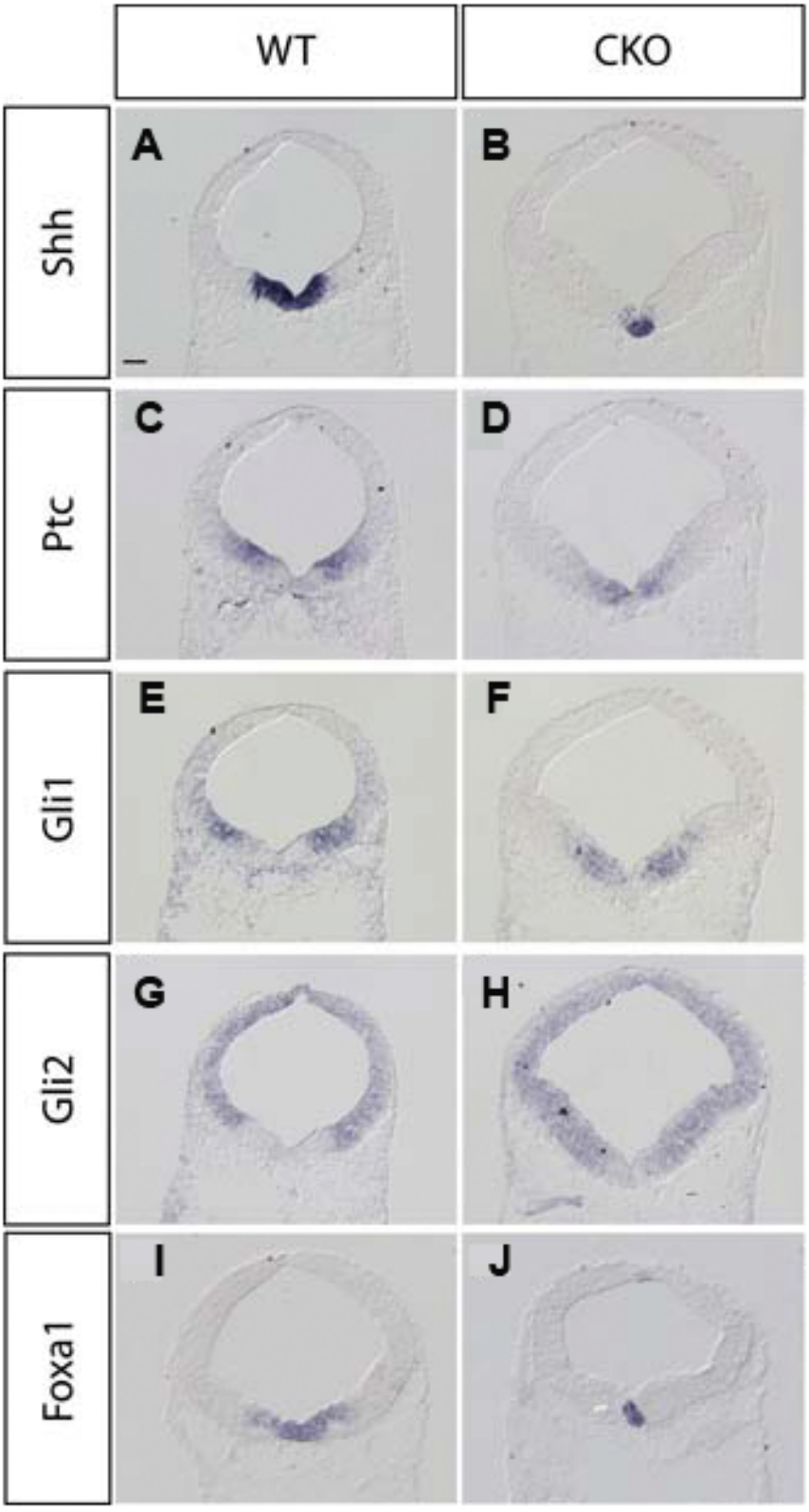

Figure 4-13:Analysis of downstream targets of Shh signalling at E10.5 in the Foxa2 CKO (conditional knockout) mouse ventral mesencephalon. A-J: Coronal sections of E10.5 wild type and Foxa2 CKO embryos. Analysis of the downstream targets of Shh signalling revealed that in E10.5 ventral mesencephalon the gene expression patterns of all the downstream targets of Shh signalling are shifted ventrally to meet the reduced Shh gene expression at the ventral midline. This suggests a possible role for Foxa2 in maintaining the expression boundary of these genes. Furthermore, Shh and Foxa1, known downstream targets of Foxa2, are reduced in these mutants. Scale bar represents 100μm. (Mavromatakis, 2008)

Primers of 54 genes identified from in vitro ChIP-Seq

Akap2 F	agagaccgtggaagcatcat			
Akap2 R	gctgccaattctttcctcag			
Akt3 F	aatcctgctggctattgtgg			
Akt3 R	tctgcaccgtcagtacttgg			
App	ggttctgggctgacaaacat			
App	cagtttttgatggcggactt			
Atg10	catccctgcaagacaaatga			
Atg10	ggctcagccatgatgtgata			
Cdh6	cagtggaatcggaaacaggt			
Cdh6	atgtccttggcctgaatcac			
Ebf2	tgagcttgttggggagagtt			
Ebf2	tgcttcatgaggaacacgag			
Ephx2	ggacgacggagacaagagag			
Ephx2	ttgatcatcccaacctgaca			
Il17rd	ttctttggcttcctcatgct			
Il17rd	tgtggttttggtgttgcact			
Ltbp1	gccctagagggaaaggtttg			
Ltbp1	ctccaaacagcaagcattca			
Mpped1	aggagaggtcacttgcctga			
Mpped1	actccagtggtgatgggaag			
Mylk	cctgaggaccgaggtttgta			
Mylk	tcactggtctgagcatcgtc			
Nedd1	tcatgggatcttcagggaaa			
Nedd1	ttcatggcgtccttaggttc			
Odz3	cgagcaaaatccatgatgtg			
Odz3	cagggaatccaggaatagca			
Pftk1	cccttgctcctcctgacata			
Pftk1	tgtagcctgcgtctcctttt			
Rgs3	ggactcttaccctcgcttcc			
Rgs3	acgctgagctggatactggt			
Rps6ka3	acaaggggtggttcacagag			
Rps6ka3	tgcaaagccaaaatcacaaa			
Sort1	gaccagcctctggatcagtc			
Sort1	atgcttctgagagccgttgt			
Tasp1	gacagtctgttgccatcgaa			
Tasp1	tcaggctctgaaatgcctct			
Tgfbr3	catggtcccctgtgtagctt			
Tgfbr3	gcggagtatcaggagtcagc			
Tmem47	gagcctcaagcagtttgctc			
Tmem47	gtgcaggtccctaaaatgga			

Tuft1	gctgcagttttgggtaggaa			
Tuft1	gctaaggtgtgcctctcagg			
Vgll4	cagtgacacaggcaggtcag			
Vgll4	gggacagtgagagaggttgc			
Xpr1	aaaccctctccctctgctgt			
Xpr1	accggacagcatcacctaac			
Itpr2	tcttccagcaaacggaagat			
Itpr2	cagagtgagatgtgcctgga			
Smad3	ggcagacttctccactgacc			
Smad3	ttggggaagatgaagaccac			
Kalrn	ccgatgctgtagctcctctc			
Kalrn	gtattggggaaaggctggat			
Kif26b	agctagaagcgaccaagcag			
Kif26b	caggtactccagggaatcca			
Gm114	cagacccaaagctttcctga			
Gm114	attgccctcgtgtcttcaat			
Plxna2	aaatgcaaagtggcttcagg			
Plxna2	aagacaaggcatcaggagga			
Tmtc2	ggattgttgccaacgacttt			
Tmtc2	caggatttatccgcactggt			
1110059E24R	ggacggaaggaagacagtga			
1110059E24R	ccctctgcaattgacttggt			
Arg1	taccagcgtggcatctacag			
Arg1	cccacccagtgatcttgact			
Ptch1	tgtggtcatcctgattgcat			
Ptch1	tagccctgtggttcttgtcc			
Sulf1	caaggtggtgacttcctggt			
Sulf1	tttccccaaccacatgactt			
Ncald	cagaaaccctggtaccctca			
Ncald	tgttgcccctacatgactga			
Gpc3	acgggatggtgaaagtgaag			
Gpc3	atttccatgctgcttgttcc			
Litaf	ccatttctccatttgctggt			
Litaf	ggatcccctaggagttcgag			
Heph	ccatgggccaagatactgac			
Heph	tgggaagagatccaccacat			
Centg2	gtttcccgatgactgatgct			
Centg2	aacccgaacaaggtcgtatg			
Tmem2	tgaccaccccactaaaggtc			
Tmem2	cccaagccaagatgttctgt			
Rab38	tgggtaagcgtcaggatagg			
Rab38	atggggtgggaaaacacata			
Jakmip1	gctgacgagaggaacgaact			
Jakmip1	gcagctcctcgttctttttg			
Meis2	atctcaaggcaaggggaagt			
Meis2	tggggaggagtgtaacttgg			
Ptprd	acagaatgaaaggcgtgctt			
Ptprd	tggaacctgtgtcagcaaag			
Dnahc2	agatcgagcctcctttgtca			
Dnahc2	agctgtccaggctcatcagt			
Ppp1r9a	cccacctcagtagccatgat			
Ppp1r9a	aagcggatggcttaggaagt			
Akr1a4	catcctgatgagccagtcct			
Akr1a4	gctgaacctgccatctaagc			

RT-qPCR primers of genes identified from the in vivo ChIP-Seq

NFIb QPCR primers	Ebf3
F: Gggactaagcccaagagacc	F: gcctagacccgtcagaagc
R: tgggtgtcctatttgacacttg	R: caaagaagttgtccccgatt
NFIC QPCR primers	Nap1l3
F: gatgtattcctccccgctct	F: aataggtgtacggggctaacag
R: aaccaggtgtaggcgaagg	R: caccaggttctgtgaccattt
NFIA QPCR primers	Zfp148
F: ggaactcgatttatatttggcatac	F: cagcgtcattgatgaaagca
R: ctggctgggactttcagatt	R: ttgtggcatctggtgaagat
Ncoa2 QPCR primers	Foxj2
F: gcgcatgtcacagagcag	F: atcagcaccatccccactc
R: ctctgtggtgcccattcc	R: gagcaccagtcaggaggaaa
Esrrb QPCR primers	Klf7
F: aactgggccaagcacatc	F: aagtgtaaccactgcgacagg
R: gtacacgatgcccaagatga	R: tcttcatatggagcgcaaga
Bnc2 QPCR primers	Runx1t1
F: ggggttgatccatctcaactt	F: ccgaccggaggaagttttat
R: cacacgtccgcaggttaat	R: ggagtgcttctcggtacgat
Trex1 QPCR primers	Arnt2
F: cagggcagaccaagaattg	F: caccaacaccaatgtcaagc
R: ggtctgtgagcccatgct	R: ctcgctgatgtacctccagtt
Tspyl1	Hivep1
F: gcttcttcacctggttctcg	F: tcgaagaagcacaaaaagagc
R: tgataatctcagcgattctgtca	R: aacgccagcctctaagacttc
Cacna1a	Rora
F: tgacaagacacccatgtctga	F: ttacgtgtgaaggctgcaag
R: tccagcctcaaaacagaagatt	R: ggagtaggtggcattgctct
Fbxw7	
F: cagacttgtcgatactggagaattt	
R: gatgtgcaacggttcatcaat	

ChIP-qPCR primers of in vitro identified regions

Sox5 1		E2f6	
LEFT PRIMER	GGAGGAATGTGGCGATAGAA	LEFT PRIMER	CACATGCCCCAAAGAAGAAT
RIGHT PRIMER	AGGACCTGGCAGACAATAGC	RIGHT PRIMER	GCAGAAATGGTTTCGGAATG
Sox5 2			
		TCF4	
LEFT PRIMER	ACACGCCAAACAAAAGGAAT		
RIGHT PRIMER	CTCTTCCGTGTGGGTGTGTA	LEFT PRIMER	CCCATGAGGACCAGTAAACG
		RIGHT PRIMER	AGAGGGGGCTGTCTCTTTTT
Sox5 3			
LEFT PRIMER	GCAAGAGAGGTCAGCACACA	Smad3	
RIGHT PRIMER	GAGGACCCCTTGGAACTCTC		
		LEFT PRIMER	TCATGCCACTGAGGACAGAG
		RIGHT PRIMER	GAGCGCGAGCATACACATTA
Med23			
LEFT PRIMER	CGGACTGCTGCCAGATCTAA	TCF12	
RIGHT PRIMER	TTCCCGGGCAATACAGATAG		
		LEFT PRIMER	AGGACAGGCTCAAGGGCTAT
		RIGHT PRIMER	CAGCCACGACATTCAGTCAG
Ankrd15			
LEFT PRIMER	CAGACAATAGGGCCTTGGAA		
RIGHT PRIMER	ATGGCTTGAGTTCAGGGGTA	Tle1	
		LEFT PRIMER	AGAGCCAAGCACTCACCTGT
Tshz3		RIGHT PRIMER	GGACAGGCGGTTTAGACAAC
LEFT PRIMER	CCAAGGGTGGAGGTTCTTCT		
RIGHT PRIMER	CTGTCTTTTTGGAGGCCTTG	Rbbp7	
		LEFT PRIMER	CTGGGATTAAAGGCGTGTGT
Nfatc1		RIGHT PRIMER	CAGATGCCCTCTTCTGGTGT
LEFT PRIMER	TGGCTGCTTTCATGGCTAGT		
RIGHT PRIMER	TGTCAACAACCTTTTTAAATTGC	Mbd5	
		LEFT PRIMER	CTTTGCTTGTCTGTGGCTTG
Tcf7l2		RIGHT PRIMER	CGCTATGCCATTCAGACAAA
LEFT PRIMER	AGAGGGAGGGAAGGCAATTA		
RIGHT PRIMER	GCCATTTCCCTTTACACAGC	Neo1	
		LEFT PRIMER	GGGCTAGTATGCCCCTTAGC
Smad1		RIGHT PRIMER	CTTCTGAAGTCCAGGGAAGC
LEFT PRIMER	CTCACTGGTGGTGAGCTGAG		
RIGHT PRIMER	CTGCGTCCTCCAGTTGACTT	Smarca2	
		LEFT PRIMER	AATGCCATGGTCGGTGTTAT
Mitf		RIGHT PRIMER	GAGGGAGCAGCTTCAGGTAA
LEFT PRIMER	GTGTTTCCAGGCAAAGGAAG		
RIGHT PRIMER	AGAATGGGATGGCTGACAAG	Rfx4	
		LEFT PRIMER	CTCTGCTGCTCTGGCTTTCT
		RIGHT PRIMER	ATGCCAAGATGGTTCCCATA

ChIP-qPCR of in vitro peaks

Slit1				Robo1				
LEFT PRIMER	TCAAGCAGAACCTGGTAGGG			LEFT PRIMER	AGAGGACCTGCCATGACATT			
RIGHT PRIMER	TTGGAGATCATCAGCCAGTG			RIGHT PRIMER	CTTTGCTTCTGGGGTGATGT			
Slit2								
				Cobl				
LEFT PRIMER	GACACGGTTGATTGCTGCTA							
RIGHT PRIMER	GCAAACATCTTGACCTGAGC			LEFT PRIMER	TCCCCTTTCCAGGTTTCTTT			
				RIGHT PRIMER	ACAGCTGGGTGGTGGTAAAC			
Bmp7								
LEFT PRIMER	CGATCTGGGATCCATCAAAC			Axin2				
RIGHT PRIMER	GTGGGGTGAGGAAATACCAA							
				LEFT PRIMER	AGCTGGGTTGCTTGATTTGA			
Corin				RIGHT PRIMER	GGGGGAGAGAGAAAAGGGTA			
LEFT PRIMER	CCGGCAACAGAGAGGATAAG							
RIGHT PRIMER	TGGGAAGTCGATTCATCTCC			Msx2				
				LEFT PRIMER	TGATTCAACACGAGGAGCTG			
FgfR2				RIGHT PRIMER	TAGAAGCCATCCTGCCAATC			
LEFT PRIMER	TACTGGGCTGGGGTAAACAG			Tcf12				
RIGHT PRIMER	TGCCAGTCTCGGCTCTTACT							
				LEFT PRIMER	AGGACAGGCTCAAGGGCTAT			
				RIGHT PRIMER	CAGCCACGACATTCAGTCAG			
Lmx1a CR2								
				Nrp2				
LEFT PRIMER	TTCTAATGCCCGATCCTGAG							
RIGHT PRIMER	GGGAATTAAGGGAGGGAGAA			LEFT PRIMER	GTGTGGCATGTTTCATCAGG			
				RIGHT PRIMER	GACATTTGGAAGGCTTCTGG			
Lmx1b CR1								
LEFT PRIMER	AGACAAGGCAGCTGTCCAAA							
RIGHT PRIMER	TAGGGGCAGGAGCTGAGTAA							

ChIP-qPCR primers to compare E12 and E14 ChIP-Seq data sets

E12 E14 overlap	E12 alone	E14 alone
Ptprt	Kif5c	Slc6a9
		F: TCGCAGAGACACAAAACTCC
F: ACACACCCGTTCCTAGACCA	F: CTTTCCTCTCCCTGTCAGCA	R: TCGCAGGCCTAGCTAAATGT
R: CACTCTCTGCCTCCCATTGT	R: GCTTTCAGTCCAATGGGAGA	
	Bnc2	Dmrt1
Ptpru		
	Bnc2 F: GTCAGCAGTGTGCAATGGA(	F: GGAGGCTGGGATGATGTCTA
F: CTCCGCCCTAACTCTGACTG	Bnc2 R: CAGCAAACACAGGCATTGA	R: CAGACCTGTGCCTTTGGATT
R: TGGGCTTTAAAGGCAGAAGA		
	Arf2	Numbl
Nfic	F: AGATGCTGTTTCCCAGGTTG	F: ACGTGCCATGCTAGTGACTG
F: GACCGAGGAGTGGGATAAGG	R: CGGCATTCACTAGGAAGGAG	R: CCACGTCACCCTATCACAGA
R: CCCACTTTCAGCTCCATCAC		
	Ednrb	Ephb6
Sorcs1		
F: CTTGCGTTTTCTCCATGGTT	F: GTCTTAGTGGGTGGCGTCAT	F: AGGACAGCTTGCTTCAGCTC
R: CAGCGCTGAAGATTAGAGCA	R: GGGGTATGGGGAGAGAAAAG	R: GGGTGGAGGGGATAGAGTTC
BMP6	Slc1a3	Atp13a2
F: ACTCCTGATGCCTCCAAGAA	F: GCCATGGAAAATAGCAGGAA	F: CTACCTGTCTCGCAGCCTGT
R: CCTTCTTTCACCCTCCCTTC	R: AGGCAGCTCTCCAGGTATGA	R: GGGAGAGGAGGGAAGAGATG
	Nmnat2	
	F:TGAGCAAGAGCAACAAGTGC	
	R:TGACTCCACCCTTTCTGACC	

Bibliography

Acampora, D., Avantaggiato, V., Tuorto, F., and Simeone, A. (1997). Genetic control of brain morphogenesis through Otx gene dosage requirement. Development *124*, 3639-3650.

Acampora, D., Mazan, S., Lallemand, Y., Avantaggiato, V., Maury, M., Simeone, A., and Brûlet, P. (1995). Forebrain and midbrain regions are deleted in Otx2-/- mutants due to a defective anterior neuroectoderm specification during gastrulation. Development *121*, 3279-3290.

Agren M., Kogerman, P., Kleman, M. I., Wessling, M. and Toftgard, R. (2004). Expression of the PTCH1 tumor suppressor gene is regulated by alternative promoters and a single functional Gli-binding site. Gene330, 101-114

Aguanno, A., Lee, M.R., Marden, C.M., Rattray, M., Gault, A., and Albert, V.R. (1995). Analysis of the neuronal promoter of the rat aromatic L-amino acid decarboxylase gene. J Neurochem *65*, 1944-1954.

Andersson, E., Jensen, J.B., Parmar, M., Guillemot, F., and Björklund, A. (2006a). Development of the mesencephalic dopaminergic neuron system is compromised in the absence of neurogenin 2. Development *133*, 507-516.

Andersson, E., Tryggvason, U., Deng, Q., Friling, S., Alekseenko, Z., Robert, B., Perlmann, T., and Ericson, J. (2006b). Identification of intrinsic determinants of midbrain dopamine neurons. Cell *124*, 393-405.

Ang, S. (2006). Transcriptional control of midbrain dopaminergic neuron development. Development *133*, 3499-3506.

Ang, S., and Rossant, J. (1994). HNF-3 beta is essential for node and notochord formation in mouse development. Cell *78*, 561-574.

Ang, S.L., Jin, O., Rhinn, M., Daigle, N., Stevenson, L., and Rossant, J. (1996). A targeted mouse Otx2 mutation leads to severe defects in gastrulation and formation of axial mesoderm and to deletion of rostral brain. Development *122*, 243-252.

Ariandna Perez-Balaguer et al. Shh dependent and independent maintenance of basal midbrain. Mech Dev (2009) vol. 126 (5-6) pp. 301-13

Bae, E.J., Lee, H.S., Park, C.H., and Lee, S.H. (2009). Orphan nuclear receptor Nurr1 induces neuron differentiation from embryonic cortical precursor cells via an extrinsic paracrine mechanism. FEBS Lett *583*, 1505-1510.

Bally-Cuif, L., and Wassef, M. (1995). Determination events in the nervous system of the vertebrate embryo. Curr Opin Genet Dev *5*, 450-458.

Barski, A., Cuddapah, S., Cui, K., Roh, T., Schones, D.E., Wang, Z., Wei, G., Chepelev, I., and Zhao, K. (2007). High-resolution profiling of histone methylations in the human genome. Cell *129*, 823-837.

Beckstead, R.M., Domesick, V.B., and Nauta, W.J. (1979). Efferent connections of the substantia nigra and ventral tegmental area in the rat. Brain Res *175*, 191-217.

Beddington, R.S., and Robertson, E.J. (1999). Axis development and early asymmetry in mammals. Cell *96*, 195-209.

Blat, Y., and Kleckner, N. (1999). Cohesins bind to preferential sites along yeast chromosome III, with differential regulation along arms versus the centric region. Cell *98*, 249-259.

Briscoe, J., and Ericson, J. (1999). The specification of neuronal identity by graded Sonic Hedgehog signalling. Semin Cell Dev Biol *10*, 353-362.

Broccoli, V., Boncinelli, E., and Wurst, W. (1999). The caudal limit of Otx2 expression positions the isthmic organizer. Nature *401*, 164-168.

Bryne, J.C., Valen, E., Tang, M.H., Marstrand, T., Winther, O., da Piedade, I., Krogh, A., Lenhard, B., and Sandelin, A. (2008). JASPAR, the open access database of transcription factor-binding profiles: new content and tools in the 2008 update. Nucleic Acids Research *36*, D102-106.

Burbach, J.P., Smits, S., and Smidt, M. (2003). Transcription factors in the development of midbrain dopamine neurons. Annals of the New York Academy of Sciences *991*, 61-68.

Dai, P., Akimaru, H., Tanaka, Y., Maekawa, T., Nakafuku, M. and Ishii, S. (1999). Sonic Hedgehog-induced activation of the Gli1 promoter is mediated by GLI3. *J. Biol. Chem*. 274, 8143-8152.

Carroll, J.S., Liu, X., Brodsky, A.S., Li, W., Meyer, C., Szary, A.J., Eeckhoute, J., Shao, W., Hestermann, E.V., Geistlinger, T.R.*, et al.* (2005). Chromosome-wide mapping of estrogen receptor binding reveals long-range regulation requiring the forkhead protein FoxA1. Cell *122*, 33-43.

Castelo-Branco, G., and Arenas, E. (2006). Function of Wnts in dopaminergic neuron development. Neurodegener Dis *3*, 5-11.

Castro, D.S., Skowronska-Krawczyk, D., Armant, O., Donaldson, I.J., Parras, C., Hunt, C., Critchley, J.A., Nguyen, L., Gossler, A., Göttgens, B.*, et al.* (2006). Proneural bHLH

and Brn proteins coregulate a neurogenic program through cooperative binding to a conserved DNA motif. Dev Cell *11*, 831-844.

Chi, C.L., Martinez, S., Wurst, W., and Martin, G.R. (2003). The isthmic organizer signal FGF8 is required for cell survival in the prospective midbrain and cerebellum. DEVELOPMENT *130*.

Chiang C., Litingtung Y., Lee E., Young KE., Corden JL., Westphal H., and PA., B. (1996). Cyclopia and defective axial patterning in mice lacking Sonic hedgehog gene function. Nature *383*, 407-413.

Chung, S., Leung, A., Han, B.S., Chang, M.Y., Moon, J.I., Kim, C.H., Hong, S., Pruszak, J., Isacson, O., and Kim, K.S. (2009). Wnt1-lmx1a forms a novel autoregulatory loop and controls midbrain dopaminergic differentiation synergistically with the SHH-FoxA2 pathway. Cell Stem Cell *5*, 646-658.

Cirillo, L.A., Lin, F.R., Cuesta, I., Friedman, D., Jarnik, M., and Zaret, K.S. (2002). Opening of compacted chromatin by early developmental transcription factors HNF3 (FoxA) and GATA-4. Mol Cell *9*, 279-289.

Clark, K.L., Halay, E.D., Lai, E., and Burley, S.K. (1993). Co-crystal structure of the HNF-3/fork head DNA-recognition motif resembles histone H5. Nature *364*, 412-420.

Cowan M W, Jessell TM, and LS, Z. (1997). Molecular and cellular approaches to neural development (Oxford university press).

Crossley, P.H., and Martin, G.R. (1995). The mouse Fgf8 gene encodes a family of polypeptides and is expressed in regions that direct outgrowth and patterning in the developing embryo. Development *121*, 439-451.

Crossley, P.H., Martinez, S., and Martin, G.R. (1996). Midbrain development induced by FGF8 in the chick embryo. Nature *380*, 66-68.

Danielian PS, M.A. (1996). Engrailed-1 as a target of the Wnt-1 signalling pathway in vertebrate midbrain development. nature *383*.

Danielian, P.S., and McMahon, A.P. (1996). Engrailed-1 as a target of the Wnt-1 signalling pathway in vertebrate midbrain development. Nature *383*, 332-334.

Di Salvio, M., Di Giovannantonio, L.G., Omodei, D., Acampora, D., and Simeone, A. (2009). Otx2 expression is restricted to dopaminergic neurons of the ventral tegmental area in the adult brain. Int J Dev Biol.

Echelard Y, E.D., St-Jacques B, Shen L, Mohler J, McMahon JA, McMahon AP (1993). Sonic hedgehog, a member of a family of putative signaling molecules, is implicated in the regulation of CNS polarity. Cell *75*.

Echelard, Y., Epstein, D.J., St-Jacques, B., Shen, L., Mohler, J., McMahon, J.A., and McMahon, A.P. (1993). Sonic hedgehog, a member of a family of putative signaling molecules, is implicated in the regulation of CNS polarity. Cell *75*, 1417-1430.

Echelard, Y., Vassileva, G., and McMahon, A.P. (1994). Cis-acting regulatory sequences governing Wnt-1 expression in the developing mouse CNS. Development *120*, 2213-2224.

Echevarría, D., Vieira, C., Gimeno, L., and Martínez, S. (2003). Neuroepithelial secondary organizers and cell fate specification in the developing brain. Brain Res Brain Res Rev *43*, 179-191.

Eells, J.B. (2003). The control of dopamine neuron development, function and survival: insights from transgenic mice and the relevance to human disease. Curr Med Chem *10*, 857-870.

Falck, B., Hillarp, N.A., Thieme, G., and Torp, A. (1962). Fluorescence of catechol amines and related compounds condensed with formaldehyde. Brain Res Bull *9*, xi-xv.

Farkas, L.M., Dünker, N., Roussa, E., Unsicker, K., and Krieglstein, K. (2003). Transforming growth factor-beta(s) are essential for the development of midbrain dopaminergic neurons in vitro and in vivo. J Neurosci *23*, 5178-5186.

Felsenfeld, G. (1992). Chromatin as an essential part of the transcriptional mechanism. Nature *355*, 219-224.

Ferri, A., Lin, W., Mavromatakis, Y., Wang, J., Sasaki, H., Whitsett, J., and Ang, S. (2007). Foxa1 and Foxa2 regulate multiple phases of midbrain dopaminergic neuron development in a dosage-dependent manner. Development *134*, 2761-2769.

Friedman, J.R., and Kaestner, K.H. (2006). The Foxa family of transcription factors in development and metabolism. Cell Mol Life Sci *63*, 2317-2328.

Fuchshofer, R., Stephan, D.A., Russell, P., and Tamm, E.R. (2009). Gene expression profiling of TGFbeta2- and/or BMP7-treated trabecular meshwork cells: Identification of Smad7 as a critical inhibitor of TGF-beta2 signaling. Exp Eye Res *88*, 1020-1032.

Gao, N., Zhang, J., Rao, M.A., Case, T.C., Mirosevich, J., Wang, Y., Jin, R., Gupta, A., Rennie, P.S., and Matusik, R.J. (2003). The role of hepatocyte nuclear factor-3 alpha (Forkhead Box A1) and androgen receptor in transcriptional regulation of prostatic genes. Molecular Endocrinology *17*, 1484-1507.

Gaudet, J., and Mango, S.E. (2002). Regulation of organogenesis by the Caenorhabditis elegans FoxA protein PHA-4. Science *295*, 821-825.

Gilbert, S.F., ed. (2003). Developmental Biology, Seventh edn (Sinauer Associates, Inc).

Goldman, J.E., Yen, S.H., Chiu, F.C., and Peress, N.S. (1983). Lewy bodies of Parkinson's disease contain neurofilament antigens. Science *221*, 1082-1084.

Goridis, C., and Rohrer, H. (2002). Specification of catecholaminergic and serotonergic neurons. Nat Rev Neurosci *3*, 531-541.

Guo, C., Qiu, H.Y., Huang, Y., Chen, H., Yang, R.Q., Chen, S.D., Johnson, R.L., Chen, Z.F., and Ding, Y.Q. (2007). Lmx1b is essential for Fgf8 and Wnt1 expression in the isthmic organizer during tectum and cerebellum development in mice. Development *134*, 317-325.

Hahn, S.L., Hahn, M., Kang, U.J., and Joh, T.H. (1993). Structure of the rat aromatic L-amino acid decarboxylase gene: evidence for an alternative promoter usage. J Neurochem *60*, 1058-1064.

Hallikas, O., Palin, K., Sinjushina, N., Rautiainen, R., Partanen, J., Ukkonen, E. and Taipale, J. (2006). Genome-wide prediction of mammalian enhancersbased on analysis of transcription-factor binding affinity. Cell 124, 47-59

Henke, R.M., Meredith, D.M., Borromeo, M.D., Savage, T.K., and Johnson, J.E. (2009). Ascl1 and Neurog2 form novel complexes and regulate Delta-like3 (Dll3) expression in the neural tube. Developmental Biology *328*, 529-540.

Hermanson, E., Joseph, B., Castro, D., Lindqvist, E., Aarnisalo, P., Wallén, A., Benoit, G., Hengerer, B., Olson, L., and Perlmann, T. (2003). Nurr1 regulates dopamine synthesis and storage in MN9D dopamine cells. Experimental Cell Research *288*, 324-334.

Hirsch, E., Graybiel, A.M., and Agid, Y.A. (1988). Melanized dopaminergic neurons are differentially susceptible to degeneration in Parkinson's disease. Nature *334*, 345-348.

Hokfelt, T., Johansson, O., and Goldstein, M. (1984). Chemical Anatomy of the Brain. Science *225*.

Holland, P.W., and Takahashi, T. (2005). The evolution of homeobox genes: Implications for the study of brain development. Brain Res Bull *66*, 484-490.

Hooper, J.E., and Scott, M.P. (2005). Communicating with Hedgehogs. Nat Rev Mol Cell Biol *6*, 306-317.

Huangfu, D., and Anderson, K.V. (2006). Signaling from Smo to Ci/Gli: conservation and divergence of Hedgehog pathways from Drosophila to vertebrates. Development *133*, 3-14.

Hynes, M., Porter, J.A., Chiang, C., Chang, D., Tessier-Lavigne, M., Beachy, P.A., and Rosenthal, A. (1995). Induction of midbrain dopaminergic neurons by Sonic hedgehog. Neuron *15*, 35-44.

Hynes, M., Stone, D.M., Dowd, M., Pitts-Meek, S., Goddard, A., Gurney, A., and Rosenthal, A. (1997). Control of cell pattern in the neural tube by the zinc finger transcription factor and oncogene Gli-1. Neuron *19*, 15-26.

Hynes M., Porter J. A., Chiang C., Chang D., Tessier-Lavigne M., Beachy P. A., and A., R. (1995a). Induction of midbrain dopaminergic neurons by Sonic hedgehog. Neuron *15*.

Hynes M., Poulsen K., Tessier-Lavigne M., and A., R. (1995b). Control of neuronal diversity by the floor plate: contact-mediated induction of midbrain dopaminergic neurons. Cell *80*, 95-101.

Jacobs, F.M., van Erp, S., van der Linden, A.J., von Oerthel, L., Burbach, J.P., and Smidt, M. (2009). Pitx3 potentiates Nurr1 in dopamine neuron terminal differentiation through release of SMRT-mediated repression. Development *136*, 531-540.

Jeong, Y., and Epstein, D.J. (2003). Distinct regulators of Shh transcription in the floor plate and notochord indicate separate origins for these tissues in the mouse node. Development *130*, 3891-3902.

Jessell, T.M. (2000). Neuronal specification in the spinal cord: inductive signals and transcriptional codes. Nat Rev Genet *1*, 20-29.

Jiang, C., Wan, X., He, Y., Pan, T., Jankovic, J., and Le, W. (2005). Age-dependent dopaminergic dysfunction in Nurr1 knockout mice. Exp Neurol *191*, 154-162.

Joksimovic, M., Yun, B., Kittappa, R., Anderegg, A., Chang, W., Taketo, M., Mckay, R., and Awatramani, R. (2009). Wnt antagonism of Shh facilitates midbrain floor plate neurogenesis. Nat Neurosci *12*, 125-131.

Joyner, A.L., Kornberg, T., Coleman, K.G., Cox, D.R., and Martin, G.R. (1985). Expression during embryogenesis of a mouse gene with sequence homology to the Drosophila engrailed gene. Cell *43*, 29-37.

Joyner, A.L., and Martin, G.R. (1987). En-1 and En-2, two mouse genes with sequence homology to the Drosophila engrailed gene: expression during embryogenesis. Genes & Development *1*, 29-38.

Jung, P., and Hermeking, H. (2009). The c-MYC-AP4-p21 cascade. Cell Cycle *8*, 982-989.

Kawasaki, H., Mizuseki, K., Nishikawa, S., Kaneko, S., Kuwana, Y., Nakanishi, S., Nishikawa, S.I., and Sasai, Y. (2000). Induction of midbrain dopaminergic neurons from ES cells by stromal cell-derived inducing activity. Neuron *28*, 31-40.

Kele, J., Simplicio, N., Ferri, A.L., Mira, H., Guillemot, F., Arenas, E., and Ang, S.L. (2006). Neurogenin 2 is required for the development of ventral midbrain dopaminergic neurons. Development *133*, 495-505.

Kessaris, N., Pringle, N., and Richardson, W.D. (2001). Ventral neurogenesis and the neuron-glial switch. Neuron *31*, 677-680.

Kiecker, C., and Lumsden, A. (2004). Hedgehog signaling from the ZLI regulates diencephalic regional identity. Nat Neurosci *7*, 1242-1249.

Kiecker, C., and Lumsden, A. (2005). Compartments and their boundaries in vertebrate brain development. Nat Rev Neurosci *6*, 553-564.

Kim, M.Y., Jeong, B.C., Lee, J.H., Kee, H.J., Kook, H., Kim, N.S., Kim, Y.H., Kim, J.K., Ahn, K.Y., and Kim, K.K. (2006). A repressor complex, AP4 transcription factor and geminin, negatively regulates expression of target genes in nonneuronal cells. Proc Natl Acad Sci USA *103*, 13074-13079.

Kingsbury, B.F. (1930). The developmental significance of the floor plate of the brain and spinal cord. J Comp Neurol *50*, 177-207.

Kittappa, R., Chang, W., Awatramani, R., and Mckay, R. (2007). The foxa2 Gene Controls the Birth and Spontaneous Degeneration of Dopamine Neurons in Old Age. Plos Biol *5*, e325.

Koudritsky, M., and Domany, E. (2008). Positional distribution of human transcription factor binding sites. Nucleic Acids Research *36*, 6795-6805.

Kumasaka, M., Sato, S., Yajima, I., Goding, C.R., and Yamamoto, H. (2005). Regulation of melanoblast and retinal pigment epithelium development by Xenopus laevis Mitf. Dev Dyn *234*, 523-534.

Kumbasar, A., Plachez, C., Gronostajski, R.M., Richards, L.J., and Litwack, E.D. (2009). Absence of the transcription factor Nfib delays the formation of the basilar pontine and other mossy fiber nuclei. J Comp Neurol *513*, 98-112.

Lacroix, M., and Leclercq, G. (2004). About GATA3, HNF3A, and XBP1, three genes co-expressed with the oestrogen receptor-alpha gene (ESR1) in breast cancer. Mol Cell Endocrinol *219*, 1-7.

Lai, E., Prezioso, V.R., Smith, E., Litvin, O., Costa, R.H., and Darnell, J.E. (1990). HNF-3A, a hepatocyte-enriched transcription factor of novel structure is regulated transcriptionally. Genes & Development *4*, 1427-1436.

Le, W.D., Xu, P., Jankovic, J., Jiang, H., Appel, S.H., Smith, R.G., and Vassilatis, D.K. (2003). Mutations in NR4A2 associated with familial Parkinson disease. Nat Genet *33*, 85-89.

Lee, H.S., Bae, E.J., Yi, S.H., Shim, J.W., Jo, A.Y., Kang, J.S., Yoon, E.H., Rhee, Y.H., Park, C.H., Koh, H.C.*, et al.* (2010). Foxa2 and Nurr1 Synergistically Yield A9 Nigral Dopamine Neurons Exhibiting Improved Differentiation, Function and Cell Survival. Stem cells (Dayton, Ohio).

Lee, K.J., and Jessell, T.M. (1999). The specification of dorsal cell fates in the vertebrate central nervous system. Annu Rev Neurosci *22*, 261-294.

Lee, S.H., Lumelsky, N., Studer, L., Auerbach, J.M., and McKay, R.D. (2000). Efficient generation of midbrain and hindbrain neurons from mouse embryonic stem cells. Nat Biotechnol *18*, 675-679.

Lenhard, B., and Wasserman, W.W. (2002). TFBS: Computational framework for transcription factor binding site analysis. Bioinformatics *18*, 1135-1136.

Levitt, M., Spector, S., Sjordsma, A., and Udenfriend, S. (1965). Elucidation of the rate-limiting step in norepineurine biosythesis in the perfused guinea-pig heart. J Pharmacol Exp Ther *148*, 1-8.

Li, Z., White, P., Tuteja, G., Rubins, N., Sackett, S., and Kaestner, K. (2009). Foxa1 and Foxa2 regulate bile duct development in mice. J Clin Invest *119*, 1537-1545.

Lin, W., Metzakopian, E., Mavromatakis, Y.E., Gao, N., Balaskas, N., Sasaki, H., Briscoe, J., Whitsett, J.A., Goulding, M., Kaestner, K.H.*, et al.* (2009). Foxa1 and Foxa2 function both upstream of and cooperatively with Lmx1a and Lmx1b in a feedforward loop promoting mesodiencephalic dopaminergic neuron development. Developmental Biology.

Liu, A., and Joyner, A.L. (2001a). Early anterior/posterior patterning of the midbrain and cerebellum. Annu Rev Neurosci *24*, 869-896.

Liu, A., and Joyner, A.L. (2001b). EN and GBX2 play essential roles downstream of FGF8 in patterning the mouse mid/hindbrain region. Development *128*, 181-191.

Liu, A., Losos, K., and Joyner, A.L. (1999). FGF8 can activate Gbx2 and transform regions of the rostral mouse brain into a hindbrain fate. Development *126*, 4827-4838.

Liu, J.K., DiPersio, C.M., and Zaret, K.S. (1991). Extracellular signals that regulate liver transcription factors during hepatic differentiation in vitro. Molecular and Cellulr Biology *11*, 773-784.

Löhr, H., Ryu, S., and Driever, W. (2009). Zebrafish diencephalic A11-related dopaminergic neurons share a conserved transcriptional network with neuroendocrine cell lineages. Development *136*, 1007-1017.

Lomvardas, S., and Thanos, D. (2002). Opening chromatin. Mol Cell *9*, 209-211.

Lupien, M., Eeckhoute, J., Meyer, C., Wang, Q., Zhang, Y., Li, W., Carroll, J.S., Liu, X., and Brown, M. (2008). FoxA1 translates epigenetic signatures into enhancer-driven lineage-specific transcription. Cell *132*, 958-970.

Mango, S.E. (2009). The molecular basis of organ formation: insights from the C. elegans foregut. Annu Rev Cell Dev Biol *25*, 597-628.

Martí, E., Takada, R., Bumcrot, D.A., Sasaki, H., and McMahon, A.P. (1995). Distribution of Sonic hedgehog peptides in the developing chick and mouse embryo. Development *121*, 2537-2547.

Martinez, S., Crossley, P.H., Cobos, I., Rubenstein, J.L., and Martin, G.R. (1999). FGF8 induces formation of an ectopic isthmic organizer and isthmocerebellar development via a repressive effect on Otx2 expression. Development *126*, 1189-1200.

Martinez-Barbera, J.P., Signore, M., Boyl, P.P., Puelles, E., Acampora, D., Gogoi, R., Schubert, F., Lumsden, A., and Simeone, A. (2001). Regionalisation of anterior neuroectoderm and its competence in responding to forebrain and midbrain inducing activities depend on mutual antagonism between OTX2 and GBX2. Development *128*, 4789-4800.

Matsunaga, E., Katahira, T., and Nakamura, H. (2002). Role of Lmx1b and Wnt1 in mesencephalon and metencephalon development. Development *129*, 5269-5277.

Matys, V., Kel-Margoulis, O.V., Fricke, E., Liebich, I., Land, S., Barre-Dirrie, A., Reuter, I., Chekmenev, D., Krull, M., Hornischer, K*., et al.* (2006). TRANSFAC and its module TRANSCompel: transcriptional gene regulation in eukaryotes. Nucleic Acids Research *34*, D108-110.

Mavromatakis, Y.E. (2006). Role of the forkhead transcription factor Foxa2 in the development of the ventral mesencephalon:. 1-367.

McMahon AP, B.A. (1990). The Wnt-1 (int-1) proto-oncogene is required for development of a large region of the mouse brain. cell *62*.

McMahon AP, J., Bradley A, McMahon JA (1992). The midbrain-hindbrain phenotype of Wnt-1-/Wnt-1- mice results from stepwise deletion of engrailed-expressing cells by 9.5 days postcoitum. cell *69*.

Meyers, E., Lewandoski, M., and Martin, G. (1998). An Fgf8 mutant allelic series generated by Cre- and Flp-mediated recombination. nature *18*.

Millen, K.J., Millonig, J.H., and Hatten, M.E. (2004). Roof plate and dorsal spinal cord dl1 interneuron development in the dreher mutant mouse. Developmental Biology *270*, 382-392.

Millet, S., Campbell, K., Epstein, D.J., Losos, K., Harris, E., and Joyner, A.L. (1999). A role for Gbx2 in repression of Otx2 and positioning the mid/hindbrain organizer. Nature *401*, 161-164.

Motallebipour, M., Ameur, A., Reddy Bysani, M.S., Patra, K., Wallerman, O., Mangion, J., Barker, M.A., McKernan, K.J., Komorowski, J., and Wadelius, C. (2009). Differential binding and co-binding pattern of FOXA1 and FOXA3 and their relation to H3K4me3 in HepG2 cells revealed by ChIP-seq. Genome Biol *10*, R129.

Naef, F., and Huelsken, J. (2005). Cell-type-specific transcriptomics in chimeric models using transcriptome-based masks. Nucleic Acids Research *33*, e111.

Nagatsu, T., Levitt, M., and Undenfriend, S. (1964). Tyrosine hydroxylase. The initial step in norepineurine biosynthesis. J Biol Chem *239*, 2910-2917.

Nakamura H, K.T., Matsunaga E, Sato T (2005). Isthmus organizer for midbrain and hindbrain development. Brain Res Brain Res Rev *49*.

Nakatani, T., Kumai, M., Mizuhara, E., Minaki, Y., and Ono, Y. (2010). Lmx1a and Lmx1b cooperate with Foxa2 to coordinate the specification of dopaminergic neurons and control of floor plate cell differentiation in the developing mesencephalon. Developmental Biology *339*, 101-113.

Nishizaki, Y., Shimazu, K., Kondoh, H., and Sasaki, H. (2001). Identification of essential sequence motifs in the node/notochord enhancer of Foxa2 (Hnf3beta) gene that are conserved across vertebrate species. Mech Dev *102*, 57-66.

Nusse, R., and Varmus, H.E. (1982). Many tumors induced by the mouse mammary tumor virus contain a provirus integrated in the same region of the host genome. Cell *31*, 99-109.

Odom, D., Dowell, R., Jacobsen, E., Gordon, W., Danford, T., Macisaac, K., Rolfe, P., Conboy, C., Gifford, D., and Fraenkel, E. (2007). Tissue-specific transcriptional regulation has diverged significantly between human and mouse. Nat Genet *39*, 730-732.

Omodei, D., Acampora, D., Mancuso, P., Prakash, N., Di Giovannantonio, L.G., Wurst, W., and Simeone, A. (2008). Anterior-posterior graded response to Otx2 controls proliferation and differentiation of dopaminergic progenitors in the ventral mesencephalon. Development *135*, 3459-3470.

Ono, Y., Nakatani, T., Sakamoto, Y., Mizuhara, E., Minaki, Y., Kumai, M., Hamaguchi, A., Nishimura, M., Inoue, Y., Hayashi, H.*, et al.* (2007). Differences in neurogenic potential in floor plate cells along an anteroposterior location: midbrain dopaminergic neurons originate from mesencephalic floor plate cells. Development *134*, 3213-3225.

Park, P.J. (2009). ChIP-seq: advantages and challenges of a maturing technology. Nat Rev Genet *10*, 669-680.

Patten, I., and Placzek, M. (2000). The role of Sonic hedgehog in neural tube patterning. Cell Mol Life Sci *57*, 1695–1708.

Placzek, M., and Briscoe, J. (2005). The floor plate: multiple cells, multiple signals. Nat Rev Neurosci *6*, 230-240.

Ptashne, M., and Gann, A. (1997). Transcriptional activation by recruitment. Nature *386*, 569-577.

Puelles, E., Annino, A., Tuorto, F., Usiello, A., Acampora, D., Czerny, T., Brodski, C., Ang, S.L., Wurst, W., and Simeone, A. (2004). Otx2 regulates the extent, identity and fate of neuronal progenitor domains in the ventral midbrain. Development *131*, 2037-2048.

Rascle, A., Neumann, T., Raschta, A., Neumann, A., Heining, E., Kastner, J., and Witzgall, R. (2009). The LIM-homeodomain transcription factor LMX1B regulates expression of NF-kappa B target genes. Experimental Cell Research *315*, 76-96.

Rausa, F.M., Tan, Y., Zhou, H., Yoo, K.W., Stolz, D.B., Watkins, S.C., Franks, R.R., Unterman, T.G., and Costa, R.H. (2000). Elevated levels of hepatocyte nuclear factor 3beta in mouse hepatocytes influence expression of genes involved in bile acid and glucose homeostasis. Molecular and Cellular Biology *20*, 8264-8282.

Ravasi, T., Suzuki, H., Cannistraci, C.V., Katayama, S., Bajic, V.B., Tan, K., Akalin, A., Schmeier, S., Kanamori-Katayama, M., Bertin, N.*, et al.* (2010). An Atlas of Combinatorial Transcriptional Regulation in Mouse and Man. Cell *140*, 744-752.

Raynal, J.F., Dugast, C., Le Van Thaï, A., and Weber, M.J. (1998). Winged helix hepatocyte nuclear factor 3 and POU-domain protein brn-2/N-oct-3 bind overlapping sites on the neuronal promoter of human aromatic L-amino acid decarboxylase gene. Brain Res Mol Brain Res *56*, 227-237.

Ren, B., Robert, F., Wyrick, J.J., Aparicio, O., Jennings, E.G., Simon, I., Zeitlinger, J., Schreiber, J., Hannett, N., Kanin, E.*, et al.* (2000). Genome-wide location and function of DNA binding proteins. Science *290*, 2306-2309.

Rick, C.E., Ebert, A., Virag, T., Bohn, M.C., and Surmeier, D.J. (2006). Differentiated dopaminergic MN9D cells only partially recapitulate the electrophysiological properties of midbrain dopaminergic neurons. Dev Neurosci *28*, 528-537.

Robertson, G., Hirst, M., Bainbridge, M., Bilenky, M., Zhao, Y., Zeng, T., Euskirchen, G., Bernier, B., Varhol, R., Delaney, A.*, et al.* (2007). Genome-wide profiles of STAT1 DNA association using chromatin immunoprecipitation and massively parallel sequencing. Nat Meth *4*, 651-657.

Roelink, H., Augsburger, A., Heemskerk, J., Korzh, V., Norlin, S., Ruiz i Altaba, A., Tanabe, Y., Placzek, M., Edlund, T., and Jessell, T.M. (1994). Floor plate and motor neuron induction by vhh-1, a vertebrate homolog of hedgehog expressed by the notochord. Cell *76*, 761-775.

Roelink, H., Porter, J.A., Chiang, C., Tanabe, Y., Chang, D.T., Beachy, P.A., and Jessell, T.M. (1995). Floor plate and motor neuron induction by different concentrations of the amino-terminal cleavage product of sonic hedgehog autoproteolysis. Cell *81*, 445-455.

Saarimäki-Vire, J., Peltopuro, P., Lahti, L., Naserke, T., Blak, A.A., Vogt Weisenhorn, D.M., Yu, K., Ornitz, D.M., Wurst, W., and Partanen, J. (2007). Fibroblast growth factor

receptors cooperate to regulate neural progenitor properties in the developing midbrain and hindbrain. J Neurosci *27*, 8581-8592.

Santagati, F., Abe, K., Schmidt, V., Schmitt-John, T., Suzuki, M., Yamamura, K. and Imai, K. (2003). Identification of Cis-regulatory elements in the mouse Pax9/Nkx2-9 genomic region: implication for evolutionary conserved synteny. *Genetics* 165, 235-242.

Santisteban, P., Recacha, P., Metzger, D.E., and Zaret, K.S. (2010). Dynamic expression of Groucho-related genes Grg1 and Grg3 in foregut endoderm and antagonism of differentiation. Dev Dyn *239*, 980-986.

Sasaki, H., and Hogan, B. (1994a). HNF-3 beta as a regulator of floor plate development. Cell *76*, 103-115.

Sasaki, H., and Hogan, B.L. (1994b). HNF-3 beta as a regulator of floor plate development. Cell *76*, 103-115.

Sasaki, H., Hui, C., Nakafuku, M., and Kondoh, H. (1997). A binding site for Gli proteins is essential for HNF-3beta floor plate enhancer activity in transgenics and can respond to Shh in vitro. Development *124*, 1313-1322.

Sasaki, H., Nishizaki, Y., Hui, C., Nakafuku, M., and Kondoh, H. (1999). Regulation of Gli2 and Gli3 activities by an amino-terminal repression domain: implication of Gli2 and Gli3 as primary mediators of Shh signaling. Development *126*, 3915-3924.

Scholpp S, L.C., Brand M (2003). Engrailed and Fgf8 act synergistically to maintain the boundary between diencephalon and mesencephalon. DEVELOPMENT *130*.

Sekiya, T., and Zaret, K.S. (2007). Repression by Groucho/TLE/Grg proteins: genomic site recruitment generates compacted chromatin in vitro and impairs activator binding in vivo. Mol Cell *28*, 291-303.

Shamim, H., Mahmood, R., Logan, C., Doherty, P., Lumsden, A., and Mason, I. (1999). Sequential roles for Fgf4, En1 and Fgf8 in specification and regionalisation of the midbrain. Development *126*, 945-959.

Shendure, J., and Ji, H. (2008). Next-generation DNA sequencing. Nat Biotechnol *26*, 1135-1145.

Shim, E.Y., Woodcock, C., and Zaret, K.S. (1998). Nucleosome positioning by the winged helix transcription factor HNF3. Genes & Development *12*, 5-10.

Simeone, A. (2000). Positioning the isthmic organizer where Otx2 and Gbx2meet. Trends Genet *16*, 237-240.

Simmons, A. (2001). Neurogenin2 Expression in Ventral and Dorsal Spinal Neural Tube Progenitor Cells Is Regulated by Distinct Enhancers. Developmental Biology *229*, 327-339.

Simon, H.H., Bhatt, L., Gherbassi, D., Sgadó, P., and Alberí, L. (2003). Midbrain dopaminergic neurons: determination of their developmental fate by transcription factors. Annals of the New York Academy of Sciences *991*, 36-47.

Smidt, M.P., Asbreuk, C.H., Cox, J.J., Chen, H., Johnson, R.L., and Burbach, J.P. (2000). A second independent pathway for development of mesencephalic dopaminergic neurons requires Lmx1b. Nat Neurosci *3*, 337-341.

Smidt, M.P., van Schaick, H.S., Lanctôt, C., Tremblay, J.J., Cox, J.J., van der Kleij, A.A., Wolterink, G., Drouin, J., and Burbach, J.P. (1997). A homeodomain gene Ptx3 has highly restricted brain expression in mesencephalic dopaminergic neurons. Proc Natl Acad Sci USA *94*, 13305-13310.

Solomon, M.J., Larsen, P.L., and Varshavsky, A. (1988). Mapping protein-DNA interactions in vivo with formaldehyde: evidence that histone H4 is retained on a highly transcribed gene. Cell *53*, 937-947.

Stern, C.D. (2001). Initial patterning of the central nervous system: how many organizers? Nat Rev Neurosci *2*, 92-98.

Sun X, , Lewandoski M, Martin G R (1999). Targeted disruption of Fgf8 causes failure of cell migration in the gastrulating mouse embryo. GENES DEV *13*.

Tuteja, G., Jensen, S.T., White, P., and Kaestner, K. (2008). Cis-regulatory modules in the mammalian liver: composition depends on strength of Foxa2 consensus site. Nucleic Acids Research *36*, 4149-4157.

Tzschentke, T.M. (2000). The medial prefrontal cortex as a part of the brain reward system. Amino Acids *19*, 211-219.

Tzschentke, T.M., and Schmidt, W.J. (2000). Functional relationship among medial prefrontal cortex, nucleus accumbens, and ventral tegmental area in locomotion and reward. Crit Rev Neurobiol *14*, 131-142.

Uittenbogaard, M., and Chiaramello, A. (2002). Expression of the bHLH transcription factor Tcf12 (ME1) gene is linked to the expansion of precursor cell populations during neurogenesis. Brain Res Gene Expr Patterns *1*, 115-121.

Van den Munckhof, P., Luk, K.C., Ste-Marie, L., Montgomery, J., Blanchet, P.J., Sadikot, A.F., and Drouin, J. (2003). Pitx3 is required for motor activity and for survival of a subset of midbrain dopaminergic neurons. Development *130*, 2535-2542.

Vokes, S.A., Ji, H., McCuine, S., Tenzen, T., Giles, S., Zhong, S., Longabaugh, W.J., Davidson, E.H., Wong, W.H., and McMahon, A.P. (2007). Genomic characterization of Gli-activator targets in sonic hedgehog-mediated neural patterning. Development *134*, 1977-1989.

Wallén, A., and Perlmann, T. (2003). Transcriptional control of dopamine neuron development. Annals of the New York Academy of Sciences *991*, 48-60.

Wallén, A., Zetterström, R.H., Solomin, L., Arvidsson, M., Olson, L., and Perlmann, T. (1999). Fate of mesencephalic AHD2-expressing dopamine progenitor cells in NURR1 mutant mice. Experimental Cell Research *253*, 737-746.

Wallerman, O., Motallebipour, M., Enroth, S., Patra, K., Bysani, M.S., Komorowski, J., and Wadelius, C. (2009). Molecular interactions between HNF4a, FOXA2 and GABP identified at regulatory DNA elements through ChIP-sequencing. Nucleic Acids Research *37*, 7498-7508.

Wederell, E.D., Bilenky, M., Cullum, R., Thiessen, N., Dagpinar, M., Delaney, A., Varhol, R., Zhao, Y., Zeng, T., Bernier, B.*, et al.* (2008). Global analysis of in vivo Foxa2-binding sites in mouse adult liver using massively parallel sequencing. Nucleic Acids Research *36*, 4549-4564.

Weigel, D., and Jäckle, H. (1990). The fork head domain: a novel DNA binding motif of eukaryotic transcription factors? Cell *63*, 455-456.

Weigel, D., Jürgens, G., Küttner, F., Seifert, E., and Jäckle, H. (1989). The homeotic gene fork head encodes a nuclear protein and is expressed in the terminal regions of the Drosophila embryo. Cell *57*, 645-658.

Weinstein, D., Ruiz i Altaba, A., Chen, W., Hoodless, P., Prezioso, V., Jessell, T., and Darnell JE. (1994). The winged-helix transcription factor HNF-3 beta is required for notochord development in the mouse embryo. Cell *78*, 575-588.

Wilkinson DG, B.J., McMahon AP (1987). Expression of the proto-oncogene int-1 is restricted to specific neural cells in the developing mouse embryo. cell *50*.

Wilson, N.K., Miranda-Saavedra, D., Kinston, S., Bonadies, N., Foster, S.D., Calero-Nieto, F., Dawson, M.A., Donaldson, I.J., Dumon, S., Frampton, J.*, et al.* (2009). The transcriptional program controlled by the stem cell leukemia gene Scl/Tal1 during early embryonic hematopoietic development. Blood *113*, 5456-5465.

Wolfrum, C., Besser, D., Luca, E., and Stoffel, M. (2003). Insulin regulates the activity of forkhead transcription factor Hnf-3beta/Foxa-2 by Akt-mediated phosphorylation and nuclear/cytosolic localization. Proc Natl Acad Sci USA *100*, 11624-11629.

Wurst, W., Auerbach, A.B., and Joyner, A.L. (1994). Multiple developmental defects in Engrailed-1 mutant mice: an early mid-hindbrain deletion and patterning defects in forelimbs and sternum. Development *120*, 2065-2075.

Wurst, W., and Bally-Cuif, L. (2001). Neural plate patterning: upstream and downstream of the isthmic organizer. Nat Rev Neurosci *2*, 99-108.

Xu, J., Watts, J.A., Pope, S.D., Gadue, P., Kamps, M., Plath, K., Zaret, K.S., and Smale, S.T. (2009). Transcriptional competence and the active marking of tissue-specific enhancers by defined transcription factors in embryonic and induced pluripotent stem cells. Genes & Development *23*, 2824-2838.

Yan, C. (2008). Genetic studies into the origin and transcriptional regulation of midbrain dopaminergic neurons in mice. In *Anatomy and Developmental Biology*, vol. PhD. London: University College London.

Ye, W., Shimamura, K., Rubenstein, J.L., Hynes, M.A., and Rosenthal, A. (1998). FGF and Shh signals control dopaminergic and serotonergic cell fate in the anterior neural plate. Cell *93*, 755-766.

Ying, Q., Stavridis, M., Griffiths, D., Li, M., and Smith, A. (2003). Conversion of embryonic stem cells into neuroectodermal precursors in adherent monoculture. Nat Biotech *21*, 183-186.

Zaret, K.S. (1995). Nucleoprotein architecture of the albumin transcriptional enhancer. Semin Cell Biol *6*, 209-218.

Zervas, M., Millet, S., Ahn, S., and Joyner, A.L. (2004). Cell behaviors and genetic lineages of the mesencephalon and rhombomere 1. Neuron *43*, 345-357.

Zhang, Y., Shin, H., Song, J.S., Lei, Y., and Liu, X. (2008). Identifying positioned nucleosomes with epigenetic marks in human from ChIP-Seq. BMC Genomics *9*, 537.

Zhou, Q.Y., and Palmiter, R.D. (1995). Dopamine-deficient mice are severely hypoactive, adipsic, and aphagic. Cell *83*, 1197-1209.

Zhou, Y., Koli, K., Hagood, J.S., Miao, M., Mavalli, M., Rifkin, D.B., and Murphy-Ullrich, J.E. (2009). Latent transforming growth factor-beta-binding protein-4 regulates transforming growth factor-beta1 bioavailability for activation by fibrogenic lung fibroblasts in response to bleomycin. Am J Pathol *174*, 21-33.